Development of polymeric nanoparticles with controlled drug release for dermal application

Inaugural-Dissertation

to obtain the academic degree

Doctor rerum naturalium (Dr. rer. nat.)

submitted to the Department of Biology, Chemistry and Pharmacy

of Freie Universität Berlin

by

BENJAMIN BALZUS

from Potsdam, Germany

2018

Die vorliegende Arbeit wurde von März 2014 bis März 2018 unter der Leitung von Prof. Dr. Roland Bodmeier im Institut für Pharmazie angefertigt.

1. Gutachter: Prof. Dr. Roland Bodmeier

2. Gutachter: Prof. Dr. Philippe Maincent

Disputation am 28.05.2018

To Katharina

Acknowledgements

First of all, I would like to thank my supervisor Prof. Dr. Roland Bodmeier for giving me the opportunity to work and study in his research group. I am very thankful for his support and for allowing me to get involved in different activities that helped me to gain valuable experience for my future career.

I kindly thank Prof. Dr. Philippe Maincent for co-evaluating my thesis.

I am deeply grateful to Dr. Fitsum Feleke Sahle for the exceptional discussions, the valuable scientific input and for proofreading parts of my thesis.

Special thanks to all my cooperation partners: Thanks to Stefan Hönzke and Prof. Dr. Sarah Hedtrich for the support regarding all pharmacological issues. Thanks to Pin Dong, Dr. Alexa Patzelt and Prof. Dr. Jürgen Lademann for their knowledge and input regarding follicular penetration. Thanks to Nadine Döge and PD Dr. Annika Vogt for their support in all dermatological issues. I am also thankful to Dr. Christian Gerecke and Prof. Dr. Burkhard Kleuser for their kind assistance and input regarding nanoparticle toxicity. Finally I would like to thank Miriam Colombo and Dr. Gaith Zoubari for providing me with their nanoparticles.

I am deeply grateful to Miriam Colombo, Prutha Gaitonde and Marina Kolbina for proofreading parts of my thesis and for their valuable comments and suggestions.

Furthermore, I thank all my colleagues of the research group for the scientific discussions, for their valuable input and assistance, and for the unforgettable lunchbreaks and group activities.

Special thanks also to Eva Ewest, Stefan Walter, Andreas Krause and Gabriela Karsubke for their assistance, generous help and support.

I would like to thank all my friends who supported me throughout my whole PhD.

I wish to express my special thankfulness to my parents, for always being good parents and for their never-ending support during my whole life.

Finally, I am eternally grateful to Katharina, for her love, encouragement and immeasurable support.

Table of contents

Abbreviations

CLSM	Confocal laser scanning microscopy
CTAB	Cetyltrimethyl ammonium bromide
DSC	Differential scanning calorimetry
EE	Encapsulation efficiency
FACS	Fluorescence-activated cell sorting
FITC	Fluorescein isothiocyanate
H2DCFDA	6-carboxy-2´,7´-dicholoro dihydrofluorecein diacetate
HEC	Hydroxyethyl cellulose
HPMCP	Hydroxypropyl methyl cellulose phthalate
KGM	Keratinocyte growth medium
LC	Loading capacity
LC-MS/MS	Liquid chromatography technique coupled with tandem mass spectrometry
MFI	Mean fluorescence intensity
MTT	3- (4,5- dimethylthiazol-2-yl)-2,5-diphenyltetrazolium bromide
MWCO	Molecular weight cut-off
NHK	Primary human keratinocytes
PBS	Phosphate buffered saline
PC	Positive control
PDI	Polydispersity index
PIPES	Piperazine-N,N′-bis(2-ethanesulfonic acid)
PLA	Polylactic acid
PLGA	Poly (lactic-co-glycolic acid)
PVA	Polyvinyl alcohol
ROS	Reactive oxygen species
RSD	Relative standard deviation
SC	Stratum corneum
SD	Standard deviation
SDS	Sodium dodecyl sulfate

Tg	Glass transition temperature
UC	Untreated cells
USP	United states pharmacopeia

1. Introduction[1]

In recent years nanotechnology-based drug delivery systems such as nanocrystals, polymeric nanoparticles, lipid nanoparticles, liposomes, nanoemulsions, microemulsions, nanofibers and dendrimers have shown promising results as novel drug delivery carriers. They offer a number of advantages such as improved drug solubility and stability, versatility to control drug release, improved membrane permeability of drugs, adjustable surface properties, drug targeting potential and flexibility to administering drugs via intravenous, intramuscular, subcutaneous and oral routes (D'Souza, 2014; Kesisoglou et al., 2007; Küchler et al., 2009b; Merisko-Liversidge et al., 2003; Sahle et al., 2016; Yoo et al., 2011). Furthermore, nanoparticles can be used to target the skin surface, furrows and hair follicles (Figure 1).

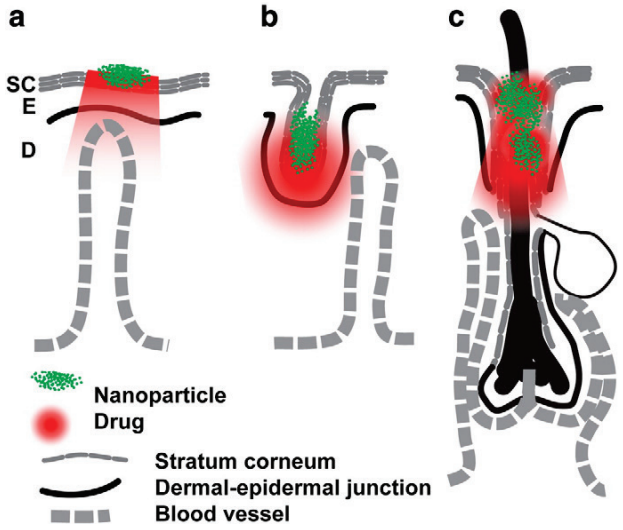

Figure 1: Sites in skin for nanoparticle delivery. Topical nanoparticle drug delivery takes place in three major sites: stratum corneum (SC) surface (panel a), furrows (dermatoglyphs) (panel b), and openings of hair follicles (infundibulum) (panel c). The nanoparticles are shown in green and the drug in red. Other sites for delivery are the viable epidermis (E) and dermis (D). (Reprinted from (Prow et al., 2011), Copyright (2011), with permission from Elsevier)

[1] Parts of this chapter were taken from:

1. B. Balzus, F.F. Sahle, S. Hönzke, C. Gerecke, F. Schumacher, S. Hedtrich, B. Kleuser, R. Bodmeier, Formulation and ex vivo evaluation of polymeric nanoparticles for controlled delivery of corticosteroids to the skin and the corneal epithelium, Eur. J. Pharm. Biopharm., 115 (2017) 122-130.
2. B. Balzus, M. Colombo, F.F. Sahle, G. Zoubari, S. Staufenbiel, R. Bodmeier, Comparison of different in vitro release methods used to investigate nanocarriers intended for dermal application, Int. J. Pharm., 513 (2016) 247-254.

Nanoparticles can potentially improve dermal local therapeutical efficiency by increasing drug penetration and permeation to the skin (Schafer-Korting et al., 2007; Shim et al., 2004). Nevertheless, until now there was just little success for nanoparticle mediated drug delivery to epidermis and dermis without barrier modification of healthy skin. However nanoparticles as drug delivery systems to improve dermal local therapeutical efficiency will be applied most likely to aged or diseased skin, where the barrier properties are changed. This might increase nanoparticle mediated drug delivery (Abdel-Mottaleb et al., 2012; Prow et al., 2011).

1.1. Skin

A main function of the skin is to protect the body against the external environment as physical barrier. Therefore the majority of environmental nanoparticles (viruses, dust, allergens or materials) cannot penetrate the skin unless the barrier is disrupted (Baroli, 2010; Prow et al., 2011). Furthermore the skin absorbs IR and UV irradiation, regulates the temperature, prevents dehydration and defends the body from entering chemicals and biological agents. The immune and enzymatic system of the skin are additional cellular and molecular barriers to neutralize, attack or degrade everything that is not physically kept outside (Baroli, 2010; Honari and Maibach, 2014).

1.1.1. Skin structure

Skin consists of three layers: epidermis, dermis and hypodermis (Figure 2). For the penetration of the skin the epidermis and dermis are the only relevant ones (Honari and Maibach, 2014).

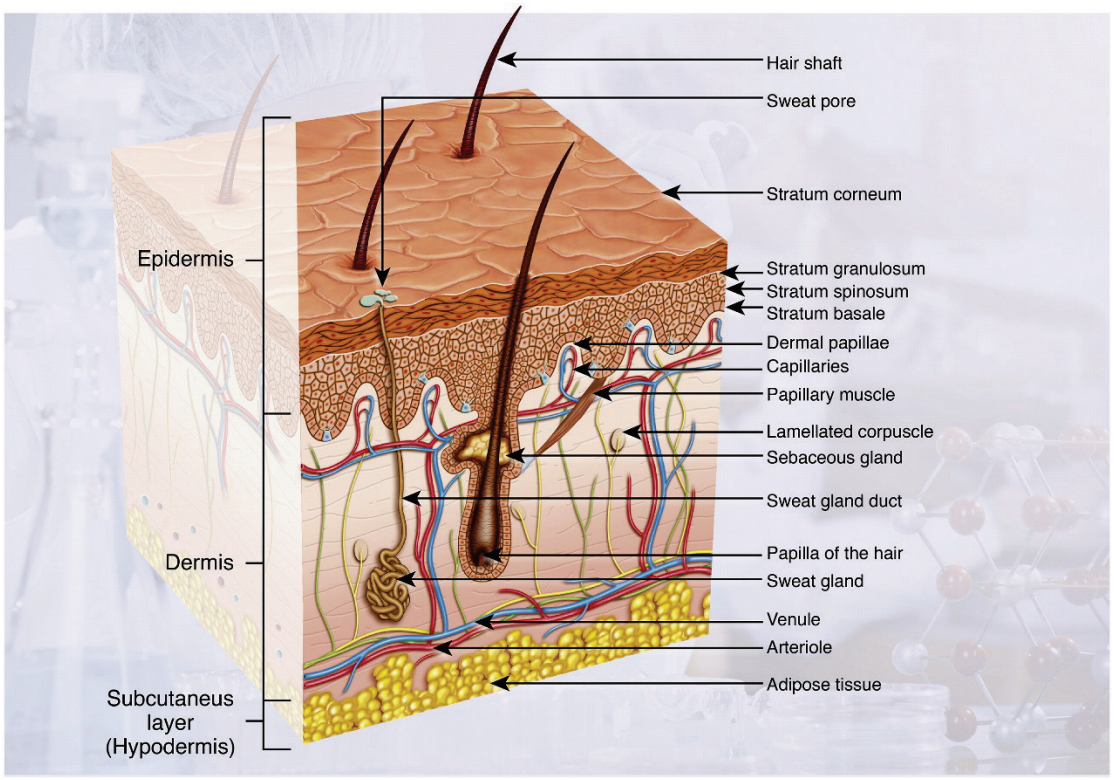

Figure 2: Schematic picture of the native skin that is sub-classified into three main compartments: epidermis, dermis and subcutis (hypodermis). Skin appendices like hair with sebaceous glands, sweat glands as well as blood vessels are embedded in the skin. (Reprinted from (Mathes et al., 2014), Copyright (2014), with permission from Elsevier)

The dermis has a capillary anastomoses function to supply the epidermis with nutrients and oxygen and clear the dermis from cell metabolic products and penetrated foreign agents. Above the dermis is the epidermis, which is separated from the dermis by a basement membrane (Woodley et al., 1983).

The epidermis is dived in five strata: the stratum basale, which is in contact with the dermis, stratum spinosum, stratum granulosum, stratum lucidum (where present) and stratum corneum, which is in contact with the external environment. The epidermis has a barrier function and is classified as stratified squamous epithelial layer with keratinocytes, which differ between the layers due to progressive modification. Keratinocytes flatten, enucleate and differentiate to corneocytes while moving up from the stratum basale to the stratum corneum. This process takes around 14 days depending on the anatomic side and age and assists the elimination of pathogens, cancerous cells or solid particulate matter (Reddy et al., 2000; Roberts and Marks, 1980). Therefore the stratum corneum is constantly renewed by keratinocytes which

undergo keratinization. The epidermis can simply be distinguished into the viable epidermis with keratinocytes and the stratum corneum with corneocytes, which are completely differentiated enucleated and keratinfilaggrin filled cells. The corneocytes are densely packed within a protein rich envelope with an outer lipid envelope surrounded by an extracellular lipid matrix arranged in bilayers (Mojumdar et al., 2016). Additionally the corneocytes are linked by corneodesmosomes, which maintain the cellular shape and regular packing of the corneocytes (Ishida-Yamamoto and Igawa, 2014). The stratum corneum is covered by a thin layer of sweat, sebum, bacteria and dead cells. However, this thin layer is expected to have a negligible effect on the barrier properties. The diffusion through the stratum corneum is expected to be the rate limiting step in substance permeation across the skin (Prow et al., 2011). Inside the viable epidermis in the stratum granulosum the existence of functional tight junctions has been demonstrated (Brandner et al., 2002; Langbein et al., 2002). Tight junctions are regarded as another important element of the physical epidermal barrier system. Additionally constituent tight junction proteins have been identified in other epithelial layers and the hair follicles (Brandner et al., 2003).

Besides the stratum corneum and the tight junctions as physical skin barriers the epidermis has a hydrophilic – lipophilic gradient with a nonhomogeneous change in hydrophobicity from the lipophilic stratum corneum to the hydrophilic stratum granulosum (Elias, 2005). This is an additional defense strategy to prevent penetration of lipophilic agents in the viable epidermis. Therefore a moderate oil water partition coefficient is a key parameter for transcutaneous absorption (Moss et al., 2002). Furthermore, there is a non linear pH gradient from stratum corneum surface (pH 4.5 - 5.5) to the stratum corneum - stratum granulosum interface (neutral) (Schirren, 1955). The skin pH gradient and acid mantle are involved in the antimicrobial defense, permeability barrier homeostasis, stratum corneum integrity and cohesiveness, regulation of pH sensitive proteolytic enzymes, desquamation processes and restriction of inflammation due to the release of inhibition of pro-inflammatory cytokines (Schmid-Wendtner and Korting, 2006). The acid mantle and the pH gradient are maintained in a lipophilic environment due to the excretion of lactic acid from sweat glands, excretion of sebum triglycerides that are transformed in free fatty acids by the normal microflora, presence of free fatty acids in the intercorneocyte lipids and

presence of membrane transporters for the exchange of sodium protons (Elias, 2005; Schmid-Wendtner and Korting, 2006).

In summary the penetration of substances and particles in the stratum corneum and towards the viable epidermis is limited by the structure of the stratum corneum and by the gradients present in the epidermis.

1.1.2. Sweat glands and pilosebaceous unit

The sweat glands and pilosebaceous units are openings and shunts in the skin surface which can potentially be used as penetration route.

Sweat glands are coiled tubular glands reaching from the stratum corneum down to the dermis or hypodermis (2 - 5 mm length). They are involved in the thermoregulation and excretion of acids and body wastes as sweat. Sweat is a hypotonic aqueous mixture of organic acids, carbohydrates, amino acids, nitrogenous substances, vitamins, and electrolytes and has a pH between 4.0 and 6.8 (Murota et al., 2015).

The pilosebaceous unit is formed by the hair follicle with the associated sebaceous gland and is supplied through the dermal papilla (Figure 3).

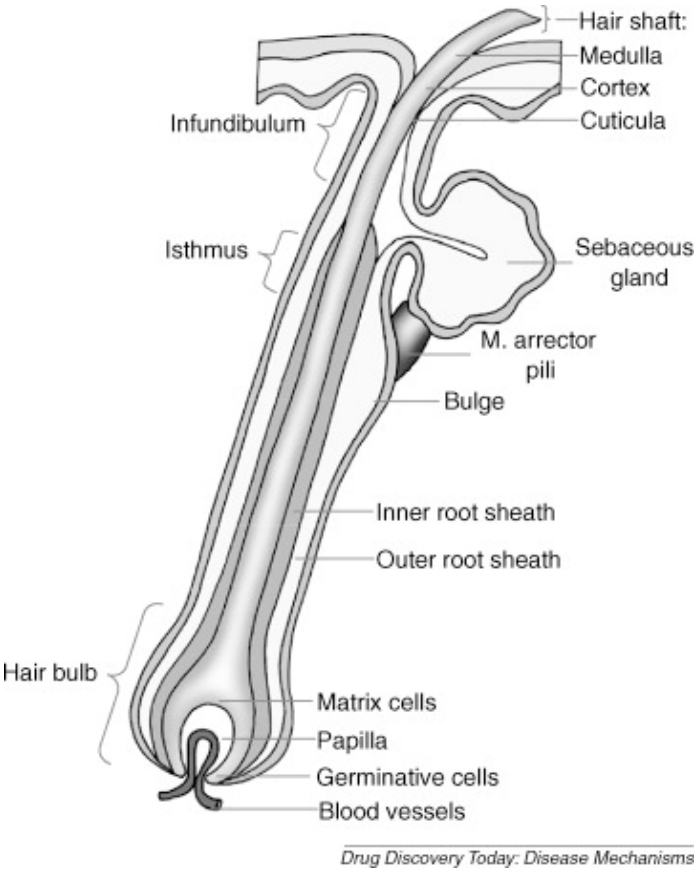

Figure 3: Morphology of the human hair follicle (Reprinted from (Patzelt et al., 2008a) Copyright (2008), with permission from Elsevier)

It is reaching down to the dermis (2 – 4 mm length) so that penetrating agents could potentially reach the viable epidermis or the blood stream depending on the penetration depth of the agents. Hair follicles consist of an inner and an outer root sheet. The hair follicle starts with its orifice at the epidermis, which is followed by the infundibulum as the compartment of the upper hair shaft. The infundibulum is less densely cornified than the stratum corneum (Vogt et al., 2007). The sebaceous gland is attached to the hair follicle and is directed to the infundibulum in depth up to 500 µm (Vogt et al., 2005). The sebaceous gland is secreting sebum into the ducts and infundibulum with a sebum flow rate of 0.1 – 2.1 µg/cm^2/min (Saint-Leger and Cohen, 1985). Sebum is a mixture of squalene, waxes, cholesterol derivatives, triglycerides, fatty acids and cell debris, which liquefy at 37 °C (Valiveti et al., 2008). However the composition of sebum is changing after secretion of the sebaceous gland. Triglycerides in the sebum composition undergo partial hydrolysis by bacterial lipases from the skin flora and epidermal esterases what liberates free fatty acids. These free fatty acids contribute to the acidic skin pH (Nakatsuji et al., 2010). The isthmus follows as

compartment between sebaceous gland and the hair bulb. Deep follicular areas reach down to the perifolliculum, where the hair shaft is surrounded by collagen fibers and the dermis. Large hair follicles of the scalp additionally exhibit arrector pili muscles (Poblet et al., 2002). The hair shaft is composed of different layers the cuticula, melanosomes, the cortex and the medulla. The deepest compartment the hair bulb consists of matrix cells, the papilla and germinative cells, which are supplied via blood vessels (Patzelt et al., 2008a).

Hair follicles are classified in vellus, lanugo, sebaceous and terminal hair follicles depending on their orifice diameter, volume, surface and depth into the dermis. Vellus hair follicles reach down to 1000 µm depth into the dermis with hair shafts of 2 cm length and a thickness of less than 30 µm. Terminal hair follicles reach down to 3000 µm depth into the dermis with characteristically pigmented hair that is longer than 2 cm and thicker than 50 µm (Vogt et al., 2007). The overall follicular density is specified as 0.1% to the whole skin what usually refers to the forearm. In contrast the forehead displays 292 follicles/cm^2 leading to a follicular orifice surface area of 13.7 mm^2 which is 13.7% of the skin surface (Otberg et al., 2004). However only active hair follicles can be accessed. Hair follicles are active during hair growth, which takes years, or during sebum flow. Inactive follicles are closed and do not contribute to the follicular density and follicular penetration (Lademann et al., 2001).

1.1.3. Skin diseases

Skin diseases significantly change the barrier structure and function of the skin. Skin disease processes affect the dermal microenvironment associated with shifts in skin conditions like skin pH and transepidermal water loss. The physiological pH of healthy skin with an average of pH 5.5 is in some skin disease conditions like atopic dermatitis, ichthyosis, diaper dermatitis, irritant contact dermatitis and tinea pedis significantly increased depending on the severity of the disease (Ali and Yosipovitch, 2013). In patients with atopic dermatitis skin pH as high as 6.13 ± 0.83 was reported (Sparavigna et al., 1999). Besides the release of mediators the microbial colonization and inflammatory infiltrates can be altered (Hamid et al., 1994; Roll et al., 2004). Additionally, the localization and expression of tight junction proteins is disturbed by skin disease processes (Brandner et al., 2015; Kirschner et al., 2009). In chronic

lesional skin with inflammatory disorders like in atopic dermatitis and psoriasis the differentiation process of keratinocytes, the biosynthesis of the stratum corneum, the lipid composition and the organization of the stratum corneum is changed resulting in an impaired barrier function (Schmuth et al., 2015; van Smeden and Bouwstra, 2016).

Among skin diseases inflammatory skin diseases are the most common ones in medical dermatology and atopic dermatitis and psoriasis are the two most common inflammatory skin diseases (Guttman-Yassky et al., 2011). Atopic dermatitis and psoriasis can be easily distinguished clinically, because both exhibit distinct histological changes and an impaired barrier function. The percutaneous absorption rates of small molecules are increased in both cases (Garcia Ortiz et al., 2009; Lin et al., 2015). However, the increased skin penetration does not apply to all molecules (Yoshiike et al., 1993). Therefore diseased skin has rather a moderate increased penetration rate in comparison to healthy skin (Gattu and Maibach, 2011). Other challenging skin diseases are inflammatory processes in and around the hair follicle e.g. follicular psoriasis and primary inflammatory hair diseases. In these cases inflammation is located at specific, poorly accessible areas in otherwise unaffected skin.

1.2. Corticosteroids

Topical corticosteroids are one of the most frequently prescribed drugs to treat inflammatory skin diseases by dermatologists. The clinical effectiveness of corticosteroids especially in the treatment of psoriasis and atopic dermatitis is mediated by their vasoconstrictive, anti-inflammatory, immunosuppressive and antiproliferative effects. The target cells of topical glucocorticoids are the keratinocytes and fibroblasts within the viable epidermis and dermis, where the glucocorticoid receptors are located (Marks et al., 1982; Ponec et al., 1981). The cellular uptake of corticosteroids is a non-mediated, passive diffusion (Ponec and Kempenaar, 1983). However certain target cells possess a specific transport system for corticosteroids (Rao, 1981). The immunosuppressive and anti inflammatory effects are related to the regulation of corticosteroid-responsive genes. Corticosteroids bind to the corticosteroid receptor forming a complex that is rapidly transported to the nucleus and binds to the glucocorticoid responsive element a DNA region. This either stimulates or inhibits the

transcription of certain genes and regulates thereby inflammatory processes (Hughes and Rustin, 1997). Corticosteroids also indirectly regulate gen transcription by blocking other transcription factors like nuclear factor κB (Scheinman et al., 1995). Furthermore corticosteroids inhibit the transcription of proinflammatory cytokine genes of interferon gamma, tumor necrosis factor alpha, interleukin-1,2 and 6. Additionally the T-cell proliferation and T-cell dependent immunity is inhibited (Almawi et al., 1991). In keratinocytes interleukin-1α inhibition has antiinflammatory effects, whereas in fibroblast interleukin-1α inhibition has antiproliferative and atrophogenic effects (Lange et al., 2000). The vasoconstrictive effect of corticosteroids additionally contributes to their anti-inflammatory activity and diminishes erythema at the lesion site. However, the exact mechanism is not completely clear.

Despite the clear therapeutical benefit of corticosteroids in inflammatory skin diseases like atopic dermatitis and psoriasis (Furue et al., 2003) there are certain problems regarding corticosteroids. The treatment with topical corticosteroids is restricted to short therapy intervals, because of the facilitated penetration of topical corticosteroids. Long-term treatments on large skin surface areas lead to relevant absorption of corticosteroids in the organism and undesirable side effects in different organ systems. Undesirable side effects of topical corticosteroids are allergic reactions, skin atrophy, vasculopathy and an increased susceptibility to skin infections (Callen et al., 2007; Furue et al., 2003). Therefore, the disadvantage result from the chronic course of atopic dermatitis and psoriasis with recurrent episodes and long-term treatments with topical corticosteroids. Consequently there is a high demand for the development of novel therapeutic strategies that overcome these drawbacks and drug delivery to the intended site without further distribution to distant or irrelevant tissues is highly desired. In conclusion the development of delivery systems, which improve the selectivity of topical corticosteroid therapy, e.g. by targeted delivery of the corticosteroids to diseased skin areas and by prolonged release from reservoirs which maintain high corticosteroid concentrations at the site of action hereby allowing the reduction of the applied drug amount and applications frequencies would be highly beneficial.

1.3. Drug penetration into the skin

The opportunity to deliver bioactive molecules to the skin is not only an important implication for the local therapy of skin diseases but also for vaccination or systemic delivery of drugs with poor peroral bioavailability. Substances can penetrate across the stratum corneum transcellular, intercellular or through the appendageal pathway (Figure 4).

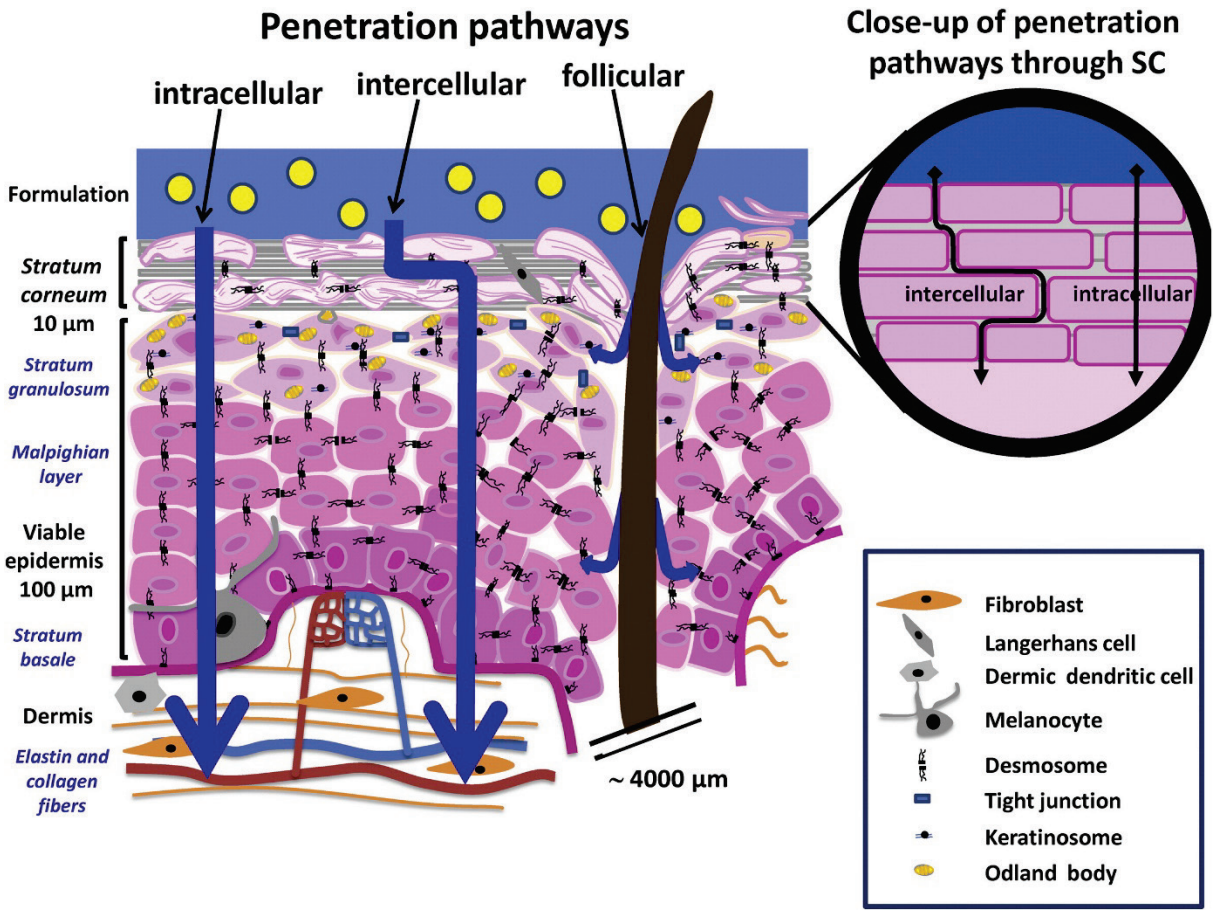

Figure 4: Sketch of the three penetration pathways: intracellular, intercellular and follicular. The upper right inset is a close-up of the stratum corneum (SC) showing the intracellular pathway and the tortuous intercellular pathway (Reprinted from (Bolzinger et al., 2012) Copyright (2012), with permission from Elsevier).

The intercellular route is favored especially for small molecules, which can freely move in the intercellular spaces. Therefore, the diffusion rate of small molecules is influenced by their physicochemical properties as lipophilicity, solubility, the hydrogen bonding ability molecular weight and volume (Potts and Guy, 1995). The transcellular pathway is unlikely compared to the intercellular route for most substances due to the repeated partitioning between lipophilic and hydrophilic compartments (Albery and Hadgraft,

1979; Elias and Friend, 1975). Conventionally drugs are topical applied in creams and ointments however there are different investigations to overcome the skin barrier and enhance drug penetration especially for drugs, which hardly penetrate the skin due to their size or relative hydrophilicity.

Drug penetration through the stratum corneum can be enhanced by substances in various ways e.g. chemically disturbance of the skin barrier (Ita, 2015), by occlusion mediated skin hydration or by diffusion enhancement. Besides the critical discussed chemical disturbance (Finnin and Morgan, 1999) there are also physical methods to disturb the skin barrier and enhance drug penetration. Low frequency ultrasound temporally disturbs the skin barrier by shock waves (Azagury et al., 2014) and acoustically-induced microjets resulting from cavitation and electroporation with high voltage pulses temporarily creates aqueous pores in cell membranes (Blagus et al., 2013). Furthermore the skin layer can be destroyed in a controlled manner by laser techniques which enhance drug penetration depth through artificial vertical channels (Sklar et al., 2014). Microneedle arrays mechanically damage the skin and form diffusion pathways for subsequently applied formulations. Microneedles can directly deposit the drug into the skin from immediately dissolving material or by hallow needles for microinjection (Haj-Ahmad et al., 2015; Sullivan et al., 2010; van der Maaden et al., 2014). Nanoparticles are another alternative or addition to enhance the drug penetration into the skin. Nowadays, the potential of nanoparticles to overcome the skin barrier and penetrate into deeper skin layers is debatable. However studies are indicating that nanoparticles enhance drug penetration and permeation through the skin (Schafer-Korting et al., 2007) and even penetrate into deeper skin layers of barrier disrupted skin (Abdel-Mottaleb et al., 2012; Zhang and Monteiro-Riviere, 2008).

1.4. Nanoparticles to enhance drug penetration into the skin

Nanoparticles can be designed to interact differently with the skin, giving the opportunity of highly interesting clinical applications. Additionally, nanoparticles can facilitate distinct transport mechanisms that do not apply for dissolved bioactive molecules. Physicochemical properties of nanoparticles like size, shape, deformability, charge and polarity have significant effects on the ability to interact with the skin and to enter the skin. Smaller nanoparticles are more likely to penetrate into the skin

compared to bigger nanoparticles (Liang et al., 2013). Spherical nanoparticles penetrate into the skin more rapidly than ellipsoid shaped nanoparticles (Ryman-Rasmussen et al., 2006). Deformable nanoparticles penetrate better into the skin compared to rigid nanoparticles, because they are potentially squeezed between the corneocytes into deeper skin layers (Jose Morilla and Lilia Romero, 2016). The negative skin charge under normal physiological conditions (Marro et al., 2001; Rojanasakul and Robinson, 1989) makes positively charged nanoparticles preferable for penetration due to electrostatic interaction. Negatively charged nanoparticles lack electrostatic interaction what impairs access to the outermost skin layer (Contri et al., 2016; Wu et al., 2010).

Another interesting advantage of nanoparticles is that they can control the drug release in contrast to the pure drug. Delayed drug release from nanoparticles allows better localization of the drug in the epidermis with low skin permeation tendency compared to conventional creams, what may significantly reduce local and systemic side effects associated with corticosteroid therapy and could improve treatment effectiveness and patient compliance (Abdel-Mottaleb et al., 2012; Abdel-Mottaleb et al., 2011). Recently, stimuli-responsive nanoparticles for dermal application such as pH- and temperature-sensitive nanoparticles have received attention. pH-responsive nanoparticles can use pH-gradients on the skin between diseased and healthy skin to target the drug to higher pH disease sites and spare healthy skin areas by selection of nanoparticles with the desired pH threshold releasing at the pH of diseased skin but not healthy skin. Besides, the easy access to the skin surface gives the opportunity to use external triggers like UV light and heat to target diseased and spare healthy skin areas.

1.5. Nanoparticles for follicular targeting

The significance of the transfollicular route was long time doubtful, because hair follicles are only covering 0.1% of the skin surface and due to the sweat and sebum outward excretion (Lademann et al., 2001; Scheuplein, 1967). However the complex vascularization and deep invagination with a thinning stratum corneum of the pilosebaceous unit has led to a reappraisal of this view (Lu et al., 2014). Nowadays different studies are indicating that the transfollicular route has a significant effect on the drug penetration (Otberg et al., 2007). Solid particles like polymer nanoparticles,

lipid nanoparticles and liposomes are known to penetrate into open hair follicles (Lademann et al., 2007) and a particle size of 300 – 600 nm is optimal for the follicular penetration, because this particle size correspond to the thickness of the overlapping cuticula hair surface (Lademann et al., 2009; Patzelt et al., 2011). In contrast 3 -10 µm microparticles enter only into the orifice or block the hair follicle (Teichmann et al., 2006). Massaging also increases the penetration depth of nanoparticles, because the movement of the hair acts as a gearing pump that pushes the particles inside the hair follicle (Patzelt et al., 2011). In a mathematical simulation model it was demonstrated that the sawtooth-like profile of the hair surface together with a well-defined corrugation amplitude explain the enhanced particle transport into the hair follicle introduced by hair motion (Radtke et al., 2017). Hair follicles are an optimal target for drug delivery, because they represent an efficient reservoir for nanoparticles and nanoparticle based drug delivery as nanoparticles stay inside the hair follicle for several days (Lademann et al., 2006). However a barrier comparable to the stratum corneum in the upper hair follicle part and tight junctions in the lower part of the hair follicle prevent nanoparticle penetration into living tissue (Brandner et al., 2003; Nohynek et al., 2007). Furthermore, with time nanoparticles are eliminated from inside of the hair follicle to the skin surface by the outward sebum flow (Lademann et al., 2006). Targeting of the hair follicles with drug-loaded nanoparticles can be exploit for controlled drug delivery to maintain constant drug level within the tissue over several days for localized therapeutic action to reduce application frequency to increase patient compliance. Besides stimuli-responsive nanoparticles can be used to release the incorporated drug into adjacent target structures, like sebaceous glans, viable skin or vasculature (Lademann et al., 2016; Patzelt et al., 2017). Additionally dendritic cells and other cells, that are involved in inflammatory processes in the skin, can be targeted through the follicular route (Lademann et al., 2005; Vogt et al., 2005). Possible internal and external triggers in the hair follicle for stimuli responsive nanoparticles are pH, temperature, radiation and sebum. The temperature on the skin surface is around 32 °C (Burton, 1935). Inside the hair follicle the temperature increases and is expected to reach the body temperature of 37 °C deep in the follicles. External radiation like IRA radiation can also be used for photo activated drug release as nanoparticles inside the hair follicle can still be reached by the radiation (Lademann et al., 2016). Additionally the composition of sebum represents a promising drug release trigger as sebum is mainly located inside the hair follicle and just small amounts are on the skin surface.

In conclusion nanoparticles can improve and control the drug penetration into the skin and effectively target hair follicles. As a result nanoparticles represent a promising option to improve topical therapy significantly, and at the same time reduce systemic side effects for skin and hair follicle associated diseases.

1.6. Drug delivery systems for dermal application

1.6.1. Nanocrystals

The majority of the new developed drug molecules are poorly soluble and therefore often have a low bioavailability (Stegemann et al., 2007). Bioavailability problems are not only relevant orally, but also for the topical application to the skin. Low bioavailability is expected for drugs with a low saturation solubility and a low dissolution rate. Low dissolved drug amounts lead to a too low concentration gradient between formulation and skin and therefore allow drug diffusion into the skin (Müller et al., 2011). A particle size reduction in general increase the kinetic saturation solubility and the dissolution rate (Buckton and Beezer, 1992). As a result nanocrystals were investigated to improve the bioavailability of poorly soluble drug molecules and since 2000 there are some drug products on the market with nanocrystals for oral application. Nanocrystals consist to 100% of the active ingredient consequently the drug loading is practically 100%. In aqueous dispersions nanocrystals are generally stabilized by surfactants or a stabilizer layer (Rabinow, 2004). The dermal drug delivery of nanocrystals to improve skin penetration was not intensively investigated in the past. Nevertheless it was demonstrated that nanocrystals increase the drug penetration into the skin compared to coarse suspension and commercial formulations and additionally penetrate into the hair follicle (Corrias et al., 2017; Pireddu et al., 2016).

1.6.2. Liposomes, ethosomes and transfersomes

Liposomes, ethosomes and transfersomes are in general lipidic vesicles in the nanometer range that enhance the skin permeation of entrapped molecules (Cevc and Blume, 2001). These lipidic vesicles can be loaded with hydrophilic and hydrophobic drugs. Hydrophilic drugs are within the inner aqueous phase whereas hydrophobic drugs partition into the lipid bilayer (Eloy et al., 2014). Challenges of lipophilic vesicles

are the poor colloidal stability. These particles tend to coalescence and fuse when submitted to dry environments, such as the skin surface (Schaller and Korting, 1996). Nevertheless there are some differences in their composition leading to differences in their physicochemical properties.

Liposomes are vesicles of one or multiple lipid bilayers with an aqueous core. Generally liposomes are mixtures of phospholipids, or phospholipids and cholesterol and can be positively or negatively charged. Cholesterol leads to stiffer lipid bilayers and by increasing the cholesterol amount in liposomal compositions the deformability of liposomes decreases (Taylor et al., 1990).

Ethosomes are lipidic vesicles with a fluid lipid bilayer and an increased elasticity due to the addition of 20 – 45% ethanol (Jain et al., 2007). Ethanol interacts with the lipid polar heads and increases the fluidity of the liquid crystalline state of the phospholipids (Kurihara-Bergstrom et al., 1990). Besides, ethanol is a penetration enhancer to increase the skin penetration of the entrapped drug. Ethosomes are negatively charged due to the high ethanol amount (Touitou et al., 2000). The permeation of ethosomes is more effective than ethanol, aqueous ethanol or ethanolic phospholipid solution suggesting a synergetic effect between ethanol, vesicles and skin lipids (Touitou et al., 2000).

Transfersomes are ultra deformable vesicles composed of phospholipids with surfactants, which act as edge activators to increase the elasticity and deformability of the lipid bilayer. The edge activators are generally single chain surfactants of high radius of curvature and mobility, like sodium cholate, sodium deoxycholate, Span 80, Tween 20 and Tween 80 (Jain et al., 2003). These particles are generally negatively charged.

The different lipidic vesicular systems were studied with a broad range of different drugs to increase the drug penetration into the skin (Baroli, 2010). However, the clear mechanism how the lipidic vesicular systems increase the skin penetration of drugs is still unknown and there are different hypothesis.

Lipidic vesicles are potentially squeezed through the corneocytes or interact with the thin sebum-sweat layer what could increase the particle adhesion to the stratum corneum. Furthermore lipidic vesicles may fuse on the skin surface and form an

occlusive lipidic layer or rupture followed by the penetration of particle contents, which disorganizes the stratum corneum lipid matrix. The ingredients of the lipidic vesicles like lipidic esters, ethanol and surfactants are known penetration enhancers (Elsayed et al., 2007). Additionally it was demonstrated that lipidic vesicles penetrate into hair follicles and release the entrapped drug inside the hair follicles (Subongkot et al., 2013).

1.6.3. Lipid nanoparticles

Lipid nanoparticles were developed to combine the advantages of nanoemulsions, liposomes and polymeric nanoparticles (Müller et al., 2002). Lipid nanoparticles are composed of solid lipids, which can be mixed with liquid lipids and are normally stabilized by surfactants. Lipid nanoparticles have generally an average particle size of 50 – 1000 nm, can be positively or negatively charged and are rigid due to their solid matrix. The lipids are generally well tolerated like in the case of nanoemulsions and liposomes (Mehnert and Mäder, 2001). Typically lipid nanoparticles are loaded with poorly water soluble substances and the loading capacity depends on the solubility of the substance in the lipids. The loading capacity reaches from below 1 % up to 50 % of very lipophilic substances like ubidecarenone (Jenning and Gohla, 2001; Westesen et al., 1997). The incorporated drugs are protected against degradation and the release of the active ingredient can be controlled due to the solid state of the particle matrix like in the case of polymeric nanoparticles (Zoubari et al., 2017). These particles are mainly intended for dermatological or cosmetic use. After application to the skin lipid nanoparticles adhere onto the skin and form an occlusive layer due to the large specific surface area of lipid nanoparticles (Dingler et al., 1999). The drug release of lipid nanoparticles and the drug partition into skin lipids can be controlled by the lipophilicity of the lipid matrix of the lipid nanoparticles (Küchler et al., 2010). However only a few intact lipid nanoparticles can be found in the first stratum corneum layers, because after topical application lipid nanoparticles are mixed with skin lipids and lose their morphology probably due to melting (Küchler et al., 2009b). Therefore the occlusive layer leading to an increased skin hydration is expected to be the primary reason for the enhanced drug penetration into the skin by lipid nanoparticles (Müller et al., 2002).

Additionally lipid nanoparticles frequently consist of lipids, which are also present in sebum. Sebum is the predominant environment in hair follicles. Therefore the hair follicles represent a potential penetration route for lipid nanoparticles and it was demonstrated that lipid nanoparticles based on lipids of sebum penetrate into the hair follicles and release the drug into sebum (Lauterbach and Müller-Goymann, 2014).

1.6.4. Polymeric nanoparticles

Polymeric nanoparticles were developed to control the release of the entrapped/encapsulated drug. Polymeric nanoparticles can be positively or negatively charged and the main polymeric nanoparticles investigated for dermal drug delivery can be classified in three groups i) large molecules with dendritic structures, ii) hydrophilic nanogels, i.e. polymer networks and iii) polymeric nanoparticles prepared by hydrophobic polymers, which form stable particulate carriers in an aqueous environment.

Large molecules with dendritic structures are synthesized macromolecules, which exhibit a distinct molecular structure like dendrimers or dendritic (hyperbranched) architectures (Figure 5).

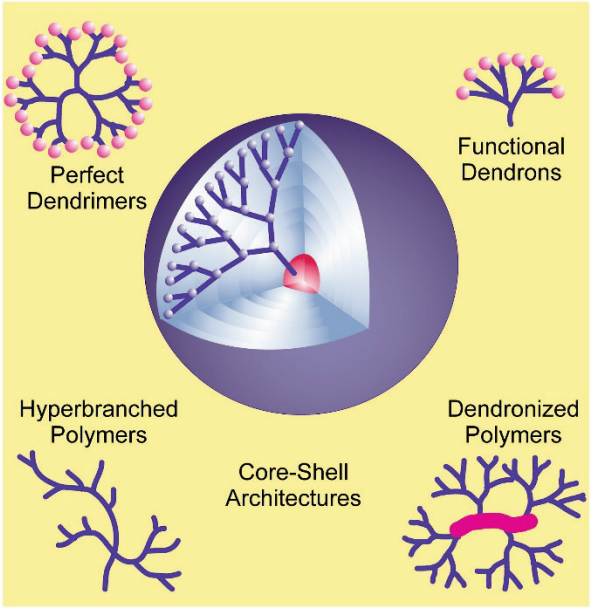

Figure 5: Overview of dendritic architectures and their nomenclature (Reprinted from (Haag and Vogtle, 2004) Copyright (2004), with permission from John Wiley and Sons).

The particle size of these dendritic structures can be optimized by the synthesis conditions and the selection of appropriate end groups for the synthesized macromolecules leading to stable nanoparticles without the need of surfactants. The structure-property-relationship was investigated with polyamidoamine dendrimers with varying functional surface groups (—NH_2, —COOH, and —OH) and particle sizes between 10 and 18 nm. Polyamidoamine dendrimers penetrate the skin through intercellular lipids and hair follicles. Positively charged polyamidoamine dendrimers enhance the skin penetration more in comparison to negatively or neutral charged polyamidoamine dendrimers due to their higher affinity to the negatively charged skin. Furthermore the skin penetration is inversely correlated to the molecular weight of the nanoparticles and nanoparticle penetration could be detected up to the viable epidermis (Venuganti and Perumal, 2009; Venuganti et al., 2011). Nevertheless the toxicity of polyamidoamine dendrimers remains an issue and the preparation of less toxic degradable nanoparticles is under investigation (Uram et al., 2013).

Hyperbranched nanoparticles like core multishell nanocarriers are composed of a hydrophobic and hydrophilic compartment and have a range in size from 20 - 30 nm. Core multishell nanocarriers consist of a dendritic polyglycerol core surrounded by an internal C18 alkyl shell and an outermost methoxy polyethylene glycol shell. Due to their structure, which is comparable to liposomes these nanoparticles can load hydrophobic and hydrophilic drugs and increase their delivery to viable skin layers (Küchler et al., 2009a; Küchler et al., 2009b). However, the drug loading is limited by the compartment volume available (Jansen et al., 1994). Additionally core multishell nanocarriers do not penetrate deep into the hair follicles due to their small size (Lohan et al., 2016).

Hydrophilic nanogels are based on a hydrophilic polymer network with a defined dimension, which swells in aqueous environment e.g. N- isopropyl acrylamide and dendritic polyglycerols. Hydrophilic nanogels can load proteins like bovine albumin, L-asparaginase II, or transglutaminase-1 with a loading capacity of up to 70 wt. %. N-isopropyl acrylamide dendritic polyglycerols are thermoresponsive. Therefore, nanogels were prepared, which collapse above 35 °C and release the loaded protein. These temperatures are typically reached within the deeper layers of the stratum corneum. Skin penetration experiments demonstrated efficient intraepidermal protein

delivery. However penetration of the nanogels themselves was not detected (Witting et al., 2015).

Furthermore thermoresponsive nanogels were investigated for follicular drug targeting with triggered drug release. Therefore thermoresponsive nanogels with a particle size of 300 – 500 nm and different cloud points between 32 – 37 °C were prepared. These nanogels effectively penetrated and released the drug above their cloud points into hair follicles (Sahle et al., 2017).

Polymeric nanoparticles prepared out of hydrophobic polymers are mainly used to encapsulate small hydrophobic molecules due to their probable affinity of matrix material and payload. The particle preparation and loading often occurs in one step by different physical methods like emulsion, nanoprecipitation or solvent displacement methods. Therefore these nanoparticles generally exhibit reasonable encapsulation efficiencies and drug loadings, because of the co localization of the polymer and the drug during preparation. Different polymers with different solubility, polarity, biocompatibility, biodegradability, swelling and charge can be used for the preparation of these polymeric nanoparticles. Eudragit®, cellulose, polylactic acid (PLA) and poly (lacitic-co-glycolic acid) (PLGA) derivates are among the most commonly used polymers for the preparation of nanoparticles.

Eudragits are copolymers of methacrylic acid and methacrylic/ acrylic esters or their derivatives, which include neutral, cationic and anionic polymers (Figure 6).

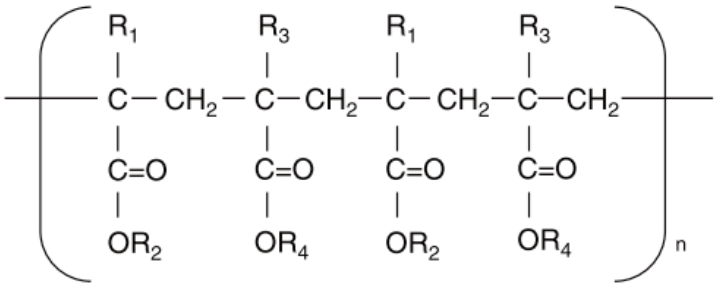

Eudragit Grade	R_1	R_2	R_3	R_4
E	CH_3	$CH_2CH_2N(CH_3)_2$	CH_3	CH_3, C_4H_9
L and S	CH_3	H	CH_3	CH_3
RL and RS	H, CH_3	CH_3, C_2H_5	CH_3	$CH_2CH_2N(CH_3)_3^+Cl^-$
NE 30D	H, CH_3	CH_3, C_2H_5	H, CH_3	CH_3, C_2H_5
L 30 D-55 and L 100-55	H, CH_3	H	H CH_3	CH_3, C_2H_5

Figure 6: Chemical structure of different Eudragit® derivates (Reprinted from (Thakral et al., 2013) Copyright (2013), with permission from Taylor & Francis).

These polymers are prepared by free-radical polymerization. The polymer chain length can be varied via various termination and transfer reactions. The polymerization can be done in solvent, emulsion, suspension, or even in bulk. The functional properties of Eudragit derivatives can be controlled by selecting from a variety of monomers. The non-functional co-monomers steer the polymer properties and the functional co-monomer adjust the solution profile of the polymer. Eudragits have various applications in drug delivery systems. The cationic Eudragit® E is soluble below a pH of 5.5 and can be used for taste masking. Eudragit® L-55, L and S are anionic and soluble above pH 5.5, 6 and 7, respectively. These polymers are used as enteric coatings or for colon targeting. Eudragit® RL, RS, NE and NM are insoluble polymers and are used in sustained drug delivery systems. These polymers differ in their permeability properties due to different swelling behavior. Eudragit® RS is a positively charged, water-insoluble copolymer of ethyl acrylate, methyl methacrylate and a low amount of methacrylic acid ester with quaternary ammonium groups. It is commonly used in controlled drug delivery systems (Thakral et al., 2013). In dermal drug delivery, Eudragit® RS nanoparticle-based heparin gels controlled the drug release into the stratum corneum in comparison to a heparin solution (Loira-Pastoriza et al., 2012). Capsaicinoids-loaded Eudragit® RS nanoparticles embedded into chitosan gels increased skin

adhesion and drug penetration in contrast to a capsaicinoids chitosan gel (Contri et al., 2014).

Cellulose-based polymers are also commonly used to prepare enteric coated, colon specific, controlled release and taste masked drug delivery systems. These polymers have a polymeric cellulose backbone which contains a basic repeating structure of β-anhydroglucose units; each unit having three replaceable hydroxyl groups. The hydroxyl groups can be substituted with ether and ester groups to adjust the physicochemical properties of the resulting cellulose derivate (Figure 7).

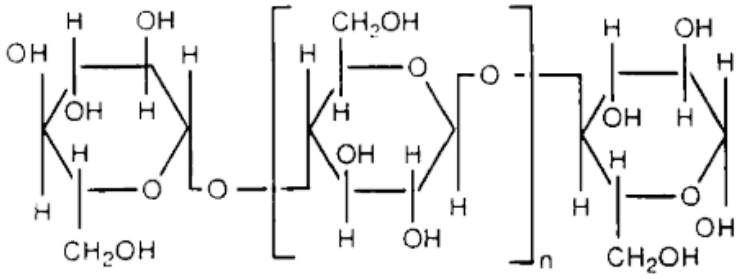

Cellulose n - 1000 approx

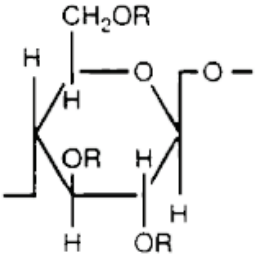

Polymer	Substituent Groups |R|	
Methylcellulose	- H	- CH_3
Hydroxypropyl methylcellulose	- H	- CH_3 - CH_2 - CH - CH_3 (OH)
Hydroxypropylcellulose	- H	- CH_2 - CH - CH_3 (OH)
Ethylcellulose	- H	- CH_2CH_3

Figure 7: The molecular structure of cellulose and cellulose derivatives (Reprinted from (Rekhi and Jambhekar, 1995) Copyright (1995), with permission from Taylor & Francis).

Cellulose ether derivatives are synthesized by mixing cellulose with sodium hydroxide. The resulting alkali cellulose can be etherified with alkyl halogens. Partially etherified cellulose derivatives like methyl cellulose, hydroxyl ethyl cellulose or hydroxyl propyl

cellulose are water soluble polymers and often used as gelling agents. High etherified cellulose derivatives like ethyl cellulose are water insoluble and can be used for controlled drug delivery systems. There are different viscosity grades of cellulose based polymers available. The viscosity of cellulose based polymer solutions increases with increasing length of the polymer molecule (Rekhi and Jambhekar, 1995). In dermal drug delivery, quercitin-loaded ethyl cellulose nanoparticles controlled the drug release with increased quercitin skin retention (Sahu et al., 2013). Furthermore it is reported that ethyl cellulose nanoparticles selectively accumulate in inflamed skin, hair follicles and sebaceous glands (Abdel-Mottaleb et al., 2012).

PLA and PLGA are biocompatible, biodegradable and safely administrable polymers approved by the Food and Drug Administration and European Medicines Agency. Therefore these polymers have widely been used in different drug delivery systems as implants, microparticles and nanoparticles. PLA is a synthetic polymer composed of lactic acid monomers, whereas PLGA is a synthetic copolymer composed of lactic acid and glycolic acid monomers (Figure 8).

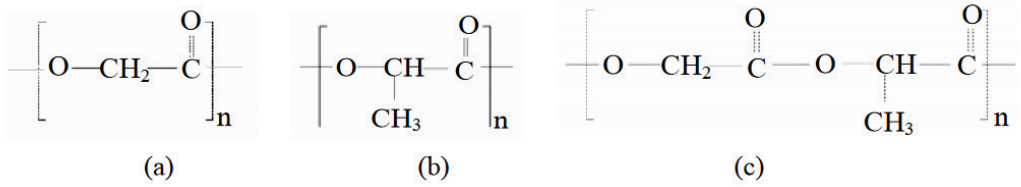

Figure 8: Polymers with hydrolysable chains: (a) Poly(glycolic acid); (b) Poly(lactic acid) and (c) Poly (D,L-lactide-coglycolide) copolymer (Reprinted from (Erbetta et al., 2012) Copyright (2012), with permission from Scientific Research Publishing).

The polymer can be synthesized by various methods among - ring opening polymerization and polycondensation reactions are the major ones (Erbetta et al., 2012). PLGA is biodegradable by hydrolysis leading to the metabolite monomers, lactic acid and glycolic acid. These monomers are eliminated from the body by the citric acid cycle (Anderson and Shive, 2012). PLGA and PLA are commercially available in different molecular weights and copolymer compositions. The degradation time of these polymers varies from several months to several years, depending on the molecular weight and copolymer ratio. The degradation rate of the polymer is effected by parameters such as molecular weight, the hydrophobicity (lactic acid > glycolic acid monomers), the degree of crystallinity (e.g., increased in L-PLA) and the glass

transition temperature of the amorphous phase (Vert et al., 1994; Visscher et al., 1985, 1986). The forms of PLGA are usually identified by the monomers ratio used. For example, PLGA 50:50 identifies a copolymer whose composition is 50% lactic acid and 50% glycolic acid. In dermal drug delivery systems PLA and PLGA nanoparticles control the drug penetration and accumulation into the skin in comparison to the free drug (Luengo et al., 2006). Furthermore PLA and PLGA nanoparticles preferential accumulate in hair follicles due to their lipophilicity and reduced the transepidermal pathway by controlling the drug release (Rancan et al., 2009; Rancan et al., 2012). Nevertheless the PLGA degradation products lactic and/or glycolic acid cause a lowering of the local pH value and pH-values lower than 3 have been observed upon degradation, which is lower than the acidic milieu of the skin. Therefore the PLGA degradation could potentially have a negative effect on the pH homeostasis and the barrier function of the skin (Liu et al., 2006).

Polymeric nanoparticles are prepared mainly by two different techniques: polymerization of monomers or dispersion of preformed polymers. Dispersion of preformed polymer is commonly realized by different methods including solvent evaporation, nanoprecipitation/solvent displacement, emulsification/solvent diffusion, salting out, dialysis or using supercritical fluid technology (Rao and Geckeler, 2011; Vauthier and Bouchemal, 2009). To choose an appropriate method, the solubility of the polymer and the drug in various solvents, safety and costs are considered (Rao and Geckeler, 2011; Yoo et al., 2011). The two most commonly used methods for the preparation of polymeric nanoparticles are nanoprecipitation/solvent displacement and solvent evaporation due to their simplicity.

Nanoprecipitation is a simple, fast, reproducible and economic method, which unlike many other techniques, needs only a one step preparation. It does not require the formation of emulsions, but involves interfacial deposition of a polymer after displacement of a semi-polar solvent, miscible with water, from a polymer solution. Rapid diffusion of the solvent into the non-solvent phase leads to a reduction in interfacial tension between the two phases, what increases the surface area and result in the formation of small droplets of polymeric solution. At the end of the preparation the remaining solvent is either evaporated by continuous magnetic stirring or under reduced pressure (Rao and Geckeler, 2011; Vauthier and Bouchemal, 2009; Yoo et al., 2011).

The solvent evaporation method is a simple and the most widely used technique to prepare polymeric nanoparticles (Rao and Geckeler, 2011). By this method, the polymer is dissolved in a solvent, which subsequently, is emulsified via high shear force or sonication into a phase, which is not miscible with the solvent to form an emulsion. Afterwards the solvent is evaporated, either by continuous magnetic stirring or under reduced pressure.

1.7. Effect of the vehicle on nanoparticles and drug penetration

Nanoparticles can be formulated in different vehicles like aqueous or organic solvent-based dispersions, gel or cream. The different vehicle properties like vehicle viscosity and lipophilicity can have an effect on the nanoparticles and drug penetration. The diffusion coefficient of molecules inside the vehicle decrease with increasing viscosities. As a result viscous vehicles reduce drug skin partitioning and adsorption. The lipophilicity of the vehicle effects the drug partitioning into the stratum corneum and potentially influences the drug release behavior of the nanoparticle (Wenkers and Lippold, 1999). An occlusive effect of the vehicle may moderately increase the drug penetration due to a higher skin hydration (Zhai and Maibach, 2001). Other ingredients like solvents, surfactants and penetration enhancers may potentially alter or damage the stratum corneum and increase the penetration of some ingredients (Benson, 2005).

After application of a nanoparticle formulation to the skin the formulation will change. Water and volatile ingredients will evaporate and non volatile ingredients are adsorbed to different extent. Furthermore, skin sweat and/or sebum components will interact with the applied formulation (Baroli, 2010). These effects could lead to destabilization/ agglomeration of the nanoparticles and the formation of supersaturated drug solutions with a potential drug recrystallization as larger microcrystals. In summary the formulation of nanoparticles with different physicochemical properties in different vehicles are critical parameters to achieve the desired drug release, drug penetration and nanoparticle stability.

1.8. Characterization of nanoparticles

Nanoparticle characterization include the determination of the particle size, particle morphology, zeta potential, drug loading, encapsulation efficiency and yield. Furthermore critical properties of nanoparticles are the drug release and their toxic potential as this are important factors to evaluate the therapeutical benefit.

1.8.1. *In vitro* drug release methods

In vitro drug release measurement is one of the most important methods used to assess the quality of a nanoparticle and to estimate its *in vivo* performance. *In vitro* and or *in vivo* release kinetics provide critical information about their behavior and are key parameter used to assess drug product safety and efficiency (D'Souza, 2014; Kroll et al., 2009).

During the various stages of drug product development especially at the initial phase, *in vitro* release testing is an important analytical tool that enables a rational and scientific approach to drug product development (Moreno-Bautista and Tam, 2011). It can also reveal fundamental information on the dosage form and its behavior. Additionally *in vitro* drug release tests provide detailed information on drug release mechanisms and their kinetics and allows the establishment of an *in vivo/in vitro* correlation (D'Souza, 2014). Furthermore *in vitro* drug release tests are used as a compendial requirement, routine assessment of quality control to support batch release and to ensure batch to batch consistency under the SUPAC guidelines.

To date, there is no compendial method or regulatory standard available to evaluate drug release from various pharmaceutical nanoparticles. Hence, several *in vitro* release methods, both compendial and non-compendial, have been utilized and reported. These methods can be broadly categorized in sample and separate, dialysis membrane, and *in situ* methods. The existing United States Pharmacopeia (USP) apparatus are primarily designed for *in vitro* drug release assessment of oral and transdermal products. Therefore there are many challenges when using compendial USP apparatus to investigate the release of nanoparticles. Certainly, the area of *in vitro* testing for nanoparticles lags behind the advances realized in drug product development.

In sample separation methods the nanoparticles are directly placed into the release media. The main release set-ups used are USP apparatus II (paddle) with volumes between 600 - 900 ml and vials with smaller volumes between 1 - 15 ml release media (Cetin et al., 2010; Sanna et al., 2012; Zhang et al., 2014). After certain time release media is withdrawn and needs to be physically separated from the nanoparticles to examine the released drug amount of the nanoparticles. In several investigations syringe filters are used to achieve physical separation between the release media and nanoparticles (Zhang et al., 2014). Besides, high energy separation techniques like centrifugation, ultracentrifugation, and ultrafiltration are used (Wallace et al., 2012). However, complete separation of the released drug from the nanoparticles is a concern, because it is challenging to separate particles that are less than a hundred nanometers in size and potentially shrink during the dissolution process like in the case of nanocrystals (Anhalt et al., 2012; Wallace et al., 2012). During filtration smaller nanoparticles may pass the filter so that a higher drug release is examined as in reality. Furthermore nanoparticles can clog the filter causing insufficient sample amounts for quantification (Kim et al., 1997). The disadvantage of centrifugation of nanoparticles is that it is time consuming and during centrifugation drug can be still released from the nanoparticles.

The dialysis methods, which involve dialysis bags/tubes or a dialyzing membrane mounted in a Franz diffusion cell, are the most popular and common techniques to examine the drug release of nanoparticles (Ammoury et al., 1990; Heng et al., 2008; Montenegro et al., 2014; Moreno-Bautista and Tam, 2011; Souto et al., 2004; Venkateswarlu and Manjunath, 2004). In the regular dialysis bag method the investigated nanosuspension is placed into a dialysis bag that is subsequently sealed and placed in a larger vessel containing release media. The release media in the vessel is agitated to minimize unstirred water layer effects. The volume inside the dialysis bag is generally smaller than the outer release media. The released drug of the nanoparticles inside the dialysis bag diffuse through the membrane in the outer release media compartment from where samples are taken for analysis (Figure 9a) (Ammoury et al., 1990; Moreno-Bautista and Tam, 2011). In contrast, in the reverse dialysis set-up, the release media is placed into the dialysis bag and afterwards the bag is subsequently sealed and placed in a larger vessel containing the nanosuspension. In this case the nanosuspension is agitated to minimize the unstirred

water layer and samples are taken from the inner compartment is sampled to determine the released drug amount (Figure 9b) (Xu et al., 2012).

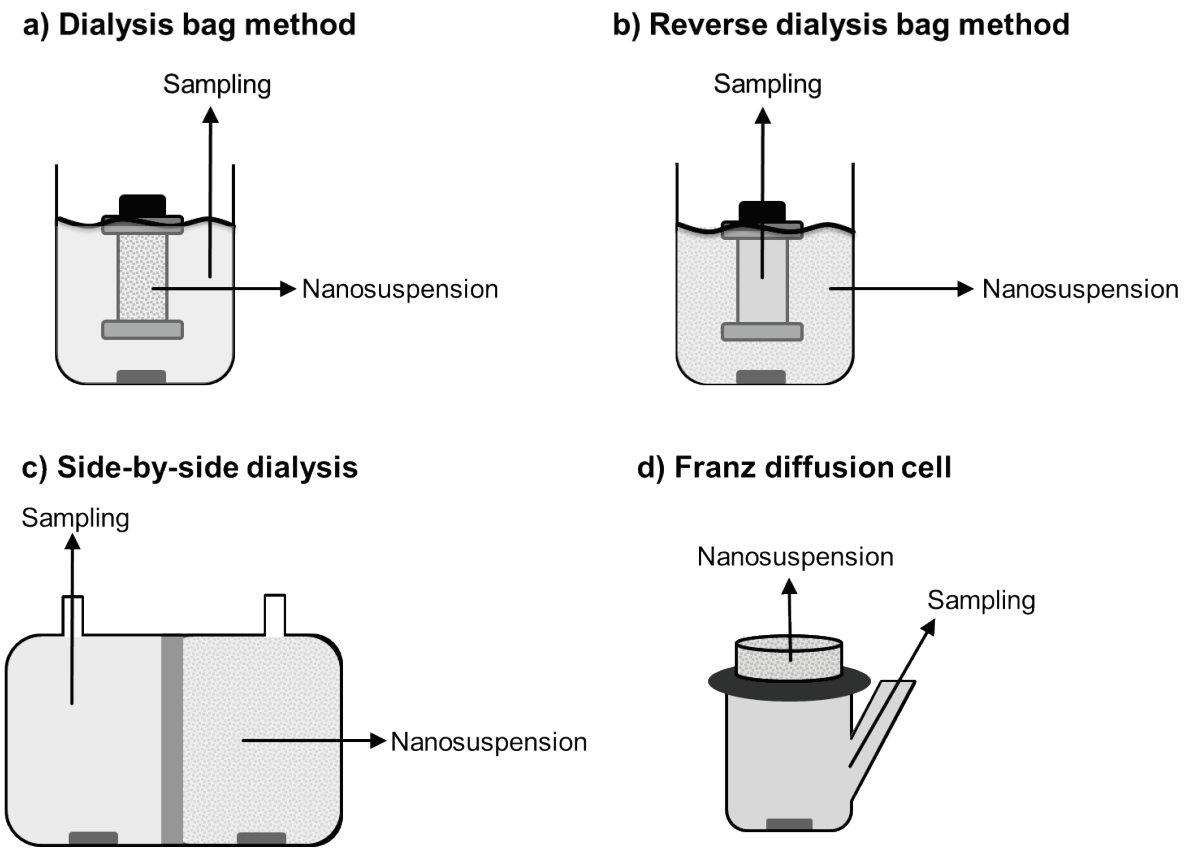

Figure 9: a) Dialysis bag method: The nanosuspension is placed into the dialysis bag and the dialysis bag is placed into the agitated release media. The sampling occurs from the outer release media. b) Reverse dialysis bag method: The release media is placed into the dialysis bag and the dialysis bag is placed into the agitated nanosuspension. The sampling occurs from the release media in the dialysis bag. c) Side-by-side dialysis: The nanosuspension and the release media are vertically separated by a dialysis membrane. The sampling occurs through a sampling port on top of the release media compartment. d) Franz diffusion cell: The nanosuspension is placed on top of the Franz diffusion cell in the donor compartment. The release media is horizontally separated by a membrane. The sampling occurs through a sampling port from the release media compartment.

In the side-by-side dialysis, the donor and receiver cell are vertically separated by a dialysis membrane and generally contain equal volumes of media. The sampling occurs from the receiver cell. The advantage is that both compartments can be stirred with a magnetic stirrer (Figure 9c) (Chidambaram and Burgess, 1999). In the Franz diffusion cell the sample is placed on top of the cell into the donor compartment, which is horizontally separated by a dialysis membrane or excised skin to the acceptor compartment. The acceptor compartment is constantly stirred with a magnetic stirrer

and the sampling occurs through a sampling port from the acceptor compartment (Figure 9d) (Souto et al., 2004). In contrast to the other dialysis methods the Franz diffusion cell can be used with excised skin instead of a dialysis membrane. Therefore, drug penetration and permeation into and through the skin can be examined *ex vivo* with Franz diffusion cell. Furthermore, Franz diffusion cell unlike the dialysis tubes and the side-by-side dialysis can be easily used with semisolid dosage forms of nanoparticles.

The disadvantage of the dialysis methods is that basically a dialysis membrane retains the nanoparticles and allows the transfer of the released drug into a receiver compartment (Venkateswarlu and Manjunath, 2004). So that, due to two diffusional barriers, the measured drug release kinetics will be artificially decreased, and depending on the drug/carrier systems, significant errors may be introduced by the membrane (Moreno-Bautista and Tam, 2011; Washington, 1989; Zambito et al., 2012). Particularly when the actual rate of drug release from the drug carriers is faster than the rate of diffusion out of the dialysis membrane, the experimental data do not fully reflect the actual release profile of the drug. It is also not possible to capture a potential initial burst release from the colloidal drug carriers. Therefore, a dialysis membrane with a low diffusional barrier and a low affinity for the drug should be used. Nevertheless, this method can still be used as a general guide in drug delivery research, because differences in equilibration time can be used as discriminatory tool to study the release behavior between fast and slow releasing dosage forms (Kim et al., 1997). Precise release kinetics assessment may also be attained by using mathematical models to compensate for the delay in drug diffusion due to the dialysis bags (Moreno-Bautista and Tam, 2011).

In situ drug release measurements lack the problems associated with sample separation or diffusion barriers. Accordingly, a number of novel *in situ* release methods based on different working principles, such as differential pulse polarography (Rosenblatt et al., 2007), voltametry and turbidimetry (D'Souza, 2014; Moreno-Bautista and Tam, 2011) and light scattering (Anhalt et al., 2012) were reported. Electrochemical methods can be used for rapid *in situ* measurements of released drug while avoiding the interference caused by the presence of undissolved dosage form in the release media (Tan et al., 2007). However, most of the electrochemical methods

are limited to a certain group of compounds, for example ionizable drugs, or require instruments that are more sophisticated.

Non-electrochemical methods like calorimetry, turbidimetry, and laser diffraction have also been evaluated as *in situ* release methods. The principle of the calorimetric measurement is based on detection of the net proportion of heat change during *in vitro* release. Concerns with calorimetric measurements are long equilibration times and that the heat produced by all the processes needs to be considered (Kayaert et al., 2010). Turbidimetric and laser diffraction approaches are based on the change in light scattering properties of nanoparticles dispersed in release media. Dissolution kinetics of nanocrystals of different sizes ranging from 120 - 270 nm could be examined and distinguished by the light scattering method (Anhalt et al., 2012; Crisp et al., 2007). Challenges of these methods are the long equilibration times, limited range of particle size, and initial concentration of samples that can be used.

Another alternative method is the *in situ* drug release measurement with a Sirius® inForm apparatus. This apparatus can measure the UV absorbance of the released drug without separating it from the nanoparticles (Colombo et al., 2017). Since nanoparticles cause a significant light scattering, which alter the UV spectra (Van Eerdenbrugh et al., 2011), the instrument makes adjustments for the amount of UV light lost using the concepts of Tyndall-Rayleigh scattering theory. However, this feature makes the method susceptible for errors, especially when used with highly turbid samples.

In summary, different techniques can be used to assess drug release from pharmaceutical nanoparticles, which may give different results as the methods are different in their working principles. Even with the same method different results might be obtained when working under sink and non-sink conditions (Mishra et al., 2009; Murdande et al., 2015). However in general non-sink conditions are reported to be more discriminative than sink conditions when investigating nanoparticles (Liu et al., 2013). The main problem is that the choice of a drug release method for analysis of nanoparticles in most cases is random without giving an account about their reproducibility and ability to discriminate release between different dosage forms. Furthermore, little information is available with regard to comparability of different *in vitro* release methods.

1.8.2. Determination of nanoparticle and drug penetration into the skin

The investigation of nanoparticle and drug penetration into the skin is essential for the development and optimization of new dermal pharmaceutical products. Different models have been established to investigate skin penetration of drugs and nanoparticles. Normally the *ex vivo* drug penetration is investigated with excised human skin from surgeries. The excised skin is placed onto Franz diffusion cells between the donor and acceptor compartment instead of the membrane to investigate the drug penetration. The drug amount which permeates through the skin reaches the acceptor compartment and can be quantified in the same. The drug amount which penetrates into the different skin layers can be quantified at the end of the experiment. The used excised human skin can be separated by heat into epidermis and dermis, which can be extracted afterwards to quantify the penetrated drug amount (Döge et al., 2016).

Another approach to quantify the drug amount in the different skin layers is the tape stripping method. Tape stripping is a simple method which is used for penetration studies for decades (Lademann et al., 2012). In this method adhesive films are successively applied to and removed from the skin after topical application of the investigated formulation. Each tape removes corneocytes layer by layer and subsequently the penetrated drug or nanoparticle amount in the respective layer. Afterwards the amount of removed corneocytes (stratum corneum) can be quantified by weighing (Weigmann et al., 1999). As a result every used tape strip contains two types of information: the amount of stratum corneum and the concentration of the topically applied substance in the respective layer. The drug concentration can be quantified for example after extracting the tape with solvents by UV or HPLC. Additionally the penetration depth of nanoparticles can be determined semi quantitative by fluorescence microscopy for example in the case of fluorescence labeled nanoparticles. Those information are used to examine the penetration depth profile of nanoparticles and/or the drug. However tape stripping can only remove the dead cells of the stratum corneum. The information about the penetrated drug amount into the living tissue is not provided. Nevertheless tape stripping can be performed easily with human volunteers to examine the drug penetration *in vivo*.

To differentiate the penetrated drug amount in the stratum corneum and hair follicles differential tape stripping was developed (Teichmann et al., 2005). This method combines the tape stripping method with a cyanoacrylate biopsy. After removing the penetrated drug amount from the stratum corneum by tape stripping the remaining drug amount in the hair follicle is extracted by a cyanoacrylate biopsy, which takes up the hair follicle contents.

However excised human skin has the disadvantage that follicular penetration cannot be investigated, because it contracts after surgical removal. The very dense network of elastic fibers around the hair follicle keeps the hair follicle closed even after stretching the excised skin. In contrast to excised human skin pig ear skin does not contract after removal due to the cartilage where it is fixed. Furthermore porcine ear skin has a hair density of 11 – 25 hairs/cm^2 with a diameter of 58 – 97 µm and an infundibular diameter of 200 µm while the infundibulum reaches a depth of 550 µm and sebaceous glands may be associated in a depth of about 500 µm which is comparable to human skin (Jacobi et al., 2007). Therefore pig ear skin represents a good model to investigate ex vivo nanoparticle and drug penetration into hair follicles.

1.8.3. Safety/Toxicity

The characterization of the toxicological potential of nanoparticles is an important property to assess the clinical potential of such innovative drug delivery systems. The broad variety of nanoparticles can mainly be classified according to their toxicological potential into less toxic nanoparticles and critical nanoparticles which might exhibit toxicity due to certain physicochemical properties. Soluble and or/ biodegradable nanoparticles disintegrate after application to skin into molecular species, like liposomes and PLGA nanoparticles and are supposed to be less toxic. In contrary insoluble and/or biopersistent nanoparticles, like quantum dots and fullerenes, can be taken up by and remain in the reticulo-endothelial system and cells especially after application repetition. Therefore those nanoparticles are supposed to exhibit a higher toxicity (Bowman et al., 2010).

Uptake of nanoparticles in keratinocytes of the stratum corneum occurs most likely through specialized processes like endocytosis on recognition by lipid rafts (Zhang and Monteiro-Riviere, 2009). In contrast lipid nanoparticles traverse the cell membrane,

distribute throughout the cytosol and localize in the perinuclear region without any toxic effects (Teskac and Kristl, 2010).

Besides this classification, nanoparticles can be characterized upon their cytotoxic and oxidative stress induction effect, which are two of the major concerns inducing toxic and genotoxic effects. The cytotoxic potential can be examined for example by the MTT assay. The MTT assay is a widely used method to determine the viability in metabolic active cells. It is based on the conversion of the yellow MTT to formazan blue by the mitochondrial reductase system of living cells. Dead cells can not reduce the yellow MTT and the color difference can be quantified to examine the amount of dead cells and the cytotoxic potential. The oxidative stress triggered by nanoparticles can be examined for example by measuring the intracellular reactive oxygen species (ROS) with the H2DCFDA assay. H2DCFDA is a chemically reduced, acetylated form of fluorescein used as an indicator for ROS in cells. This nonfluorescent molecule is deacetylated by intracellular esterases and can be oxidized to fluorescent dichlorofluorescein by radicals such as hydroxyl, peroxyl, alkoxyl, nitrate and carbonate to a fluorescent molecule and quantified by fluorescence measurements.

1.9. Research objectives

The purpose of this work was to prepare nanoparticles which potentially increase treatment effectiveness and minimize corticosteroid associated side effects to improve patient compliance by controlled drug release into the skin and hair follicles. Additionally different *in vitro* drug release methods for nanoparticles should be compared.

The specific goals were:

- To prepare dexamethasone-loaded polymeric nanoparticles which adhere well to the skin and release the drug slowly in a controlled manner.
- To prepare dexamethasone-loaded polymeric nanoparticles, which penetrate deep into the hair follicle and release the drug within the hair follicle triggered by their dissolution in sebum.
- To optimize the dexamethasone-loaded polymeric nanoparticles regarding their particle size, encapsulation efficiency, loading capacity and drug release.

- To assess and compare the reproducibility and discriminative power of three *in vitro* drug release methods under sink and non-sink conditions for nanoparticles, namely dialysis bags, Franz diffusion cells and an *in situ* drug release method using Sirius® inForm apparatus.

2. Materials and methods

2.1. Materials

2.1.1. Drug, drug formulation and dye

Dexamethasone (Fagron GmbH & Co. KG, Barsbuettel, Germany); DEXAMETHASON Creme LAW; 0.05% (Riemser Pharma GmbH, Greifswald, Germany); Nile red (Sigma-Aldrich GmbH, Schnelldorf, Germany)

2.1.2. Polymers

Ethyl cellulose (Ethocel® Standard 4 Premium, Colorcon Ltd., Dartford, UK); poly(methacrylic acid-co-methyl methacrylate, 1:1) (Eudragit® L 100), poly(methacrylic acid-co-methyl methacrylate, 1:2) (Eudragit® S 100), ammonio methacrylate copolymer type B (Eudragit® RS 100), PLGA 503 H, (Evonik Industries AG, Darmstadt, Germany); hydroxypropyl methyl cellulose phthalate 55 (HPMCP-55), (Shin-Etsu Chemical Co., Ltd., Tokyo, Japan); hydroxyethyl cellulose (HEC), (Natrosol® 250 HX, Ashland Industries Europe GmbH, Schaffhausen, Switzerland); PLA (PURASORB PDL 02, Corbion, Amsterdam, Netherlands); PLGA 503 (Resomer 503), PLGA 502 S (Resomer RG 502 S) (Boehringer Ingelheim Pharma GmbH & Co. KG; Ingelheim, Germany)

2.1.3. Lipids

Stearoyl macrogolglycerides (Gelucire® 50/13, Gattefossé GmbH, Bad Krozingen, Germany); solid triglycerides containing hydrogenated coco-glycerides, beeswax and ceteareth-25 as additive (Witepsol® S55, Cremer Oleo GmbH & Co. KG, Hamburg, Germany); cetyl palmitate, olive oil, palmitic acid, squalene (Carl Roth GmbH & Co. KG, Karlsruhe, Germany); liquid paraffin (Caesar & Loretz GmbH, Hilden, Germany); cotton seed oil, coconut oil (Sigma-Aldrich GmbH, Schnelldorf, Germany); cholesterol, oleic acid (Alfa Aesar GmbH & Co KG, Karlsruhe, Germany); paraffin (solidification point 57-60 °C) (Merck KGaA, Darmstadt, Germany)

2.1.4. Surfactants

Poloxamer 188 (Kolliphor® P188), poloxamer 407 (Kolliphor® P407) (BASF SE, Ludwigshafen, Germany); polyvinyl alcohol 4-88 (PVA) (Emprove®, Merck KGaA, Darmstadt, Germany); polyethylene glycol sorbitan monooleate (Tween® 80), sodium deoxycholate (Carl Roth GmbH & Co. KG, Karlsruhe, Germany); cetyl trimethylammonium bromide (CTAB) (Sigma-Aldrich GmbH, Schnelldorf, Germany)

2.1.5. Reagents and kits

Disodium hydrogen phosphate dodecahydrate (Merck KGaA, Darmstadt, Germany); sodium chloride, potassium dihydrogen phosphate, ethyl acetate, fluorescence-activated cell sorting (FACS) buffer (PBS containing 0.5% BSA and 0.1% NaN_3), sodium dodecyl sulfate (SDS) (Carl Roth GmbH & Co. KG, Karlsruhe, Germany); phosphate buffered saline (PBS) (Dulbecco; BIOCHROM GmbH, Berlin, Germany); 6-carboxy-2´,7´-dichloro dihydrofluorescein diacetate (H2DCFDA) (Molecular Probes Inc., Darmstadt, Germany); keratinocyte growth medium (KGM) supplemented with Bullet Kit (Lonza AG, Cologne, Germany); silver nanoparticles 40 nm, 3-(4,5-dimethylthiazol-2-yl)-2,5-diphenyltetrazolium bromide (MTT) (Sigma-Aldrich GmbH, Schnelldorf, Germany); dexamethasone-4,6α,21,21-d4 (C/D/N ISOTOPES Inc., Quebec, Canada); acetone, acetonitrile (VWR International GmbH, Darmstadt, Germany); trypsin (PAA Laboratories GmbH, Pasching, Austria); Piperazine-N,N′-bis(2-ethanesulfonic acid) (PIPES) buffer (Ampliqon A/S, Odense, Denmark)

All other reagents and solvents used were of analytical grades. Ultra-purified water purified by a Milli-Q® apparatus (Millipore GmbH, Darmstadt, Germany) was used.

2.2. Methods[2]

2.2.1. Particle preparation

2.2.1.1. Nanocrystals

Dexamethasone nanocrystals were prepared by wet bead milling. Dexamethasone was suspended in an aqueous surfactant solution and homogenized by an Ultra Turrax (T25, IKA® -Werke GmbH, Staufen, Germany) at 20,500 rpm for 30 s. 0.1 mm zirkonium beads (Hosokawa Alpine AG, Augsburg, Germany) and the suspension (suspension:beads, 1:3 w/w) were added into a 100 ml erlenmeyer flask and milled for 3 h under magnetic stirring at ~800 rpm. The nanosuspension was filtered through a 1.2 µm glass microfiber filter (Whatman® GE Healthcare UK Ltd., Buckinghamshire, UK) to exclude larger particles.

After preparation, whenever necessary, nanocrystals were formulated into gels by using 2.5% and 5.0% (w/w) HEC.

2.2.1.2. Polymeric nanoparticles

Dexamethasone-loaded ethyl cellulose, Eudragit® RS and ethyl cellulose/Eudragit® RS nanoparticles were prepared by the solvent evaporation method. The drug and the polymer were dissolved in ethyl acetate and the polymeric drug solution was emulsified in 30 ml aqueous surfactant solution via high shear homogenization using an Ultra Turrax at 8,000 rpm for 10 s and then at 9,500 rpm for 20 s. The emulsion was sonicated (Bandelin Sonopuls HD 3200, Bandelin electronic GmbH & Co. KG, Berlin, Germany) at 200 W (amplitude 50%, tip MS73) for 3 min in an ice bath and ethyl acetate was removed by continuous stirring of the dispersion overnight under a fume

[2] Parts of this chapter were taken from:

3. B. Balzus, M. Colombo, F.F. Sahle, G. Zoubari, S. Staufenbiel, R. Bodmeier, Comparison of different in vitro release methods used to investigate nanocarriers intended for dermal application, Int. J. Pharm., 513 (2016) 247-254
4. B. Balzus, F.F. Sahle, S. Hönzke, C. Gerecke, F. Schumacher, S. Hedtrich, B. Kleuser, R. Bodmeier, Formulation and ex vivo evaluation of polymeric nanoparticles for controlled delivery of corticosteroids to the skin and the corneal epithelium, Eur. J. Pharm. Biopharm., 115 (2017) 122-130.

hood. Afterwards, the remaining organic solvent was removed at 40 °C using a rotary evaporator (BUECHI rotavapor-R, BÜCHI Labortechnik AG, Flawil, Swizerland). The colloidal dispersion was first filtered through a 1.2 µm and then 0.7 µm glass microfiber filter (Whatman® GE Healthcare UK Ltd., Buckinghamshire, UK) to exclude lager particles. Drug-free or Nile red-loaded nanoparticles were prepared by the same procedure without the drug and instead of the drug dissolving Nile red in the polymer solutions, respectively.

After preparation, whenever necessary, polymeric nanoparticles were formulated into gels by using 2.5% and 5.0% (w/w) HEC.

2.2.1.3. Lipid nanoparticles

Dexamethasone-loaded lipid nanoparticles were prepared by high shear homogenization technique. First, the lipid components were melted and mixed at 60 °C and the drug was dispersed in the molten lipid mixture. Then water heated to 60 °C was poured into the molten lipid mixture and the two phases were homogenized at 13,500 rpm for 1 min and then at 8,000 rpm for 3 min using an Ultra Turrax. Finally, the dispersion was cooled to room temperature to solidify the lipid phase and obtain the lipid nanoparticles.

2.2.1.4. Microparticles

Ethyl cellulose microparticles were prepared by the solvent evaporation method. The polymer was dissolved in ethyl acetate and the polymer solution was emulsified in 30 ml aqueous surfactant solution via high shear homogenization using an Ultra Turrax at 8,000 rpm for 10 s and then at 9,500 rpm for 20 s. The ethyl acetate was removed by continuous stirring of the dispersion overnight under a fume hood and the remaining organic solvent was removed at 40 °C using a rotary evaporator. The microparticles were collected by filtration through a 0.45 µm cellulose nitrate filter (Whatman® GE Healthcare UK Ltd., Buckinghamshire, UK) and dried under a fume hood.

2.2.2. Drying of nanoparticle suspensions

After preparation, whenever necessary, the nanoparticle suspensions were freeze dried or spray dried.

2.2.2.1. Freeze drying

The nanoparticle suspension was shock frozen with liquid nitrogen and subsequently freeze dried (Alfa® 2-4 LD Plus freeze-dryer, Martin Christ Gefriertrocknungsanlagen GmbH, Osterode am Harz, Germany). Freeze-drying was performed at −47 °C and 0.055 mbar.

2.2.2.2. Spray drying

The nanoparticle suspension was subsequently spray dried (Buechi 190 mini spray-dryer; BUECHI, Flawil, Switzerland) using the following conditions: inlet temperature 120 °C; pump flow 6 g/min; spray flow 600 nl/h, aspirator pressure 40 mbar; outlet temperature 80 °C.

2.2.3. Artificial sebum preparation

The lipid mixture of artificial sebum consisted of 15% squalene, 10% paraffin (solidification point 57-60 °C), 15% cetyl palmitate, 10% olive oil, 25% cotton seed oil, 12% coconut oil, 6% oleic acid, 6% palmitic acid and 1% cholesterol (all by weight). The lipid components were mixed and heated to 60 °C to form a transparent lipid melt. Upon slow cooling of the transparent lipid mixture at ambient temperature, a homogeneous semi-solid mass was obtained. The artificial sebum contains the typical quantities of lipids in human sebum (Lu et al., 2009) based on commercially available materials.

2.2.4. Measurement of the particle size and zeta potential of nanoparticles

The particle size, polydispersity index (PDI) and zeta potential of the nanoparticles were measured at 25 °C by dynamic light scattering (Zetasizer® Nano ZS, Malvern Instruments Ltd., Malvern, UK). Prior to the measurement the samples were diluted to

0.1% (w/v) polymer with Milli-Q water to measure the particle size and with conductivity adjusted Milli-Q water (50 µS/cm) to measure the zeta potential.

2.2.5. Measurement of the particle size of microparticles

The particle size of microparticles was measured by laser diffractometry (Mastersizer® 2000, Malvern Instruments Ltd., Malvern, UK). The dispersion medium was purified water. The obscuration was adjusted from 4 to 6%. Stirring speed was set to 750 rpm and no sonication was used. As characteristic parameters the $d_{0.1}$, $d_{0.5}$ and $d_{0.9}$ were obtained.

2.2.6. Determination of encapsulation efficiency, loading capacity and yield

The total drug amount in the nanocrystal and polymeric nanoparticle suspensions were determined spectrophotometrically (Agilent HP 8453, Agilent Technologies Inc., Santa Clara, US) at 242 nm after dissolving the nanoparticles in water and 60% (w/w) isopropanol, respectively. In the case of Eudragit® RS nanoparticles and ethyl cellulose/Eudragit® RS nanoparticles quantification was conducted at 260 nm due to UV absorption by Eudragit® RS at 242 nm. During spectrometric measurements drug free nanoparticles treated the same way were used as blank standards. The determination of the drug content of lipid nanoparticles was not necessary as the samples were not filtered.

The encapsulation efficiency and loading capacity of the nanocrystals, polymeric nanocarriers and lipid nanoparticles were determined indirectly by determining the amount of dexamethasone dissolved in the aqueous phase.

The separation of the nanocrystals and polymeric nanoparticles from the external aqueous phase was done by centrifugation (Hereaus™ Biofuge™ Stratos™, Thermo Electron Corp., Osterode, Germany) of the colloidal dispersion at 17,000 rpm and 23 °C for 8 h. The amount of drug in the aqueous phase was quantified spectrophotometrically at 242 nm. During spectrometric measurements drug free nanoparticles treated the same way were used as blank standards.

In case of lipid nanoparticles the continuous phase was separated from the lipid nanoparticles by centrifugation of the colloidal dispersion in a 10 kDa molecular weight cut-off (MWCO) filter (Vivaspin® 500, VWR International GmbH, Darmstadt, Germany) for 4 h at 15,000 g at 10 °C to avoid melting of the lipid phase during centrifugation.

The amount of nanoparticle recovered after preparation and filtration was determined by freeze drying 2 ml of the aqueous nanosuspension.

The percentage drug encapsulation efficiency (%EE) was calculated as (mass of total drug - mass of non-entrapped drug)/mass of total drug * 100%. The percentage drug loading capacity (%LC) was calculated as mass of entrapped drug/mass of nanoparticles recovered * 100%. The percentage yield was calculated as mass of nanoparticles recovered/theoretical mass * 100%.

2.2.7. Redispersibility

The redispersibility of the freeze-dried nanoparticles was investigated visually and by measuring the particle size of the nanoparticles after redispersing the dried nanoparticles in Milli-Q water.

2.2.8. Microscopy

2.2.8.1. Optical light microscopy and cross polarized light microscopy

Microscopic and cross polarized light microscopic images were taken using a cross polarized light microscope (Zeiss Axioskop, Carl Zeiss Microscopy GmbH, Jena, Germany) equipped with an Axiocam 105 color camera and ZEN software (Carl Zeiss Microscopy GmbH, Jena, Germany). Furthermore, the microscope was equipped with a Mettler Toledo FP82HT hot stage (Mettler-Toledo GmbH, Giessen, Germany) to heat the sample if necessary.

2.2.8.2. Confocal laser scanning microscopy (CLSM)

Histological sections of porcine ear skin containing hair follicles, obtained after follicular penetration experiments, were examined under a CLSM (LSM 700, Carl Zeiss, Jena,

Germany) using a Plan-Apochromat 10×/0.45 M27 objective. The penetration of Nile red (at an excitation wavelength of 555 nm, laser intensity 2.0, pinhole 1 AU, Gain 600, digital offset 0, digital gain 1.0 and emission wavelengths of 590 nm) was tracked in the hair follicles. Skin samples without nanoparticle suspensions were used as negative controls for configuration of the microscope settings.

The accumulated fluorescence intensity of Nile red in hair follicles was determined with ImageJ software. The area in each hair follicle was sectioned from image of the fluorescence channel, and then the marked area was analyzed by imageJ. The value of the sum of the values of the pixels was taken as the accumulated fluorescence intensity of Nile red in hair follicle.

2.2.9. Determination of solubilities and partition coefficients

2.2.9.1. Dexamethasone solubility in aqueous media

An excessive amount of dexamethasone was added to the investigated aqueous media and stirred at 600 rpm for 3 days. Afterwards the suspension was centrifuged at 17,000 rpm and 23 °C for 8 h. The amount of drug in the supernatant was quantified spectrophotometrically at 242 nm.

2.2.9.2. Dexamethasone solubility in artificial sebum and paraffin

The dexamethasone solubility in artificial sebum and paraffin was determined half quantitatively. Therefore, various dexamethasone amounts (0.005%, 0.01%, 0.02%, 0.05% and 0.1% w/w) were added to artificial sebum and liquid paraffin, respectively. Afterward the dexamethasone artificial sebum and dexamethasone liquid paraffin mixtures were placed in an oven (T6120, Heraeus Instruments, Osterode, Germany) at 60 °C and stirred at 600 rpm. After 24 h the dexamethasone artificial sebum and dexamethasone liquid paraffin mixtures were investigated visually if dexamethasone was dissolved.

2.2.9.3. Dexamethasone solubility in polymer films.

Polymer films with various drug to polymer ratios (1:20, 1:10, 1:5 and 1:2) were prepared to estimate drug solubility in pure polymer. The polymer and the drug were dissolved in acetone (5% w/w) and a thin film of the organic drug-polymer solution was casted on a microscopic slide. The organic solvent was evaporated under a fume hood and the remaining solvent was removed in a vacuum oven (Heraeus^{TM} VT 5042 EK, Thermo Electron Corp., Osterode, Germany) at room temperature for 2 h. The polymer films were observed visually for clarity and under a cross polarized light microscope for drug recrystallization.

2.2.9.4. Polymer solubility in artificial sebum

The solubility of different polymers in artificial sebum was determined half quantitatively. Therefore, various polymer amounts (0.1%, 0.5%, 1%, 2%, 5%, 10%, 20% and 30% w/w) were added to artificial sebum and stirred at 600 rpm at 60 °C in an oven. After 24 h the artificial sebum polymer mixtures were investigated visually if the polymer was dissolved.

2.2.9.5. Artificial sebum/water and paraffin/water partition coefficient of dexamethasone

The artificial sebum/water and liquid paraffin/water partition coefficient of dexamethasone were determined indirectly by measuring the amount of dexamethasone dissolved in the aqueous phase. 4 ml of an aqueous 43.8 ± 0.3 µg/ml dexamethasone solution was added to 4 ml artificial sebum and respectively to 4 ml liquid paraffin, heated to 60 °C and mixed to form an emulsion. These emulsions were placed in an oven at 37 °C and stirred at 600 rpm for 24 h. Afterwards the emulsions were centrifuged at 17,000 rpm and 37 °C for 8 h. The amount of dexamethasone in the supernatant was quantified spectrophotometrically at 242 nm. During spectrometric measurements dexamethasone free water treated the same way was used as blank standard. The partition coefficients were calculated as dexamethasone

amount in water at the beginning – dexamethasone amount in water after 24 h/dexamethasone amount in water after 24 h.

2.2.10. Recrystallization of dexamethasone from saturated dexamethasone solutions

1.8 ml saturated dexamethasone solution was put in a petri dish (d = 35 mm). The petri dish was placed in an oven at 32 °C and at predefined time points (1 h, 2 h, 4 h, 6 h, 8 h and 24 h) the evaporated amount of water was determined by weight loss. Afterwards the remaining solution was observed under a cross polarized light microscope for drug recrystallization.

2.2.11. Differential scanning calorimetry (DSC) measurements

Thermograms of powders, artificial sebum and artificial sebum powder mixtures were recorded using a DSC 6000 (PerkinElmer, Inc. Waltham, MA, USA). Powders (5 – 10 mg), artificial sebum (15 - 20 mg) and artificial sebum mixtures (15 - 20 mg) were weighed accurately in 50 µl aluminum pans with pierced lid. DSC scans were recorded for a heating, cooling, heating run at a heating rate of 10 ºC/min within 0 °C and 160 ºC and a cooling rate of 40 °C/min. The thermogram of the second heating run was recorded, because the glass transition temperature (Tg) of polymers determined in the first heating run is affected by the thermal history of the polymer. Heating polymers first above the Tg and then quench cooling, eliminate the thermal history of polymers (Grijpma and Pennings, 1994). The Tg was evaluated with the Pyris software (PerkinElmer, Inc. Waltham, MA, USA).

2.2.12. Viscosity measurements

The viscosity and viscoelasticity of viscous and viscoelastic fluids were measured using a rheometer (MCR 302, Anton Paar, Graz, Austria). The viscosity was measured at varying shear rate (2 - 50 s^{-1}) and the viscoelasticity was examined in oscillatory amplitude sweep measurements with a fixed angular frequency of 10 rad/s and at varying strain (0.1% - 100%). Aqueous nanosuspensions were measured with a double gap measuring system DG27 and gels, artificial sebum and artificial sebum powder

mixtures were measured with a cone plate measuring system CP25 TG. Aqueous nanosuspensions and gels were investigated at 25 °C and artificial sebum and artificial sebum powder mixtures were investigated at 37 °C.

2.2.13. Erosion and dissolution behavior of microparticles in artificial sebum

The swelling, erosion and dissolution behavior of 20% (w/w) of ethyl cellulose microparticles in artificial sebum was investigated under a microscope at 37 °C.

2.2.14. *In vitro* drug release

Drug release from the nanoparticles was investigated using three different *in vitro* release methods. Experiments were conducted under sink and non-sink conditions where the amount dexamethasone in the receiver compartment at 100% drug release equals 10% and 50% (w/v) of its saturation solubility, respectively. The saturation solubility of dexamethasone differed between the used dexamethasone batches. The dexamethasone batch used for the experiments in section 3.1 and section 3.2. had a saturation solubility of 66 ± 1 µg/ml in pH 7.4 phosphate buffer. The dexamethasone batch used for the experiments in section 3.3. Had a saturation solubility of 90 ± 1 µg/ml in pH 7.4 phosphate buffer.

2.2.14.1. In situ drug release investigations using Sirius® inForm

The calculated amount of the nanoparticle dispersions was added manually into 40 ml release medium in an *in situ* release study apparatus (Sirius® inForm, Sirius Analytical Instruments Ltd., Forest Row, UK) which was maintained at 32 °C. The pH of the release medium was automatically adjusted to 7.4 and stirred at 100 rpm. The UV absorbance of the released dexamethasone was read between intervals using a 5 mm UV probe immersed in the release medium. Prior to the release experiment the molecular extinction coefficient of dexamethasone was determined, which was later used to automatically calculate the percentage of drug released as a function of time. Analysis of the results was preceded by simple background correction for nanocrystals

and Tyndall background corrections for lipid nanoparticles and polymeric nanoparticles to adjust for the effect of light lost due to scattering by the nanocarriers.

2.2.14.2. Dialysis bags

The calculated amount of the nanoparticle dispersion containing the required amount of dexamethasone was placed in a preconditioned dialysis bag (Float-A-Lyzer® G2, 20 kDa MWCO, Spectrum Laboratories, Inc., CA, USA) and the bag was put in a container containing pH 7.4 phosphate buffer as a release medium. Then the whole set-up was placed in an incubation shaker which was maintained at 32 °C and continuously shaken at 120 rpm. 1 ml (under sink condition) or 0.4 ml of the sample (under non-sink condition) was withdrawn at predefined time intervals (1, 3, 7, 24 and 48 h) and replaced by fresh release media. The released dexamethasone was quantified by a UV- spectrometer at 242 nm.

2.2.14.3. Franz diffusion cells

An appropriately conditioned regenerated cellulose membrane (Spectra/Por® 2 Dialysis Membrane, RC discs of MWCO 12–14 kDa, Spectrum Laboratories, Inc., CA, USA) was mounted on a Franz diffusion cell, the acceptor compartment was filled with pH 7.4 phosphate buffer, and the whole diffusion cell was placed in a thermostatic bath, which was maintained at 32 °C. The calculated amount of the nanoparticle suspension was placed on the donor compartment and closed using a wax foil (Parafilm M®, Bemis Company Inc., Oshkosh, WI, USA) to prevent water evaporation. The acceptor compartment was stirred at 600 rpm throughout the release experiment and 0.4 ml sample was withdrawn at predefined time interval (0.25, 0.75, 1.5, 3, 5, 7 and 24 h) and replaced by fresh buffer media. The released dexamethasone was quantified by a UV- spectrometer at 242 nm.

Franz diffusion cell experiments to investigated sebum responsive drug release were optimized to investigate the responsive drug release. Drug release from the nanoparticles was investigated under non-sink condition (20 µg/ml, in the acceptor compartment at 100% drug release). Before mounting the membranes on the Franz diffusion cell, the membranes were soaked either in water, paraffin or artificial sebum

for 15 h at 37 °C. The temperature of the thermostatic bath during the experiment was change to 37 °C and the donor compartment was not closed with a wax foil to simulate the physiological conditions inside the hair follicle. The predefined time intervals were changed to 1, 2, 4, 6, 8 and 24 h.

2.2.14.4. Determination of drug flux through the dissolution membrane

Dexamethasone flux (µg/cm^{2}h) through the dissolution membranes was measured by determining the slope of the linear part of the drug release curve at the initial stages of drug release.

2.2.15. *Ex vivo* drug release and penetration studies with excised human skin

The ex vivo skin drug penetration and release studies were performed in cooperation with the research groups of Prof. Dr. Sarah Hedtrich and PD Dr. med. Annika Vogt.

Cutaneous absorption of dexamethasone was investigated using female human, abdominal skin with no damages, stretch marks or scars (obtained from plastic surgeries with permission and informed consent) in accordance with a validated protocol (OECD guideline no. 428 (2004a)). Immediately after surgical removal, the subcutaneous layer of the skin was removed, the skin was washed with PBS and kept in a freezer (- 20 °C).

2.2.15.1. Franz diffusion cell

During the experiment, the defrosted skin (< 6 months) was mounted on Franz diffusion cells and the formulations equivalent to 10 µg/cm^2 dexamethasone were applied on the skin surface and were incubated at 32 °C for 6 h. The donor compartment was filled with PBS. Then the excess material loosely attached to the skin surface was carefully removed by tape-stripping twice. Epidermis and dermis were heat separated (1 min in 60 °C hot water) and the dermis was horizontally cut into 50 µm sections at - 24 °C using a freeze microtome (Frigocut 2800N, Leica Microsystems Holding GmbH, Bensheim, Germany). Epidermis and dermis skin slices were subjected to 5 freeze-

thaw cycles. Following the addition of 50 pmol Dex-d_4 as internal standard, samples were extracted 3 times with 500 µl ethyl acetate. Combined extracts were exsiccated by vacuum rotation and the dried residues were reconstituted in 200 ml acetonitrile. Dexamethasone concentrations in extracts of *ex vivo* human skin samples were quantified by LC-MS/MS as described previously (Döge et al., 2016).

2.2.15.2. Microdialysis

For microdialysis studies, the recesses in the device were filled with culture medium (KGM-Gold™ Keratinocyte Growth Medium, Lonza Group AG, Basel, Switzerland) and 2.5 × 4 cm^2 areas of intact skin were pinned, dermis side down, on the device. For topical administration of the dexamethasone formulations, a lid containing 9 holes (1 cm^2) was screwed on top of the device with carefully positioning of each skin sample (3 donors) directly below a hole. 5 h after topical application, the lid of the device was removed and a microdialysis probe (Ep High Flux Probes 45 kDa MWCO, EP Medical ApS, Copenhagen, Denmark) was inserted in the emerged 1 cm^2 skin using a guide canula (0.60 mm × 25 mm, 100 Sterican®, B. Braun Melsungen AG, Melsungen, Germany). The position was controlled by optical coherence tomography (VivoSight Michelson Diagnostics Ltd., Maidstone, UK). The canula was withdrawn leaving the fiber placed within the skin. Probes were perfused with PIPES buffer (pH 7.4) at a constant flow rate of 3 µl/min using a pump (Univentor 864 Syringe Pump, Univentor Limited, Zejtun, Malta). Microdialysis samples were collected manually at 6, 12 and 24 h after topical application for a period of 1 h (time-intervals: 6 – 7 h, 12 – 13 h and 24 – 25 h) at room temperature using a new probe for the last collection step. During the intervals, the skin was kept in an incubator. The amount of dexamethasone in microdialysis samples was quantified by LC-MS/MS as described previously (Döge et al., 2016).

2.2.16. *Ex vivo* hair follicular penetration studies

The *ex vivo* hair follicular penetration studies were performed in cooperation with the group of Prof. Dr. Dr.-Ing. Jürgen Lademann. For the *ex vivo* follicular penetration study fresh porcine ear skin from a local abattoir was used. The porcine ears were stored in the refrigerator for less than 3 days before use. The skin was thoroughly washed with

distilled water and dried with tissue paper afterwards. The hairs were trimmed using a pair of scissors and an adhesive solution was put around the application area (2 cm × 2 cm) and dried for 90 min, to prevent lateral diffusion of the colloidal dispersion. Then 80 µL of Nile red-loaded ethyl cellulose or Eudragit® RS nanoparticle suspension was uniformly spread over the application area and was massaged for 2 min using a mini massager (Rehaforum Medical GmbH, Elmshorn, Germany). Then the skin was incubated at 32 °C for 1 h. The Nile red-loading was 0.004% based on the polymer amount. Afterwards, cryo spray was used and biopsies of about 0.6 cm × 0.6 cm were cut out using a scalpel. The biopsies were put in an Eppendorf tube, frozen in liquid nitrogen and stored at −20 °C. Finally, the biopsies were mounted in a frozen tissue freezing medium and 10 µm histological sections containing hair follicles (n = 7) were cut out using a cryostat (Microm HM 560, Microm GmbH, Walldorf, Germany). The histological sections were observed under a CLSM to determine the penetration depth and fluorescence intensity of the dye. Approval to conduct the *ex vivo* experiments using the porcine ear skin was obtained from the Veterinaeramt Berlin.

2.2.17. Toxicity study

The toxicity studies were performed in cooperation with the research group of Prof. Dr. Burkhard Kleuser.

2.2.17.1. Isolation and cultivation of primary human keratinocytes

Primary human keratinocytes (NHK) were isolated from juvenile foreskins (with ethical consent). The cells were isolated and cultivated according to a standard protocol (Gysler et al., 1997). The NHK cells were grown in KGM supplemented with Bullet Kit at 37 °C in a humidified atmosphere with 5% CO_2. The cells used in all the experiments did not exceed passage 4 and were seeded and maintained during experiments in KGM.

2.2.17.2. 3-(4,5-dimethylthiazol-2-yl)-2,5-diphenyltetrazolium bromide (MTT) assay

The MTT assay is a widely used method to determine the viability in metabolic active cells. The assay was carried out as described previously (Kumar et al., 2014). It is based on the conversion of the yellow MTT to formazan blue by the mitochondrial reductase system. NHKs were seeded into 96-well plates (TPP AG, Trasadingen, Germany) with a density of 10,000 cells per well. After 24 h, the nanoparticles (prepared without dexamethasone) were added to the well plates forming a final concentration of 50 and 500 µg/ml and were further incubated for 24 h and 48 h. Subsequently, the cells were incubated with 100 µl MTT solution (0.5 mg/ml in PBS) for 4 h. After removing the supernatants, 50 µl dimethyl sulfoxide was added to dissolve the formazan salt and its optical density was measured using a microplate reader (Tecan AG, Crailsheim, Germany) setting the excitation to 540 nm. As a positive control 0.003% SDS was used. Untreated cells and the solvent control (1% w/v PVA solution) served as references. The measured absorbance values of the untreated cells were considered as 100% cell viability. A cell viability <80% predicts cytotoxic effects.

2.2.17.3. 6-carboxy-2´,7´-dichlorodihydrofluorescein diacetate (H2DCFDA) assay

Intracellular reactive oxygen species (ROS) levels were measured using the H2DCFDA assay. H2DCFDA is a chemically reduced, acetylated form of fluorescein used as an indicator for ROS in cells (Jaeger et al., 2012). This nonfluorescent molecule is deacetylated by intracellular esterases and can be oxidized by radicals such as hydroxyl, peroxyl, alkoxyl, nitrate and carbonate to a fluorescent molecule (excitation 495 nm, emission 525 nm). NHKs were seeded in 12-well plates (100,000 cells per well) and grown for 24 h (37 °C, 5% CO_2) in KGM supplemented with Bullet Kit. Then cells were incubated with 50 and 500 µg/ml nanoparticles (prepared without dexamethasone) for 1 h in KGM. After exposure, cells were loaded with 25 µM H2DCFDA in the same media for 1 h at 37 °C. The cells were harvested by trypsin incubation and collected in 2 ml reaction tubes. Thereafter, cell pellets were washed 5 times with ice-cold FACS buffer. After resuspending the cell pellet in 200 ml FACS buffer, the samples were analyzed by FACSCanto II (BD Biosciences, Heidelberg,

Germany). The H2DCFDA fluorophor was measured in the fluorescein isothiocyanate (FITC) channel (488 nm excitation). Silver nanoparticles (40 nm) served as positive control. Untreated cells and the solvent control served as references. Fluorescence was measured in 10,000 cells and the mean value of the fluorescence was examined. The results are presented as mean fluorescence intensity (MFI).

2.2.18. Statistical analysis

Unless otherwise stated all measurements were conducted in triplicates and the data were given as mean ± standard deviation (SD). One-way ANOVA with Tukey test was performed to compare means at the statistical significance level (P) ≤ 0.05. Drug release profiles were compared by using two-way ANOVA followed by the Tukey test at $p \leq 0.05$.

3. Results and discussion

List of contributions from other research scientists (research groups):

Nanoparticles provided by other research scientists:

Nanocrystals provided and characterized by Miriam Colombo (Table 7, Figure 32-39 and Figure 41).

Lipid nanoparticles provided and characterized by Gaith Zoubari (Table 7, Figure 33 and Figure 35-38).

Experiments performed by other research scientists (research groups):

In situ drug release investigations using Sirius® inForm performed by Miriam Colombo (Figure 33-34).

Ex vivo drug release and penetration study performed by Stefan Hönzke (research group of Prof. Dr. Sarah Hedtrich) (Figure 15 and Figure 41).

Intradermal micro dialysis experiments using excised human skin performed by Nadine Döge (research group of Dr. Annika Vogt) (Figure 41).

Ex vivo follicular penetration study performed by Pin Dong (research group of Prof. Dr. Jürgen Lademann) (Figure 30-31).

MTT and H2DCFDA assay performed by Dr. Christian Gerecke (research group of Prof. Dr. Burkhard Kleuser) (Figure 16-17).

3.1. Part I: Preparation and optimization of polymeric nanoparticles with controlled drug release[3]

Corticosteroids are commonly used for the treatment of inflammatory skin diseases. However, treatment effectiveness using corticosteroids is highly dependent on drug release at the application site because high drug concentration often leads to serious local and systemic side effects like skin atrophy (Schoepe et al., 2006).

Therefore, nanoparticles that adhere and penetrated to/into the skin and release the drug in a controlled manner may significantly reduce local and systemic side effects associated with corticosteroid therapy and improve treatment effectiveness and patient compliance.

Nanoparticles offer a number of advantages for dermal drug delivery, including improved drug solubility and stability, adjustable surface properties, increased surface adhesion, drug targeting, controlled drug release and increased drug penetration and permeation through the skin (Kesisoglou et al., 2007; Küchler et al., 2009b; Merisko-Liversidge et al., 2003; Sahle et al., 2016; Schafer-Korting et al., 2007; Shim et al., 2004). Nanoparticles penetrate deep into a barrier-disrupted skin, whereas a healthy skin restricts the penetration of the nanoparticles, thus, minimizing side effects (Abdel-Mottaleb et al., 2012; Contri et al., 2016; Kimura et al., 2012; Zhang and Monteiro-Riviere, 2008). Moreover, delayed drug release from the nanoparticles allows better localization of the drug in the epidermis with low skin permeation tendency (Abdel-Mottaleb et al., 2011). Nanoparticles can also penetrate deep into the hair follicles and stay there for several days to release the drug slowly (Lademann et al., 2015). The follicular route might also be used to target dendritic cells and other cells that are involved in inflammatory processes (Lademann et al., 2005; Vogt et al., 2005).

Nanoparticle surface charge has a significant effect on adhesion and penetration of nanoparticles through the skin (Contri et al., 2016; Wu et al., 2010). The skin is negatively charged under normal physiological conditions (Marro et al., 2001;

[3] Parts of this chapter were taken from: B. Balzus, F.F. Sahle, S. Hönzke, C. Gerecke, F. Schumacher, S. Hedtrich, B. Kleuser, R. Bodmeier, Formulation and ex vivo evaluation of polymeric nanoparticles for controlled delivery of corticosteroids to the skin and the corneal epithelium, Eur. J. Pharm. Biopharm., 115 (2017) 122-130.

Rojanasakul and Robinson, 1989) and positively charged nanoparticles may adhere. Cationic amino-functionalized polystyrene and Eudragit® RS nanoparticles penetrated deeper into the skin in comparison to negatively charged nanoparticles. This is attributed to lack of electrostatic interaction with negatively charged nanoparticles that impaired access to the outermost skin layer (Contri et al., 2016; Wu et al., 2010). Different polymers with different solubility, polarity, biocompatibility, biodegradability, swelling and charge can be used for the preparation of polymeric nanoparticles. Eudragits and cellulose derivates are among the most commonly used polymers. Eudragits are copolymers of methacrylic acid and methacrylic/acrylic esters or their derivatives, which include neutral, cationic and anionic polymers. Eudragit® RS is a positively charged, water-insoluble copolymer of ethyl acrylate, methyl methacrylate and a low content of a methacrylic acid ester with quaternary ammonium groups. It is commonly used in controlled drug delivery systems (Thakral et al., 2013). In dermal drug delivery, Eudragit® RS nanoparticle-based heparin gels controlled drug release into the stratum corneum in comparison to a heparin solution (Loira-Pastoriza et al., 2012). Capsaicinoids-loaded Eudragit® RS nanoparticles embedded into chitosan gels increased skin adhesion and drug penetration in contrast to a capsaicinoids chitosan gel (Contri et al., 2014). Cellulose-based polymers are also commonly used to prepare controlled release drug delivery systems. Ethyl cellulose is a water insoluble polymer and is commonly used for the preparation of controlled drug delivery systems (Rekhi and Jambhekar, 1995). Quercitin-loaded ethyl cellulose nanoparticles controlled the drug release with increased quercitin skin retention (Sahu et al., 2013).

The objective of this study was to prepare dexamethasone-loaded Eudragit® RS and ethyl cellulose nanoparticles, which can adhere well to the skin or penetrate into the hair follicle to release the drug slowly and in a controlled manner to minimize corticosteroids therapy associated side effects and improve patient compliance and treatment effectiveness.

3.1.1. Nanoparticle preparation and characterization

Nanoparticles were prepared by the solvent evaporation method with ethyl acetate a class 3 residual solvent (ICH Q3C(R6) guideline). Different ethyl cellulose- and Eudragit® RS-based polymeric nanoparticles were formulated with different surfactants for controlled delivery of dexamethasone into the skin. The two polymers and

surfactants differ in their physicochemical properties, e.g. chemical structure, charge and hydrophobicity and are stable in aqueous formulations (Rekhi and Jambhekar, 1995; Thakral et al., 2013). Therefore, nanoparticles with different properties and drug release profiles were expected.

3.1.1.1. Nanoparticle preparation with different surfactants – Effect on particle size, PDI and encapsulation efficiency

To prepare stable aqueous formulations of dexamethasone-loaded ethyl cellulose nanoparticles the following surfactants were screened PVA, poloxamer 188, poloxamer 407, Tween® 80, CTAB and sodium deoxycholate. Furthermore the effect of the different surfactants on the particle size, PDI and encapsulation efficiency of the nanoparticles was investigated.

First, the dexamethasone solubility in different surfactants was determined (Table 1).

Table 1: Critical micelle concentration and dexamethasone saturation solubility of different aqueous surfactant solutions

Surfactant solution (2.5% w/v)	**Reported critical micelle concentration**	**Dexamethasone saturation solubility (µg/ml)**
- (water)	-	66 ± 1
PVA	no data	115 ± 1
Poloxamer 188	0.1% (Saski and Shah, 1965)	88 ± 2
Poloxamer 407	0.7% (Guzmán et al., 2007)	100 ± 4
Tween® 80	0.0013% (Katakam et al., 1995)	320 ± 7
CTAB	0.083% (Haque et al., 1999)	6378 ± 61
Sodium deoxycholate	0.032% (Chattopadhyay and London, 1984)	338 ± 7

2.5% (w/v) aqueous PVA, poloxamer 188 and 407 solutions exhibited the lowest dexamethasone solubility, whereas the dexamethasone solubility in 2.5% (w/v) aqueous Tween® 80 and sodium deoxycholate solutions was already ~5 times increased compared to the dexamethasone solubility in water. The dexamethasone solubility in 2.5% (w/v) aqueous CTAB solution was highly increased. CTAB was excluded from further studies for the nanoparticle preparation, because due to its high

solubilizing capacity of dexamethasone in the external aqueous phase a low encapsulation efficiency was expected.

There was no considerable effect on the particle size observed for dexamethasone-loaded ethyl cellulose nanoparticles in different surfactant solutions. All prepared nanoparticles were in a size range of ~170 – 220 nm (Table 2).

Table 2: Size, PDI and encapsulation efficiency of aqueous nanosuspensions prepared with 5% (w/w) ethyl cellulose nanoparticles, 0.1% (w/w) dexamethasone and 2.5% (w/v) of different surfactants.

Dexamethasone-loaded ethyl cellulose nanoparticles			
Surfactant	**Size (nm)**	**PDI**	**Encapsulation efficiency (%)**
PVA	168	0.118	88.7
Poloxamer 188	171	0.194	76.1
Poloxamer 407	190	0.191	82.7
Tween® 80	195	0.243	55.8
Sodium deoxycholate	215	0.349	53.9

However, the PDI was affected by the choice of surfactant. Thus ethyl cellulose nanoparticles prepared with sodium deoxycholate had a PDI above the limit value of 0.25 for a narrow particle distribution (Tantra et al., 2010) , while formulations with the other surfactants had a PDI below 0.25. The nanoparticle size distribution ranking from broad to narrow with different surfactant was the following: deoxycholate, Tween® 80, poloxamer 188, poloxamer 407 and PVA. The encapsulation efficiency of the dexamethasone-loaded ethyl cellulose nanoparticles prepared with sodium deoxycholate and Tween® 80 was lower than the encapsulation efficiency of the ethyl cellulose nanoparticles prepared with PVA, poloxamer 188 and poloxamer 407 (Table 2). This observation was in accordance with the higher dexamethasone solubility in the surfactant solutions of sodium deoxycholate and Tween® 80 which increased the non-encapsulated solubilized drug in the external aqueous phase and thus decreased the encapsulation efficiency, compared to the surfactant solutions of PVA, poloxamer 188 and poloxamer 407.

In conclusion, according to the evaluated parameters PVA was considered the best surfactant among studied ones for the preparation of dexamethasone-loaded ethyl

cellulose nanoparticles. Nanoparticles in aqueous PVA solution had the smallest size and PDI and the highest encapsulation efficiency.

However, all surfactants were screened at a surfactant to ethyl cellulose ratio of 1:2, which might be not the optimal for all surfactants. Therefore, a smaller particle size, PDI and higher encapsulation efficiency values might be possible to achieve by optimizing the surfactant concentration for each formulation.

3.1.1.2. Effect of surfactants on the recrystallization of dexamethasone from saturated dexamethasone solutions

The stability of aqueous nanosuspension after application to the skin is a critical practical aspect, which needs to be considered during formulation development. The evaporation of volatile components results in a rapid concentration increase of the remaining formulation components. This concentration effect could lead to destabilization/agglomeration of the nanoparticles and the formation of supersaturated drug solutions with a potential drug recrystallization in larger microcrystals (Coldman et al., 1969). Therefore, the effect of different surfactants, namely PVA, poloxamer 188, poloxamer 407, Tween® 80, CTAB and sodium deoxycholate on the recrystallization of dexamethasone in saturated dexamethasone solutions during evaporation of the aqueous phase was investigated (Figure 10). Saturated solutions were used instead of a fixed dexamethasone concentration, because the nucleation time depends on the degree of saturation (Raghavan et al., 2001). All surfactants were used as 2.5% (w/v) aqueous solution except CTAB, because the solubility of dexamethasone was highly increased in an aqueous 2.5% (w/v) CTAB solution (Table 1). Instead, an aqueous 0.025% (w/v) CTAB solution had a dexamethasone saturation solubility of 82 ± 1 µg/ml, which was comparable to the dexamethasone solubility in water. Therefore, 0.025% (w/v) CTAB was screened as additive to inhibit the dexamethasone recrystallization during evaporation of the aqueous phase by its strong dexamethasone solubilization. An aqueous saturated dexamethasone solution served as a control.

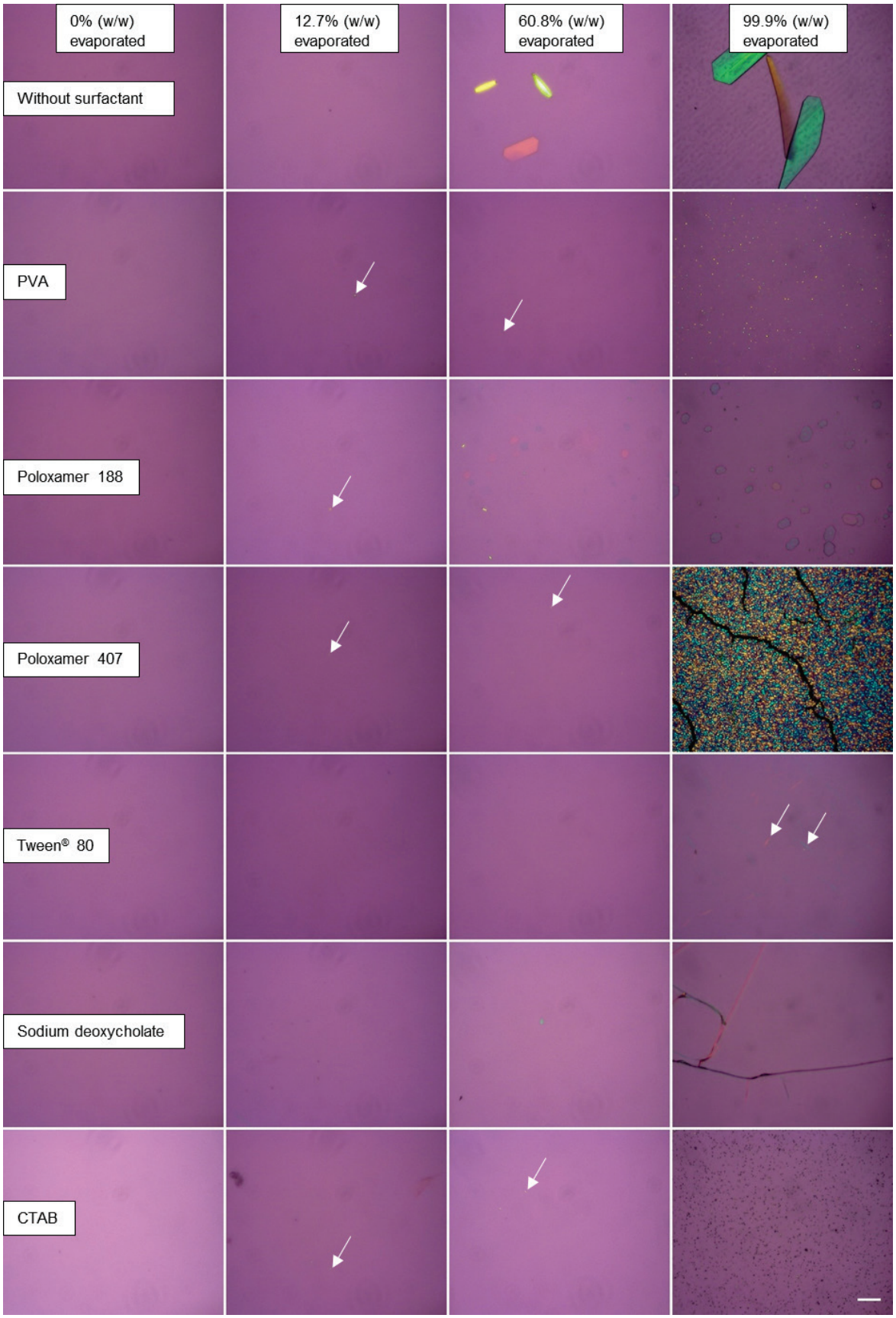

Figure 10: Aqueous saturated dexamethasone solutions without surfactant, with 0.025% (w/v) CTAB, 2.5% (w/v) PVA, poloxamer 188, poloxamer 407, Tween® 80 or sodium deoxycholate after evaporation of certain amounts of water % (w/w), arrow indicates crystal, scale bar 50 µm.

For saturated dexamethasone solution without surfactant crystals were observed when 60.8% of the aqueous phase was evaporated. In formulation with Tween® 80 no crystals were visible until 78.8% water loss. In case of sodium deoxycholate the first crystals appeared after 42.6% water loss however after evaporation of the complete aqueous phase no crystals were visible anymore. In formulations with CTAB, PVA, poloxamer 188 and poloxamer 407 crystals could be observed already after 12.7% water loss. (Table 3). Poloxamer 407 formed a film after complete water evaporation, which was shiny under the polarized light microscope (Figure 10). Due to this phenomenon dexamethasone recrystallization could not be investigated in the poloxamer 407 film by polarized light microscopy.

Table 3: : Saturated dexamethasone solutions without surfactant, with 0.025% (w/v) CTAB, 2.5% (w/v) PVA, poloxamer 188, poloxamer 407, Tween® 80 or sodium deoxycholate after evaporation of certain amounts of water % (w/w).

Water evaporated (% (w/w))	Water	2.5% (w/v) PVA	2.5% (w/v) Poloxamer 188	2.5% (w/v) Poloxamer 407	2.5% (w/v) Tween® 80	2.5% (w/v) Sodium deoxycholate	0.025% (w/v) CTAB
12.7 ± 1.0	-	Crystals	Crystals	Crystals	-	-	Crystals
22.7 ± 1.4	-	Crystals	Crystals	Crystals	-	-	Crystals
42.6 ± 2.7	-	Crystals	Crystals	Crystals	-	Crystals	Crystals
60.8 ± 3.0	Big crystals (50 µm)	Crystals	Big crystals (10 µm)	Crystals	-	Crystals	Crystals
78.8 ± 3.9	Big crystals (50 µm)	Crystals	Big crystals (10 µm)	Crystals	-	Crystals	Crystals
99.9 ± 0.1	Big crystals (100 µm)	Crystals	Big crystals (20-50 µm)	Crystals	Crystals	-	Crystals

Surfactants were reported to inhibit or promote crystal growth (Raghavan et al., 2001; Rodriguez-Hornedo and Murphy, 2004). However, in all cases except Tween® 80, surfactants promoted the crystal growth since crystals appeared earlier than in the saturated dexamethasone solution without surfactants. This could be explained by the solubilization of drug molecules inside micelles and thereby concentrating the solute molecules (Garti and Zour, 1997). Furthermore, surfactants reduce interfacial surface tension what led to the decrease in the activation energy for crystal nucleation (Christoffersen et al., 1991). All surfactants were used at concentrations above their critical micelle concentration (Table 1), except CTAB, therefore both, drug solubilization in micelles and reduction of activation energy for nucleation could be valid explanation of the promotion of crystal growth.

Although, sodium deoxycholate induced crystal nucleation less than PVA, poloxamer 188, poloxamer 407 and CTAB it could not inhibit nucleation as well as Tween® 80 did. It has been reported that the recrystallization inhibition is dependent on the drug-surfactant interactions and as a result the selection of crystallization inhibitors is usually drug specific (Margulis-Goshen et al., 2011).

The size and shape of the crystals formed during the evaporation study differed between the different surfactants (Figure 10). Crystals in aqueous saturated dexamethasone solution without surfactant and with poloxamer 188 had a prismatic shape and were bigger in size compared to the other surfactants. Crystals in an aqueous saturated dexamethasone Tween® 80 solution were needle shaped. The other surfactants led to small crystals, hence the shape could not be analyzed under light microscope.

Differences in crystal size were related to differences in nucleation and crystal growth rates (Rodriguez-Hornedo and Murphy, 2004). When nucleation rate was faster than the crystal growth rate small crystals were formed whereas big crystals were formed when crystal growth rate was faster than the nucleation rate (Li et al., 2012). Therefore, polymers inhibited the interaction of drug molecules and thus prevented crystal growth. Long needle shaped crystals as in the case of Tween® 80 indicated in some cases a high degree of supersaturation with a fast recrystallization (Boistelle and Astier, 1988; Rodriguez-Hornedo and Murphy, 2004) what is consistent with the best recrystallization inhibition by Tween® 80 due to its capacity to maintain the highest supersaturation degree of dexamethasone.

The ethyl cellulose nanosuspensions (Table 2) were also studied regarding the recrystallization of dexamethasone. However, recrystallization could not be investigated during the evaporation due to the high light scattering caused by the dispersed nanoparticles, which significantly reduced the light intensity of the microscope.

3.1.1.3. Dexamethasone solubility in ethyl cellulose and Eudragit® RS films

Prior to drug loading, the dexamethasone solubility in ethyl cellulose, Eudragit® RS and ethyl cellulose/Eudragit® RS blends was estimated by a film casting method. Films

prepared with individual polymers appeared clear but films of polymer blends were hazy at all ratios investigated (3:1, 1:1 and 1:3) even in the absence of dexamethasone (Figure 11a-c). This might be attributed to polymer aggregation because of non-specific polymeric interactions. Besides, in all cases, dexamethasone recrystallized at drug to polymer ratios of ≥1:5 (Figure 11d-f).

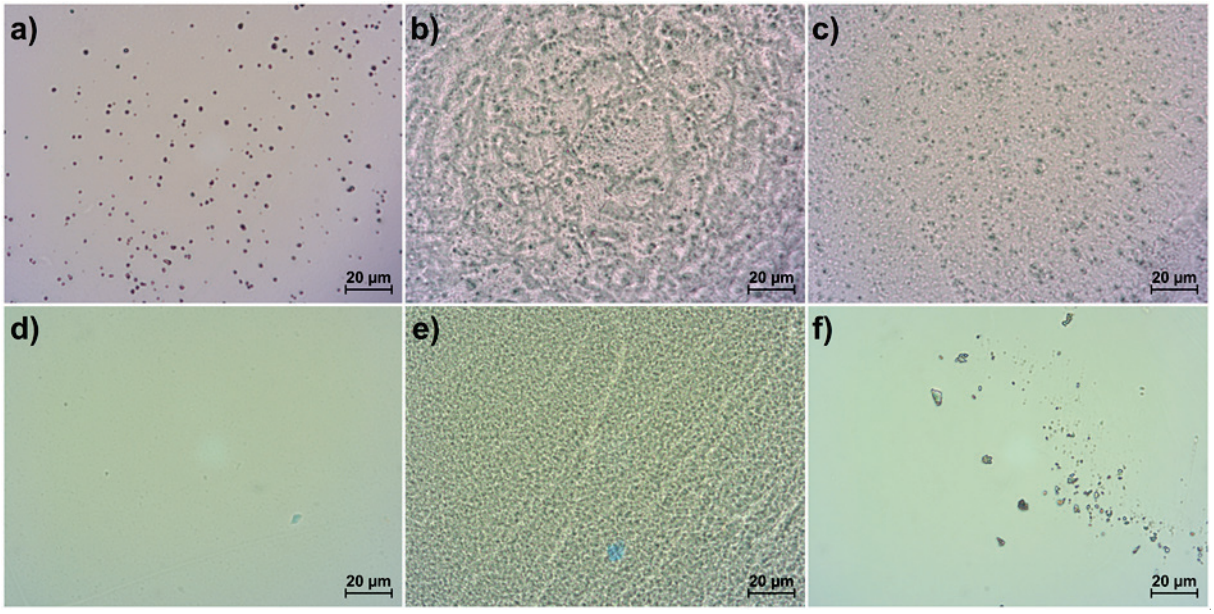

Figure 11: Films of ethyl cellulose/Eudragit® RS blends without dexamethasone (a) 3:1, (b) 1:1 and (c) 1:3 and films of (d) ethyl cellulose, (e) ethyl cellulose/Eudragit® RS (1:1) and (f) Eudragit® RS with a drug to polymer ratio of 1:5.

3.1.1.4. Optimization of ethyl cellulose and Eudragit® RS nanoparticles

Ethyl cellulose nanoparticles were larger than Eudragit® RS nanoparticles (Table 4). This can be attributed to the permanent positive charge at the surface of Eudragit® RS, which minimizes the tendency of nanoparticle-nanoparticle aggregation, and to the lower viscosity of the organic solution of Eudragit® RS (1.53 ± 0.04 mPa s) when compared to ethyl cellulose (9.56 ± 0.66 mPa s). Eudragit® RS exhibits a self-stabilizing effect (Bodmeier et al., 1991). Ethyl cellulose nanoparticles had a negative zeta potential due to adsorption of hydroxyl ions (Jin et al., 2012), whereas Eudragit® RS nanoparticles had a positive zeta potential due to the quaternary ammonium groups on the polymer surface. Ethyl cellulose nanoparticles also had higher dexamethasone encapsulation efficiency and loading capacity than Eudragit® RS nanoparticles, which

can be attributed to the higher hydrophilicity and surface charge of the Eudragit® RS which will led to a lower affinity towards the lipophilic dexamethasone.

Table 4: Compositions and characteristics of dexamethasone-loaded polymeric nanoparticles (stabilized by 1% w/v PVA in aqueous phase)

Formulation	Ethyl cellulose to Eudragit® RS ratio (w/w)	*Polymer (% w/w)	Drug to polymer ratio (w/w)	Organic to aqueous phase ratio (w/w)	Zeta potential (mV)	Encapsulation efficiency (% w/w)	Loading capacity (% w/w)	Yield (%)	Size (nm)	PDI	Redispersibility Size (nm); (PDI)
NP-1	1:0	1	1:20	1:3	-18	54.9	1.4	96.6	120	0.074	NR
NP-2	1:0	2	1:20	1:3	-21	47.8	1.7	93.2	125	0.088	NR
NP-3	1:0	5	1:100	1:3	-36	87.0	0.8	95.1	172	0.150	NR
NP-4	1:0	2	1:20	1:2	-21	66.4	2.2	97.4	139	0.058	NR
NP-5	1:0	2	1:40	1:3	-22	72.3	1.2	97.4	124	0.082	NR
NP-6	0:1	1	1:20	1:3	32	12.7	0.3	101.0	64	0.201	64; (0.199)
NP-7	0:1	2	1:20	1:3	35	14.1	0.5	95.5	70	0.191	70; (0.196)
NP-8	0:1	5	1:20	1:3	44	16.1	0.7	94.3	94	0.214	95; (0.216)
NP-9	0:1	2	1:20	1:4	36	14.4	0.5	95.5	64	0.218	64; (0.209)
NP-10	0:1	2	1:20	1:2	33	14.9	0.5	94.9	78	0.182	80; (0.174)
NP-11	0:1	5	1:100	1:3	41	71.1	0.6	94.1	90	0.214	91; (0.203)
NP-12	1:1	2	1:40	1:3	34	67.0	1.1	97.4	102	0.110	105; (0.110)

* Percentage based on the aqueous phase; NR = not redispersible. The relative standard deviation (RSD, %) of the particle size, PDI, zeta potential, encapsulation efficiency, loading capacity and yield were 0.1 - 1.3, 0.5 - 27.4, 0.5 - 7.8, 0.1 - 1.3, 0.1 - 1.3 and 0.01 - 3.75, respectively. At a drug to polymer ratio of 1:20, dexamethasone was not completely soluble in 5% ethyl cellulose or 2% ethyl cellulose with an organic to aqueous phase ratio of 1:4.

Generally, particle size, zeta potential, encapsulation efficiency and loading capacity of the polymeric nanoparticles increased with increasing polymer concentration and organic phase ratio (Table 4). The size increase can be attributed to a higher polymer concentration in the organic phase droplets or to the larger organic phase droplets in the emulsion. Increasing the polymer amount increased the zeta potential because less PVA is covering the nanoparticle surface and shielding the charge of the polymer. At high organic phase ratio, the rate of organic solvent evaporation with respect to the total organic phase is slower so that the solvent/drug flux out of the solvent/polymer droplet is reduced improving drug loading and entrapment. However, the changes were not considerable.

Nanoparticle size decreased slightly with increasing PVA concentrations (Figure 12), owing to the stabilizing effect of the surfactant. Eudragit® RS nanoparticles could be prepared without PVA because of the self-stabilizing effect of the polymer.

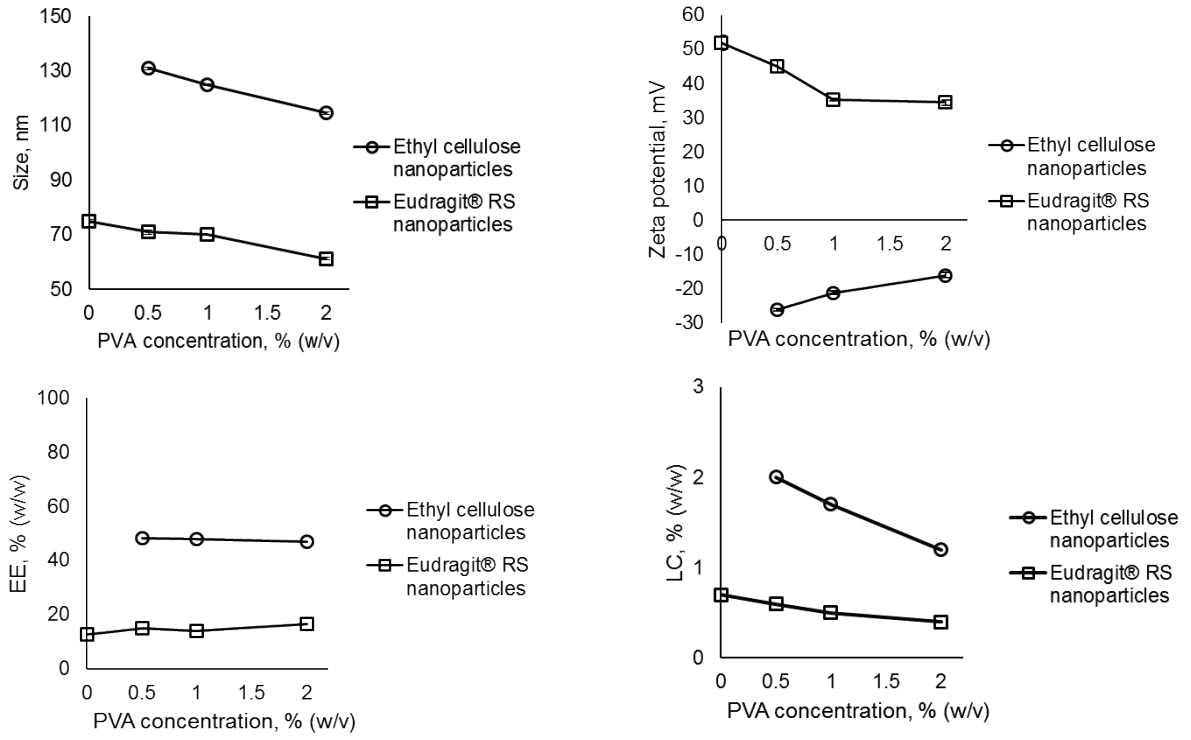

Figure 12: Effect of PVA concentration on the particle size, zeta potential, entrapment efficiency and loading capacity of ethyl cellulose and Eudragit® RS nanoparticles.

As expected, the absolute value of the zeta potential slightly decreased with increasing PVA concentration, because PVA is covering the nanoparticle surface and shielding the charge on the nanoparticle surface. PVA concentration had no significant effect on the encapsulation efficiency whereas the loading capacity decreased with increasing PVA concentration. This can be attributed to the drug solubilizing effect of PVA.

As expected, the size of the ethyl cellulose/Eudragit® RS nanoparticles increased with increasing the ratio of ethyl cellulose (Figure 13). By increasing the percentage of ethyl cellulose in the ethyl cellulose/Eudragit® RS nanoparticles, the encapsulation efficiency and loading capacity increased significantly. At 75% (w/w) ethyl cellulose, there was partial nanoparticle aggregation (yield = 52.9%) and resulted in reduced drug encapsulation efficiency and loading capacity. In addition, the polymer ratio showed no significant effect on zeta potential and at all ratios investigated the ethyl

cellulose/Eudragit® RS nanoparticles had a positive zeta potential due to the permanent positive charge of the quaternary ammonium groups of Eudragit® RS.

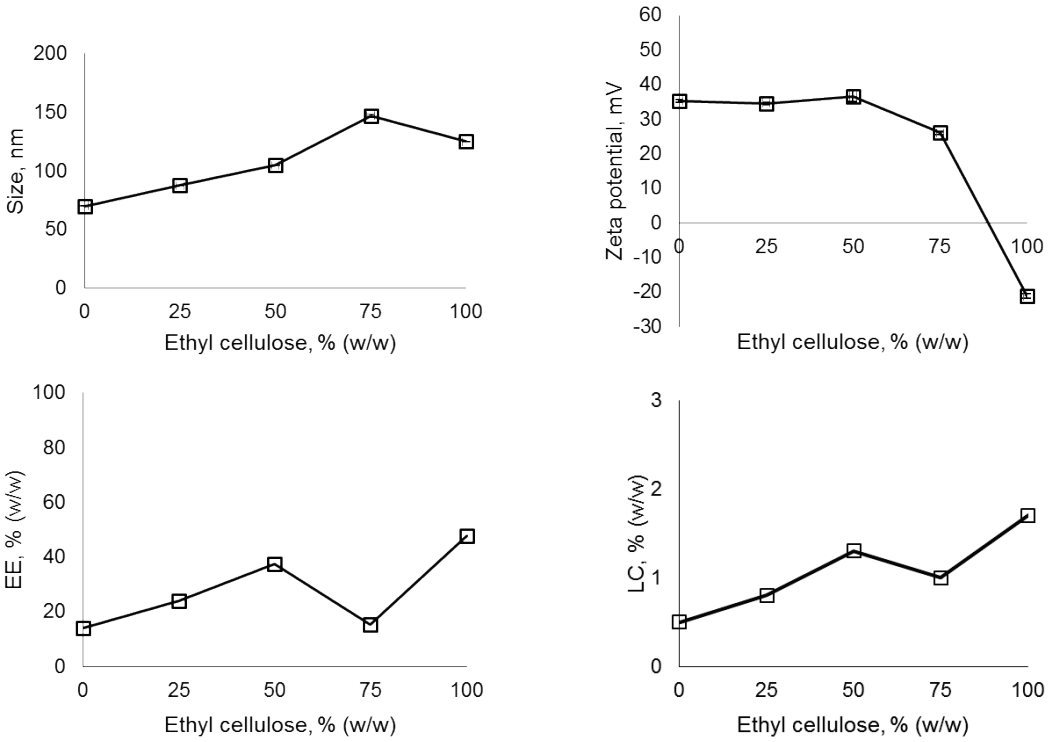

Figure 13: Effect of percentage ethyl cellulose in ethyl cellulose/Eudragit® RS nanoparticles on particle size, zeta potential, entrapment efficiency and loading capacity.

Eudragit® RS and ethyl cellulose/Eudragit® RS nanoparticles were redispersible due to the self-stabilizing and hydrophilic character of Eudragit® RS because of their quaternary ammonium functional groups. However, ethyl cellulose nanoparticles were not redispersible (Table 4) because of their poor wettability (Schmidt and Bodmeier, 1999).

3.1.2. *In vitro* drug release

Dexamethasone release from 2% ethyl cellulose, 2% Eudragit® RS and 2% ethyl cellulose/Eudragit® RS (1:3, 1:1, 3:1) nanoparticles, prepared at drug to polymer ratio of 1:20, was investigated *in vitro* (Figure 14a).

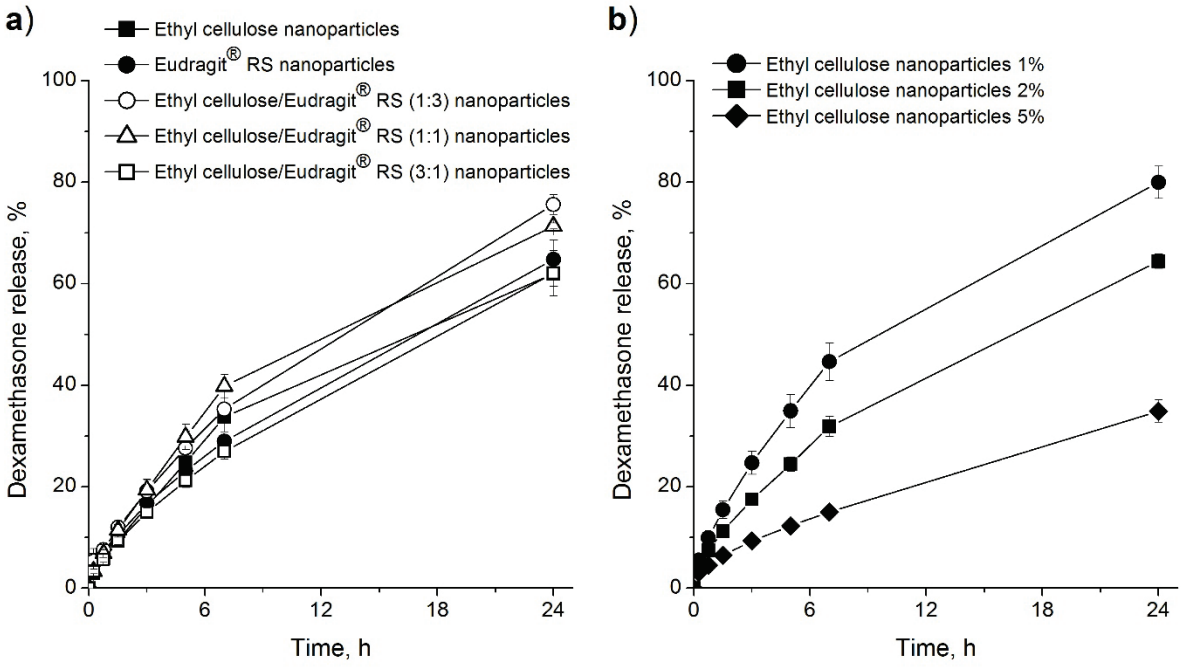

Figure 14: Effect of (a) ethyl cellulose to Eudragit® RS ratio and (b) polymer amount in the nanosuspension on dexamethasone release.

There was no significant difference in drug release between ethyl cellulose, Eudragit® RS and the ethyl cellulose/Eudragit® RS (3:1) nanoparticles. However, ethyl cellulose/Eudragit® RS (1:1 and 1:3) nanoparticles led to a faster drug release.

Fast release of the hydrophobic dexamethasone is expected from hydrophilic Eudragit® RS nanoparticles. However, its low drug loading (0.5%) compared to ethyl cellulose nanoparticles (1.7%) might slow down the release and, hence, it had drug release comparable to ethyl cellulose nanoparticles. Upon blending the two polymers, a proportional change in polymer hydrophilicity and drug loading capacity was expected and there might have been no significant changes in drug release. However, the two polymers are not soluble in each other (Figure 11a-c) and when mixed at 1:1 the more heterogeneous mixture was obtained. This might result in a porous matrix with an increased drug loading capacity and fast drug release.

Interestingly, drug release decreased considerably with decreasing drug to polymer ratio (which was achieved by increasing the amount of the polymer in the dispersed phase to keep the amount of suspension applied in the donor phase constant) (Figure 14b). This is expected because there is a high degree of drug encapsulation and probable formation of a high tortuous path. It is thus possible to control drug release by choosing the appropriate amount of the polymer within the nanosuspension.

3.1.3. *Ex vivo* drug release and penetration

The *ex vivo* drug release and penetration experiments with excised human skin were performed in cooperation with the research group of Prof. Dr. Sarah Hedtrich.

Drug release from nanoparticles into the skin is a complex process. Nanoparticle adhesion to and penetration into the outer layer of the skin lead to a longer retention time of the nanoparticles, where the drug can be released deeper and over a longer period of time.

Dexamethasone release and penetration from 2% ethyl cellulose, 5% Eudragit® RS and 2% ethyl cellulose/Eudragit® RS (1:1) nanoparticles (Table 4) and a marketed cream, each loaded with 0.05% dexamethasone, were investigated *ex vivo* using excised human skin (Figure 15).

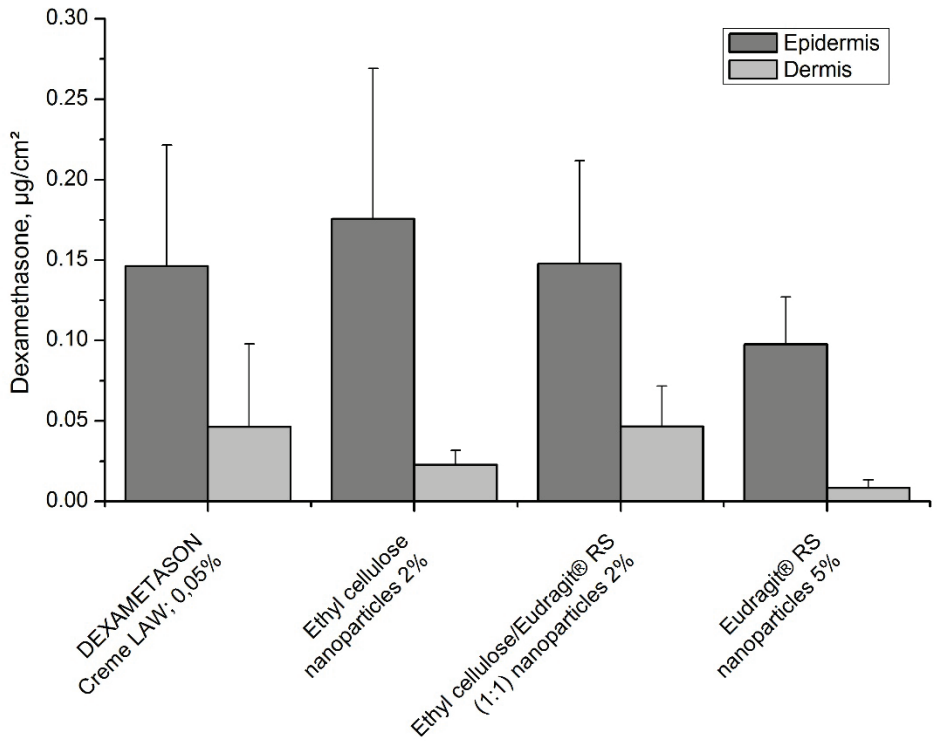

Figure 15: Amount of dexamethasone in epidermis and dermis recovered 6 h after topical application of 0.05% dexamethasone-loaded ethyl cellulose, Eudragit® RS and ethyl cellulose/Eudragit® RS (1:1) nanoparticles and DEXAMETHASON Creme LAW; 0,05%.

In all the cases, over 6 h, an insignificant amount of dexamethasone was recovered in the acceptor compartment. More dexamethasone was recovered on the epidermis, with lesser degree of penetration into deeper layers, with ethyl cellulose nanoparticles

than the commercial cream. This can be attributed to slow release of dexamethasone from the nanoparticles. Dexamethasone release and penetration into the deeper layers increased when Eudragit® RS was blended with ethyl cellulose. This is in line with the results of the release study where drug release from ethyl cellulose/Eudragit® RS (1:1) nanoparticles was significantly faster than the pure polymers (Figure 14a). The ethyl cellulose/Eudragit® RS nanoparticles were also positively charged, which also have high tendency to adhere and penetrate through the skin than negatively charged or neutral nanoparticles (Wu et al., 2010). Thus, the increase in degree of drug penetration might be attributed to the charge and improved dexamethasone release from the ethyl cellulose/Eudragit® RS nanoparticles. Interestingly, dexamethasone penetration in both epidermis and dermis was lower from 5% Eudragit® RS nanoparticles (Figure 15). At high percentage of the polymer (low drug to polymer ratio) drug release decreased significantly (see Section 3.1.2) and low degree of drug penetration into the deeper layers of the skin might be attributed to slow drug release. The small amount of drug penetrated on the upper layer might also be associated with low amount of drug release and a high degree of adhesion of the cationic nanoparticles to the negatively charged skin surface, which was most likely taken away with the first two layers of tape strips. Thus, over longer period of time, slow drug release and penetration might be obtained. Therefore, by preparing polymeric nanoparticles and controlling the drug to polymer ratio it was possible to control drug release on the skin surface, which would also enhance treatment effectiveness of some skin diseases using corticosteroids.

However for nanoparticles, follicular penetration is assumed to be the major penetration pathways through the skin and, follicular penetration from excised human skin is insignificant because the follicles remained closed after surgical removal of the skin (Patzelt et al., 2008b). Thus, penetration of the nanoparticles into deeper layer of the hair follicles is expected to improve the degree of penetration of the corticosteroids and basically drug release from nanoparticles in the hair follicles is quite slow and a more sustained release over an expected period of time is expected *in vivo*. In addition, there is a high concentration of dendritic cells in the follicular walls. Thus *in vivo* the nanoparticles are expected to perform even better.

3.1.4. Toxicity study

The toxicity study of the polymeric nanoparticles was performed in cooperation with the research group of Prof. Dr. Burkhard Kleuser.

The MTT assay showed that there was no significant reduction in cell viability after exposing the cells to 50 and 500 µg/ml Eudragit® RS and ethyl cellulose nanoparticles for 24 h and 48 h (Figure 16). In contrast, cell proliferation increased, which can be associated with increased cell metabolism as a result of stress response. The same effect was observed with high concentrations of the well-established biocompatible and biodegradable PLGA nanoparticles (Swed et al., 2014). Oxidative stress triggered by nanoparticles is one of the major concerns for inducing genotoxic effects (Nel et al., 2006). The H2DCFDA assay showed that the Eudragit® RS nanoparticles bear no cytotoxicity potential but ethyl cellulose nanoparticles, especially when used at high concentration (500 µg/ml) (Figure 17). It has been suggested that the general trend of nanomaterials cytotoxicity is similar among various types of nanoparticles and that non-specific oxidative stress is one of the largest concerns in nanoparticle-induced toxicity (Nel et al., 2006).

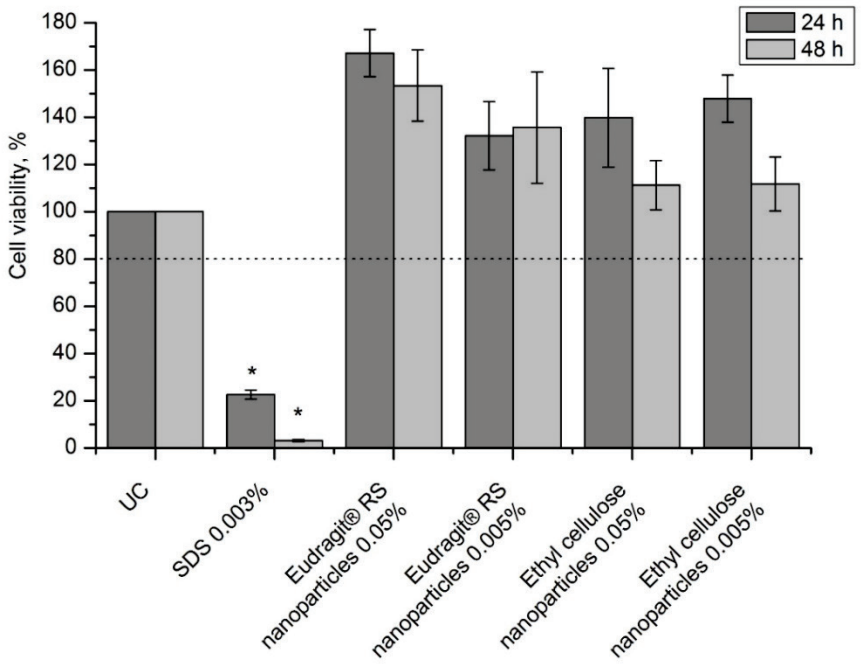

Figure 16: Percent cell viability of NHK cells determined by MTT assay after exposing them to different concentrations of ethyl cellulose and Eudragit® RS nanoparticles for different period of time. UC = untreated cells (negative control) and SDS (positive control). * indicates significant differences from the cytotoxicity limit 80%; $p < 0.05$

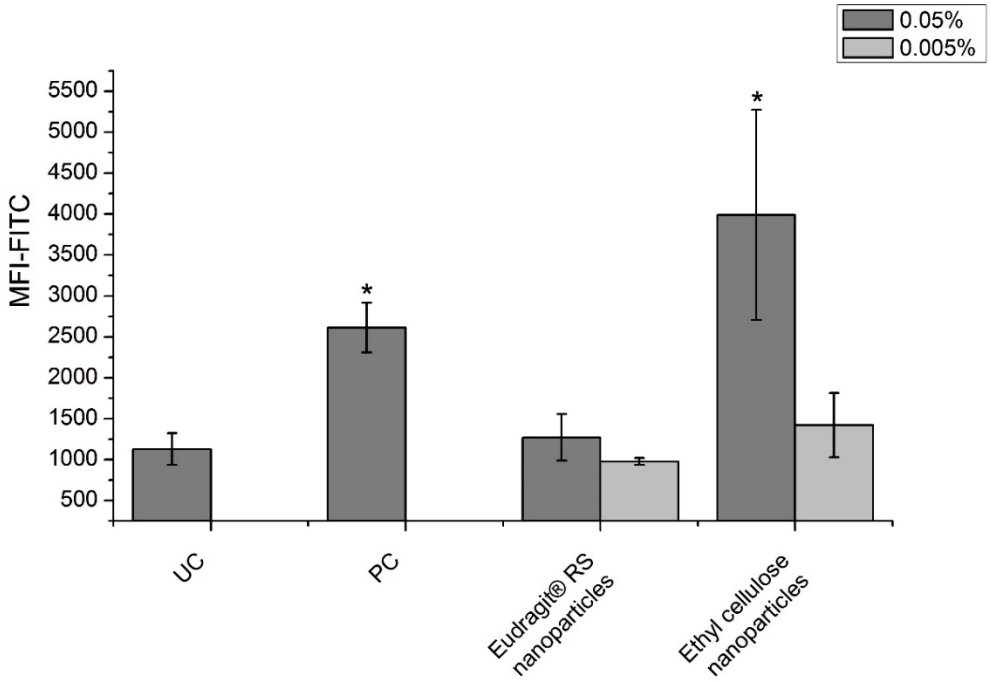

Figure 17: ROS levels in NHK cells after exposing them to different concentrations of ethyl cellulose and Eudragit® RS nanoparticles for 1 h as determined by the H2DCFDA assay. UC = untreated cells (negative control); PC = positive control (40 nm silver nanoparticles). * $p < 0.05$

3.1.5. Conclusions

Promising dexamethasone-loaded ethyl cellulose and Eudragit® RS nanoparticles were prepared and characterized. The nanoparticles showed no toxicity potentials *ex vivo*, except ethyl cellulose particles, which exhibited ROS generating potentials. Drug release from the nanoparticles could be controlled by choosing appropriate type and amount of polymer. *Ex vivo*, drug release and penetration into the skin from the nanoparticles was slower than a commercial cream. Thus, these nanoparticles could be used for the delivery of corticosteroids, whereby slow release on the skin surface could significantly improve their treatment effectiveness. However, *ex vivo* drug release and penetration investigations using excised human skin might neglect the follicular pathway and the results should be supported by *in vivo* data.

3.2. Part II: Sebum-responsive nanoparticles for follicular targeting

Inflammatory processes in and around the hair follicle e.g. follicular psoriasis and primary inflammatory hair diseases are challenging skin diseases, because in these cases inflammation is located at specific, poorly accessible areas in otherwise unaffected skin.

Solid particles like polymer nanoparticles, lipid nanoparticles and liposomes are known to penetrate into open hair follicles (Lademann et al., 2007). Additionally a particle size of 300 – 600 nm is optimal for the follicular penetration, because this particle size corresponds to the thickness of the overlapping cuticula hair surface (Lademann et al., 2009; Patzelt et al., 2011).

Hair follicles are an optimal target for drug delivery, because they represent an efficient reservoir for nanoparticles and nanoparticle-based drug delivery as nanoparticles stay inside the hair follicle for several days (Lademann et al., 2006). Furthermore dendritic cells and other cells, that are involved in inflammatory processes in the skin, can be targeted through the follicular route (Lademann et al., 2005; Vogt et al., 2005).

However the drug release from nanoparticles within a confined environment, for example hair follicles, remains a challenge (Lademann et al., 2015). The upper section of the hair follicle is mainly filled with sebum, which is secreted by the sebaceous gland (Lu et al., 2009). Sebum is a mixture of squalene, waxes, cholesterol derivatives, triglycerides, fatty acids and cell debris, which liquefy at 37 °C (Valiveti et al., 2008). Therefore sebum could be used to trigger nanoparticle swelling, erosion and dissolution and by this increasing the drug release or even lead to pulsatile site-specific drug release in the hair follicle.

The objective of this study was to prepare sebum-responsive nanoparticles, which penetrate deeply into the hair follicle and will swell, erode and/or dissolve in sebum to trigger the drug release.

3.2.1. Screening of sebum-responsive polymers

The solubility of different polymers in artificial sebum was determined at 60 °C, where the artificial sebum is in a molten state and visually clear. The artificial sebum solubility of Eudragit® L 100, Eudragit® S 100, HPMCP-55, PLA, PLGA 503, PLGA 503 H, PLGA 502 S and PVA was < 1% (w/w) and were considered not sufficiently sebum-responsive for this study. Eudragit® RS particles were small and transparent when observed under the microscope and as a result it was difficult to discern if Eudragit® RS was soluble enough in the sebum. Consequently Eudragit® RS particles were mixed with artificial sebum and observed under the microscope at 37 °C for 16 h. After 16 h there was no change in particle size or shape of the Eudragit® RS nanoparticles (Figure 18) and Eudragit® RS was also considered as insoluble in sebum.

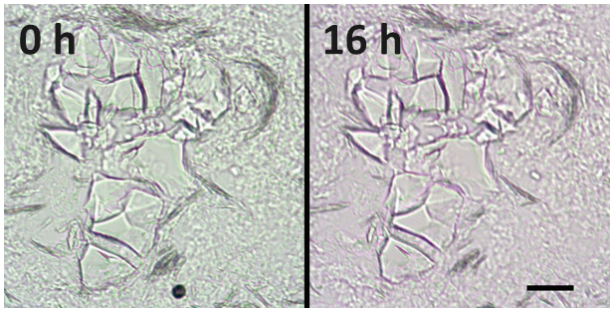

Figure 18: Eudragit® RS particles after 0 h (start) and 16 h incubation time in artificial sebum at 37 °C; scale bar 50 µm.

Interestingly, ethyl cellulose particles dissolved in artificial sebum and when the ethyl cellulose concentration increased the solution appeared hazy (Figure 19a-c). However, when observed under the microscope all the particles were dissolved up to 20% (w/w) ethyl cellulose but some undissolved particles were obtained at 30% (w/w) ethyl cellulose (Figure 19d-f). Thus, ethyl cellulose was chosen to prepare and evaluate sebum-responsive nanoparticles.

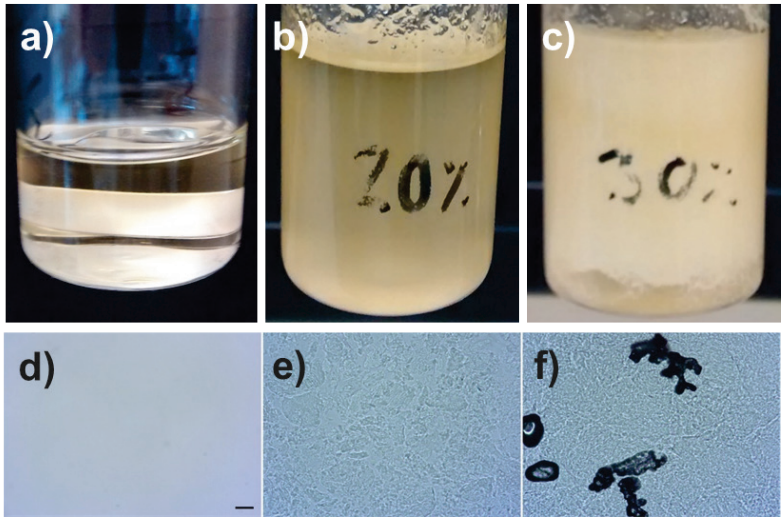

Figure 19: Macroscopic (a-c) and microscopic (d-f) pictures of artificial sebum (a, d), artificial sebum with 20% (w/w) ethyl cellulose (b, e) and 30% (w/w) ethyl cellulose (c, f) at 60 °C after 24 h; scale bar 50 µm.

3.2.2. Sebum-responsive nanoparticle preparation and size optimization

All the nanoparticles were prepared by solvent evaporation method. However, the follicular penetration of nanoparticles is highly dependent on nanoparticles size and nanoparticles in the range of 600 - 700 nm are excellent candidates to target the hair follicles (Patzelt et al., 2011). Therefore, the potentials of the two emulsion homogenization techniques, namely sonication and high shear homogenization to obtain the desired nanoparticle size were assessed. The effect of sonication amplitude and sonication time in case of sonication and rotational speed and emulsification time in case of high shear homogenization on the particle size and PDI of the prepared ethyl cellulose nanoparticles was investigated.

3.2.2.1. Effect of sonication amplitude and sonication time on the particle size and PDI

Sonication is a well established method to produce nanoparticles. Generally the size of nanoparticles prepared by sonication is dependent on the ultrasound amplitude and sonication time, which determine the total energy input (Abbas et al., 2014).

The effect of the amplitude on the particles size and PDI was investigated at a fixed sonication time of 2 min and the amplitude was varied from 10% to 25%. The effect of the sonication time on the particle size and PDI was studied at a fixed amplitude of 15% at different sonication times (0.5, 2 and 4 min).

Both factors had an insignificant effect on the particle size and already a low amplitude and a short sonication time led to a small particle size below 250 nm (Figure 20). The PDI was in all cases below the limit value of 0.25 for a narrow particle size distribution (Tantra et al., 2010). Therefore, sonication was too powerful to prepare ethyl cellulose nanoparticles in the range of 600 - 700 nm.

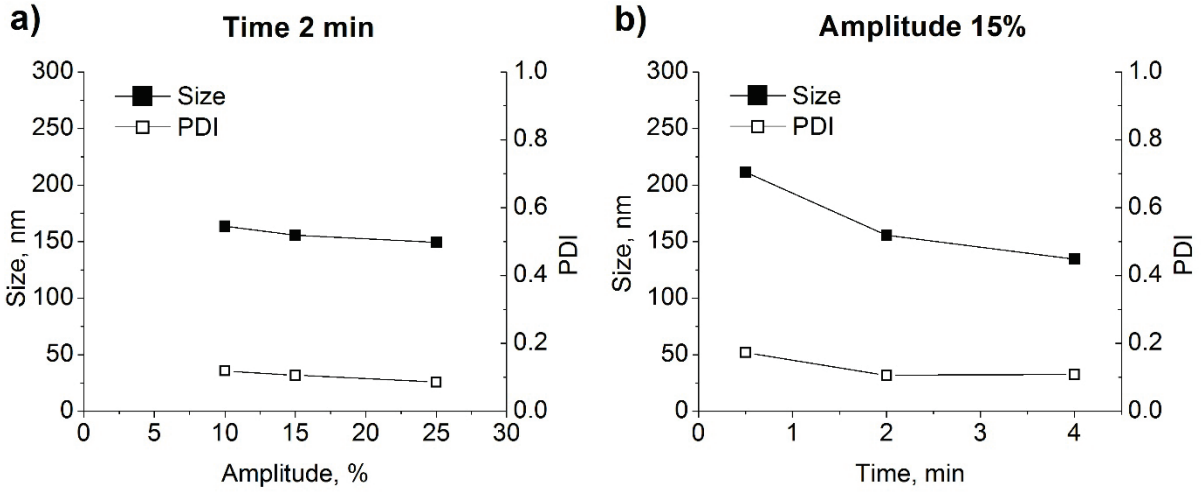

Figure 20: Effect of sonication amplitude (a) and sonication time (b) on the sizes and PDI values of ethyl cellulose nanoparticles prepared by sonication for 2 min and 15% ultrasound amplitude, respectively.

3.2.2.2. Effect of rotational speed and emulsification time on the particle size and PDI

High shear homogenization is hardly used to prepare nanoparticles, because often high amounts of microparticles are obtained (Mehnert and Mäder, 2001). Nonetheless, a number of nanoparticle preparations by high shear homogenization indicate that the method is sufficient for the preparation of nanoparticles (Puglia et al., 2013; Triplett and Rathman, 2008). The rotational speeds and emulsification times of high shear homogenization may determine the particle size and PDI of the obtained nanoparticles.

Ethyl cellulose nanoparticles were prepared with different rotational speeds and emulsification times to investigate their effect on the particle size and PDI. Interestingly

rotational speeds below 13,500 rpm gave only microparticles and by varying the rotational speed from 13,500 to 24,000 rpm the size of the nanoparticles could be controlled in the range of 900 - 400 nm (Figure 21). However, a PDI value of 0.25 was only obtained at a high rotational speed of 24,000 rpm and with longer homogenization times of 4 - 6 min. Otherwise the PDI was between 0.3 - 0.5 and higher than the limit value of 0.25 indicating a relatively broad particle distribution. High shear homogenization was an adequate method to control the size of ethyl cellulose nanoparticles over a broad range. The PDI values could be adjusted by formulation optimization regarding high shear homogenization (Triplett and Rathman, 2008).

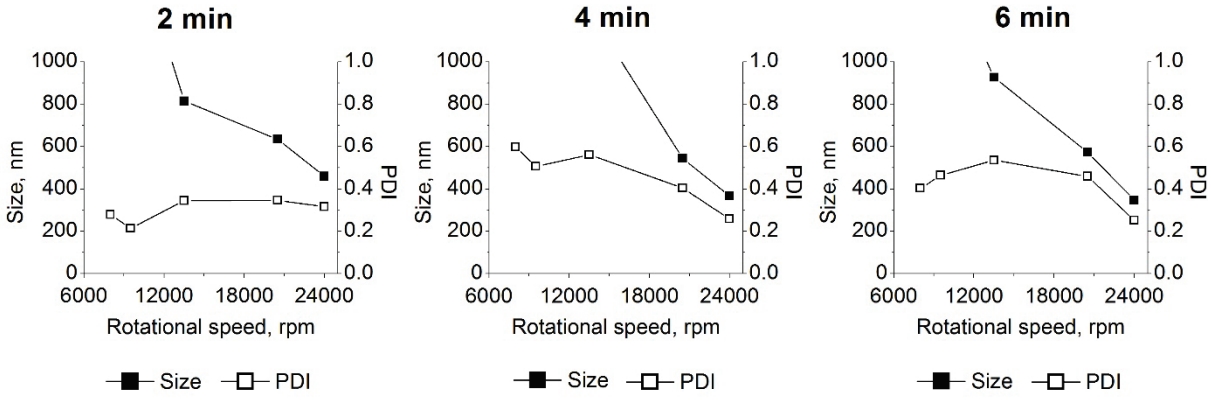

Figure 21: Effect of rotational speed and emulsification time on the particle size and PDI of ethyl cellulose nanoparticles.

3.2.3. Investigation of polymer sebum interactions

The changes in the thermal behavior, viscosity and viscoelasticity of the sebum-responsive and sebum-unresponsive polymers in artificial sebum were thoroughly investigated to better understand the sebum-responsive nature of the nanoparticles. For the investigation ethyl cellulose and Eudragit® RS were used as sebum-responsive and sebum-unresponsive polymers, respectively.

3.2.3.1. Ethyl cellulose microparticle dissolution in artificial sebum

The swelling, erosion and dissolution of ethyl cellulose microparticles in artificial sebum was investigated under the microscope at 37 °C. The prepared ethyl cellulose microparticles were composed of 80% (w/w) ethyl cellulose and 20% (w/w) PVA. The

$d_{0.1}$, $d_{0.5}$ and $d_{0.9}$ of the microparticles determined by laser diffraction were 3.0, 5.3 and 9.8 µm, respectively (Figure 22).

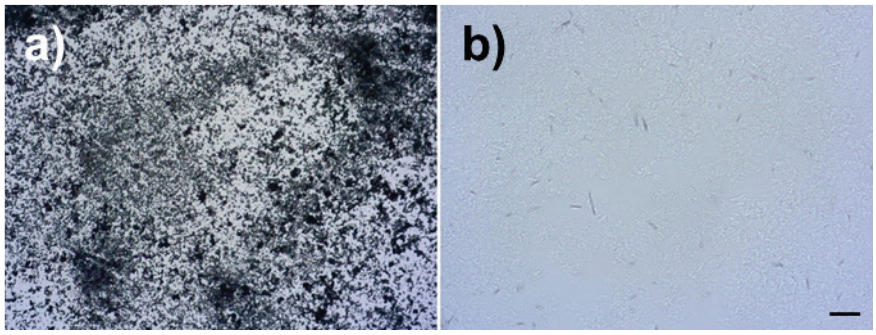

Figure 22: Microscopic pictures of ethyl cellulose microparticles (a) and artificial sebum (b) at 37 °C, scale bar 50 µm.

Dispersion of 20% (w/w) ethyl cellulose microparticles in artificial sebum resulted in rapid erosion and dissolution of the microparticles where the majority of the microparticles dissolved with in less than 2 min. However, complete dissolution of the microparticles took 2 h because the system was not subjected to any mixing under the microscope (Figure 23).

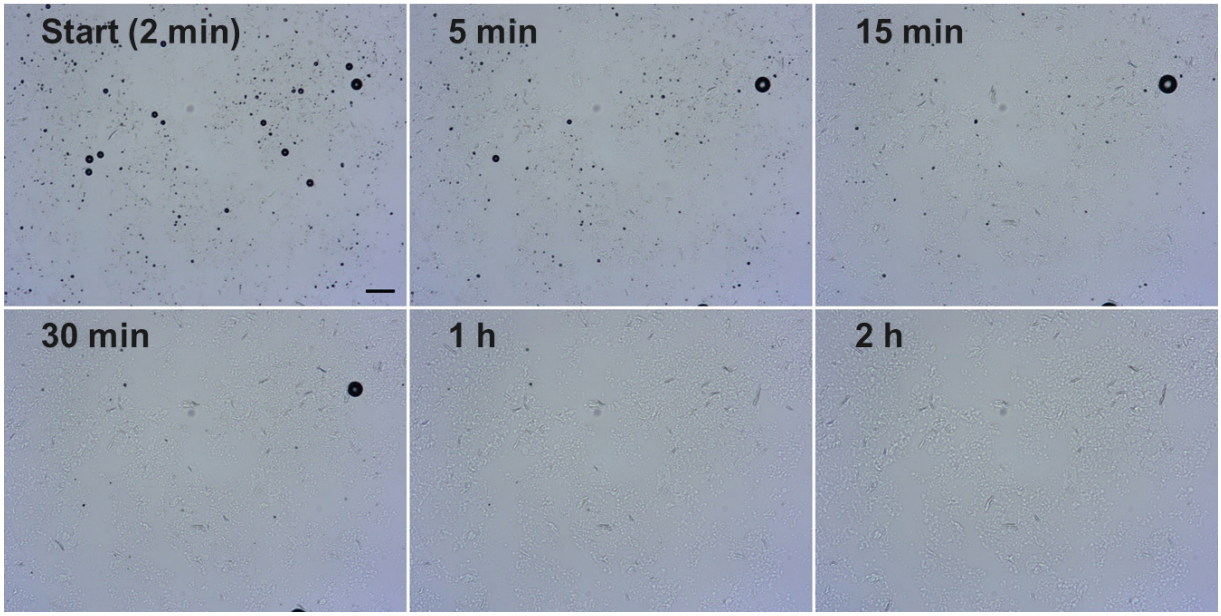

Figure 23: Microscopic pictures of 20% (w/w) ethyl cellulose microparticles in artificial sebum after mixing with artificial sebum at 37 °C at certain time points; scale bar 50 µm.

The fast dissolution of ethyl cellulose microparticles after mixing with sebum suggests that there would be fast dissolution of the sebum-responsive nanoparticles, which have an immense surface area to volume ratio. Furthermore sebum-triggered drug release

from the ethyl cellulose nanoparticles inside the upper section of the hair follicle and the sebaceous glands, which are filled with sebum is expected (Lu et al., 2009).

3.2.3.2. Effect of ethyl cellulose and Eudragit® RS nanoparticles on the thermal properties of artificial sebum

The Tg of PVA, ethyl cellulose and Eudragit® RS was 68 °C, 119 °C and 42 °C, respectively (Figure 24). The physical mixture of ethyl cellulose:PVA (8:2) and ethyl cellulose nanoparticles exhibited a Tg value close to the Tg value of ethyl cellulose and the Tg of PVA vanished indicating good miscibility of the polymers (Lu and Weiss, 1992). Nevertheless, the amount of PVA inside the physical mixture and the ethyl cellulose nanoparticle formulation was low and could be below the detection limit of the DSC. Contrarily, the physical mixture Eudragit® RS:PVA (8:2) and Eudragit® RS nanoparticles exhibited a Tg at 64 °C, which was slightly lower and broader than the PVA peak but higher and narrower than the Eudragit® RS Tg. The changes in the Tg in case of physical mixtures of Eudragit® RS:PVA (8:2) and Eudragit® RS nanoparticle formulation indicated a good miscibility of the polymers with plasticizing effect between them.

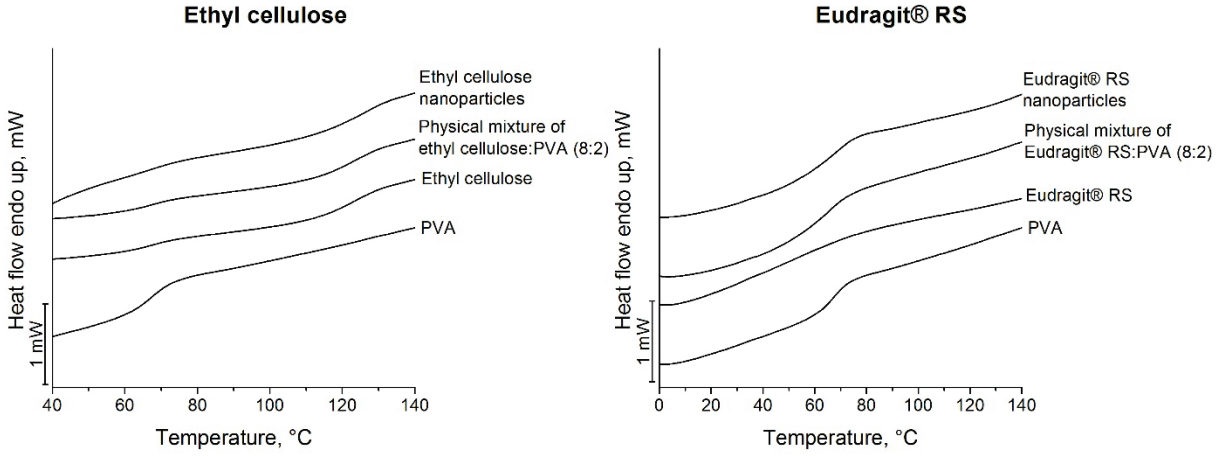

Figure 24: DSC thermograms of PVA, ethyl cellulose, Eudragit® RS, physical mixtures (8:2) of ethyl cellulose and Eudragit® RS with PVA, ethyl cellulose nanoparticles and Eudragit® RS nanoparticles.

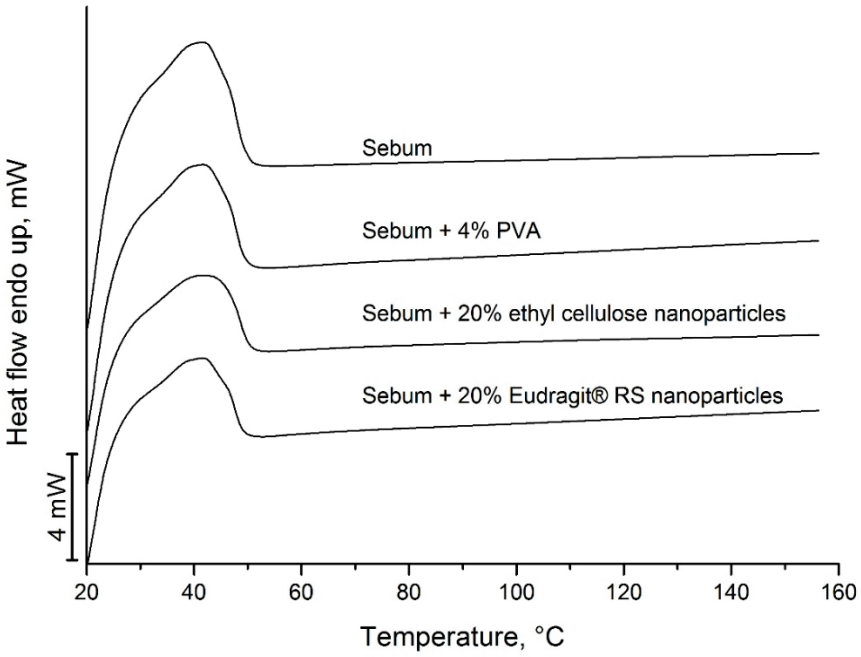

Figure 25: DSC thermograms of artificial sebum and artificial sebum with 4% (w/w) PVA, 20% (w/w) ethyl cellulose nanoparticles and 20% (w/w) Eudragit® RS nanoparticles.

The artificial sebum exhibited a broad melting peak (Figure 25), because it is a complex mixture with waxy materials like human sebum. Therefore, sebum is lacking a sharp melting peak (Lu et al., 2009). Mixing 4% (w/w) PVA (corresponding to the PVA amount in 20% (w/w) nanoparticle formulation), 20% (w/w) ethyl cellulose and 20% (w/w) Eudragit® RS nanoparticles with artificial sebum did not affect the thermal behavior of the artificial sebum as the broad melting peak of the artificial sebum remained unchanged (Figure 25). Furthermore, Tg peaks of PVA, ethyl cellulose and Eudragit® RS were not visible. This could indicate that the ethyl cellulose nanoparticles were dissolved within the artificial sebum. In the case of Eudragit® RS nanoparticles and PVA which were insoluble in artificial sebum (see section 3.2.1.) the Tg could be shifted below 50 °C due to the plasticizing effect of the artificial sebum and mixed with the broad melting peak of the artificial sebum. However, the amount of ethyl cellulose, Eudragit® RS and especially of PVA could be below the detection limit of the DSC, too.

3.2.3.3. Effects of ethyl cellulose and Eudragit® RS nanoparticles on the rheological properties of artificial sebum

The effect of nanoparticles on the rheological properties of sebum can be diverse, because on the one hand, sebum is complex mixture of waxy and liquid components

(Lu et al., 2009) and on the other hand there could be interaction between sebum and nanoparticles, between solid and liquid structures inside the sebum and between the nanoparticles itself.

The viscosity of artificial sebum decreased with increasing shear rates. Hence, artificial sebum is a non-Newtonian fluid with a shear thinning flow behavior (Figure 26). The artificial sebum had a pseudo plastic flow behavior with a yield stress as it only started to flow when a certain stress value was exceeded (Figure 27). Furthermore, the viscosity decreased with time under shear stress characterizing a thixotropic flow behavior (Figure 26).

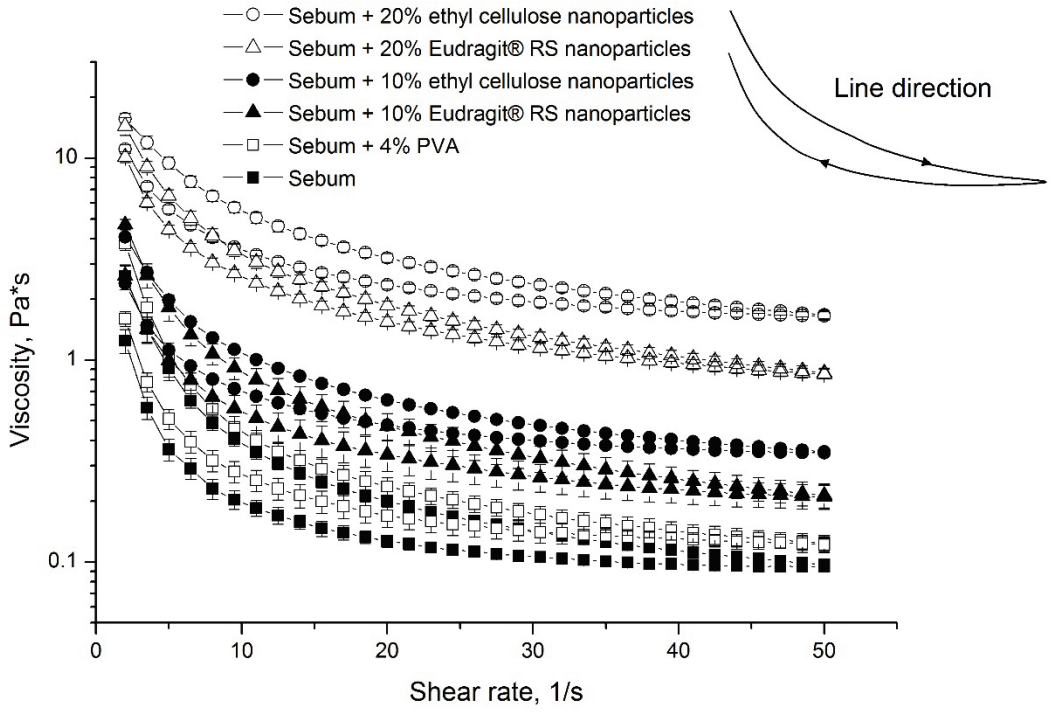

Figure 26: Viscosity as a function on shear rate of artificial sebum and artificial sebum mixtures with PVA, ethyl cellulose nanoparticles and Eudragit® RS nanoparticles at 37 °C.

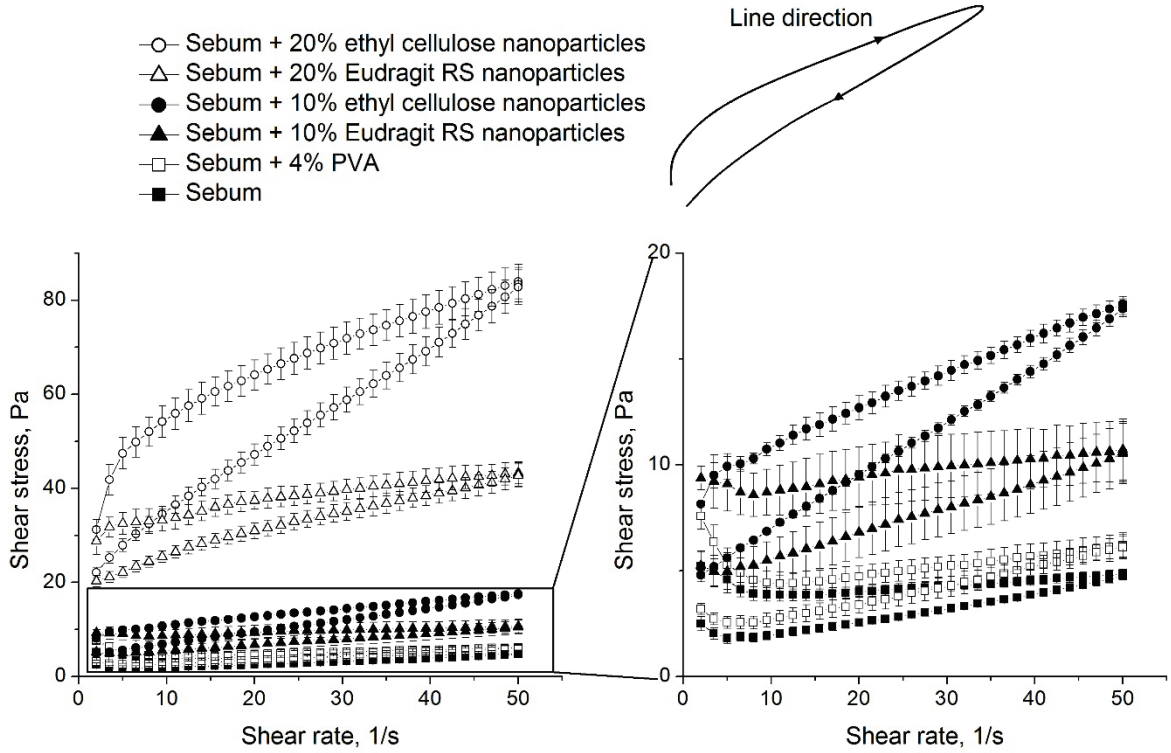

Figure 27: Shear stress as a function of shear rate of artificial sebum and artificial sebum mixtures with PVA, ethyl cellulose nanoparticles and Eudragit® RS nanoparticles at 37 °C.

Addition of PVA, ethyl cellulose nanoparticles and Eudragit® RS nanoparticles had no effect on the shear thinning pseudo plastic thixotropic flow behavior of the artificial sebum. 2% (data not shown) and 4% (w/w) PVA in artificial sebum had an insignificant effect on the viscosity of artificial sebum what correspond to the amount of PVA after the addition of 10% and 20% (w/w) nanoparticle formulation to artificial sebum, respectively. However, in case of ethyl cellulose and Eudragit® RS nanoparticles the viscosity of the artificial sebum increased proportional to the percentage of nanoparticles added (Figure 26).

Generally, ethyl cellulose nanoparticles increased the viscosity of the artificial sebum more than Eudragit® RS nanoparticles due to their dissolution in the sebum unlike the Eudragit® RS nanoparticles. In fact ethyl cellulose is an established gelling agent in oils (Davidovich-Pinhas et al., 2015). The increased viscosity in case of Eudragit® RS nanoparticles can also be explained by the Krieger-Dougherty equation (Equation 1).

$$\frac{\eta}{\eta_0} = (1 - \frac{\varphi}{\varphi_m})^{-[\eta]\varphi_m}$$ Equation 1

where η is the viscosity of the suspension, η_0 is the viscosity of the medium, [η] is the intrinsic viscosity (2.5 for spheres), φ is the volume concentration of particles, φ_m is φ at the maximum packing.

The viscosity increases at high volume fraction of the dispersed phase (φ) as the particles become more closely packed and their free movement is hindered. Additionally charged nanoparticles increase the viscosity higher than uncharged nanoparticles, because charge increases the effective diameter of particles, what is comparable to an increase of the volume fraction of already constrained particles (Heine et al., 2010).

The viscoelastic behavior of the artificial sebum alone and when mixed with PVA, ethyl cellulose nanoparticles or Eudragit® RS nanoparticles was investigated by amplitude sweep tests. Thereby the ability of artificial sebum to store energy, what characterize an elastic behavior of solids (storage modulus, G´), and to dissipate energy as it flows, what characterize a viscous behavior of liquids (loss modulus, G´´), was measured.

At low strains the storage modulus (G´) values were bigger than the loss modulus (G´´) values indicating a gel like behavior of a viscoelastic solid. The intersection of the G´ and G´´ curve at higher strains is the gel-sol transition point where the gel structure of the artificial sebum was liquefied. After the gel-sol transition point the G´´ values were bigger than the G´ values indicating the viscoelastic behavior of a liquid (Figure 28).

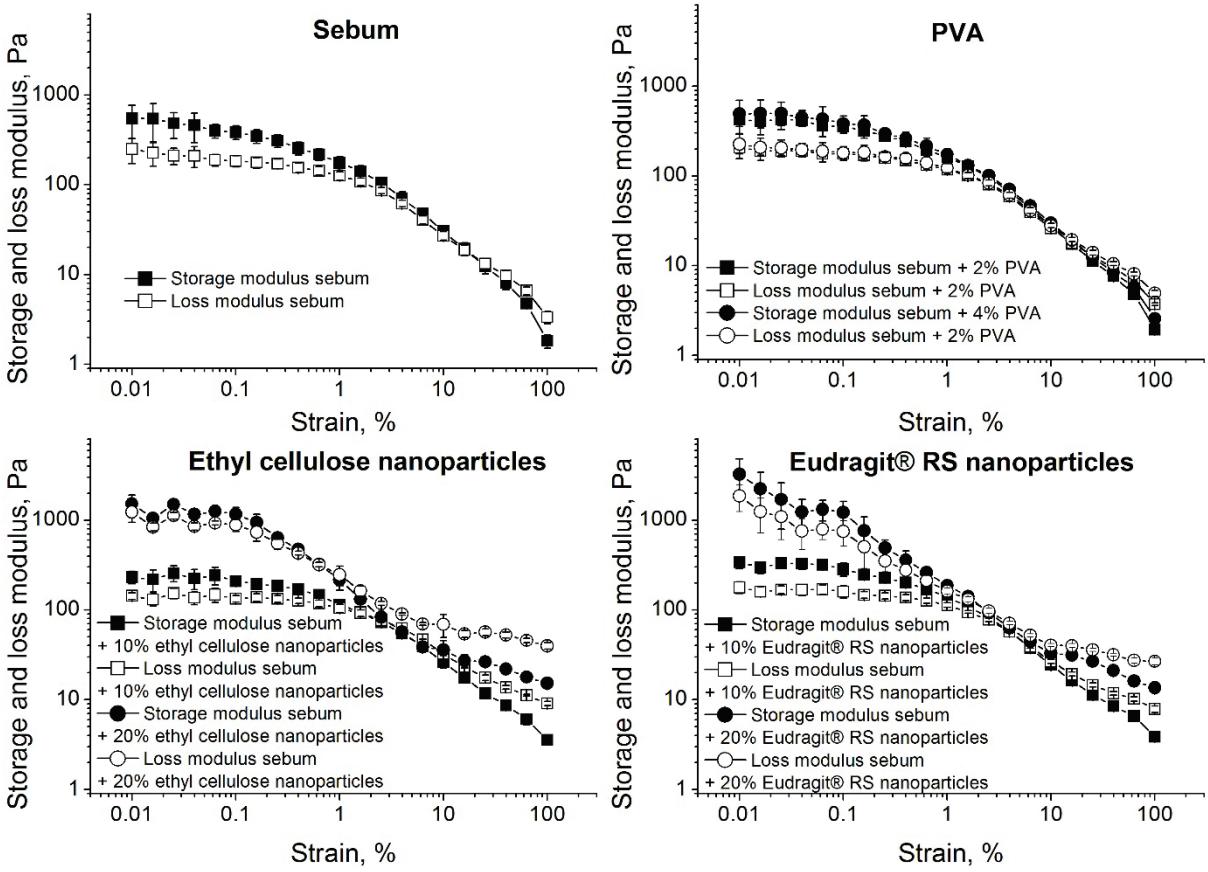

Figure 28: Storage and loss moduli as a function of strain of artificial sebum and artificial sebum mixtures with PVA, ethyl cellulose and Eudragit® RS nanoparticles at 37 °C.

2% and 4% (w/w) PVA in artificial sebum had an insignificant effect on the viscoelastic properties of artificial sebum. The addition of 10% (w/w) ethyl cellulose nanoparticles to artificial sebum slightly increased the viscosity and the G´´ values especially at high stress and strain values. Increasing the ethyl cellulose nanoparticles amount to 20% (w/w) increased both, the G´ and the G´´, values. The distance between G´ and G´´ values decreased and the gel-sol transition point shifted to a lower strain after the addition of ethyl cellulose nanoparticles and with increasing ethyl cellulose nanoparticle concentrations in comparison to artificial sebum (Table 5). Thus, the gel like structure of the artificial sebum was preserved after the addition of ethyl cellulose nanoparticles. However, the smaller difference of G´ and G´´ and the shift in the gel-sol transition point after addition of ethyl cellulose nanoparticles suggest that the interactions inside sebum, which formed the gel like structure were disturbed by ethyl cellulose, because the gel like structure liquefied under smaller strain values in comparison to artificial sebum.

Table 5: Gel-sol transition points of artificial sebum and artificial sebum mixtures with PVA, ethyl cellulose nanoparticles and Eudragit® RS nanoparticles

Mixture	Gel-sol transition point (Strain, %)
Sebum	17.63% ± 3.35%
Sebum + 2% (w/w) PVA	13.67% ± 2.87%
Sebum + 4% (w/w) PVA	14.53% ± 1.50%
Sebum + 10% (w/w) ethyl cellulose nanoparticles	1.96% ± 0.89%
Sebum + 20% (w/w) ethyl cellulose nanoparticles	0.67% ± 0.03%
Sebum + 10% (w/w) Eudragit® RS nanoparticles	4.78% ± 1.12%
Sebum + 20% (w/w) Eudragit® RS nanoparticles	2.06% ± 0.57%

The addition of 10% (w/w) Eudragit® RS nanoparticles had no effect on the viscoelastic properties of the artificial sebum. However, 20% (w/w) Eudragit® RS nanoparticles increased the G´ and G´´ value (Figure 28) and the gel-sol transition point decreased to lower strain values by increasing the amount of Eudragit® RS nanoparticles (Table 5). The effect was less pronounced in comparison to ethyl cellulose nanoparticles, which dissolve inside sebum what increase possible interferences. It indicated that, although Eudragit® RS nanoparticles were insoluble inside sebum, the high amounts of undissolved nanoparticles perturb the gel organization by their accommodation and decreased the rigidity and viscoelasticity of the gel-like structure of the artificial sebum (Pal et al., 2009).

Nanoparticles deeply penetrate into hair follicles, because of the pumping and ratchet effect of the hair follicle surface structure (Patzelt et al., 2011; Radtke et al., 2017). Furthermore, nanoparticles remain inside the hair follicle for up to 10 days, because of the slow sebum flow out of the hair follicle (Lademann et al., 2006; Lademann et al., 2007). However, the examined effects of nanoparticles on the rheological properties of artificial sebum could be another reason. The shift in gel-sol transition to lower strains by their interaction with the sebum potentially led to a liquefied sebum due to the hair movement and a deeper penetration of the nanoparticles. The increase in sebum viscosity potentially reduce the sebum flow out of the hair follicle and increase the nanoparticle retaining time inside the hair follicle.

Nevertheless, the effect of nanoparticles on the rheological properties of sebum could led to hair follicle and skin irritations, as sebum is a significant factor for example in the acne formation (Youn, 2010).

3.2.4. *In vitro* drug release

The *in vitro* drug release of the different dexamethasone-loaded nanoparticles namely, nanocrystals, Eudragit® RS and ethyl cellulose nanoparticles (Table 6) was investigated with Franz diffusion cells. During the measurement the regenerated cellulose membrane, which was mounted on the Franz diffusion cells, was soaked in water, paraffin or artificial sebum to investigate the effect of paraffin and artificial sebum on the *in vitro* drug release of the different nanoparticles.

Table 6: Composition, size, PDI and loading capacity of the different nanoparticles investigated that contained 0.06% (w/w) dexamethasone.

Nanocarrier	Composition	Z-Average (nm)	PDI	Loading capacity (%)
Nanocrystals	0.5% (w/v) PVA	355	0.150	-
Eudragit® RS nanoparticles	5% (w/w) Eudragit® RS, 1.25% (w/v) PVA	90	0.233	0.8
Ethyl cellulose nanoparticles (LC 2%)	2% (w/w) ethyl cellulose, 0.5% (w/v) PVA	137	0.075	2.1
Ethyl cellulose nanoparticles (LC 1%)	5% (w/w) ethyl cellulose, 1.25% (w/v) PVA	168	0.143	0.9

The solubility of dexamethasone in water, paraffin and artificial sebum at 60 °C was 157 ± 12 µg/ml (examined quantitative), 50 µg/ml and 100 µg/ml (examined half quantitative), respectively. Its paraffin/water and sebum/water partitioning coefficient at 37 °C was 0.25 ± 0.08 and 0.96 ± 0.12, respectively. Dexamethasone nanocrystals were used as control to investigate the effect of artificial sebum on the dexamethasone partitioning between donor and acceptor compartment. The paraffin soaked membrane was used as solvent control, because ethyl cellulose is insoluble in paraffin. The amount of paraffin and artificial sebum on the membranes after soaking them for 15 h was 131 ± 31 mg and 49 ± 14 mg, respectively.

Membrane soaking had no significant effect on the *in vitro* drug release of dexamethasone nanocrystals (Figure 29a). This result indicated that neither the additional lipid layer as compartment with a partition coefficient between the donor and

acceptor nor the higher viscosity of the artificial sebum compartment had an effect on the dexamethasone partitioning from donor to acceptor compartment.

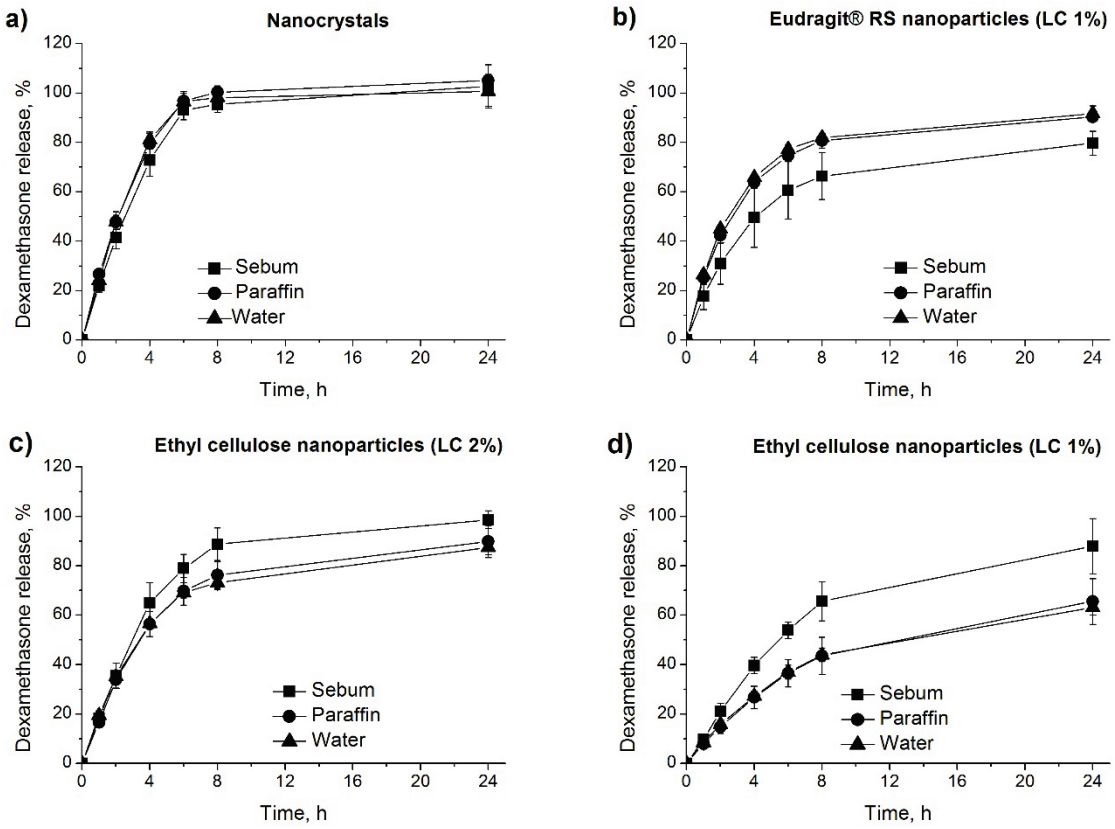

Figure 29: *In vitro* drug release of dexamethasone nanocrystals (a), dexamethasone-loaded Eudragit® RS nanoparticles with 1% loading capacity (b), dexamethasone-loaded ethyl cellulose nanoparticles with 2% loading capacity (c) and dexamethasone-loaded ethyl cellulose nanoparticles with 1% loading capacity (d) investigated with Franz-diffusion cells with regenerated cellulose membranes soaked with artificial sebum, paraffin or water.

The dexamethasone release from Eudragit® RS nanoparticles was significantly slower with artificial sebum soaked membranes compared to the water and paraffin soaked membranes. However, there was no significant difference in drug release between water and paraffin soaked membranes (Figure 29b). The slower dexamethasone release from Eudragit® RS nanoparticles with artificial sebum soaked membrane indicated an interaction between sebum and Eudragit® RS nanoparticles, which decreased the drug release. Potentially the increased viscosity of the artificial sebum, after the addition of Eudragit® RS nanoparticles (Figure 26) decreased the dexamethasone release of Eudragit® RS nanoparticles what can be explained by the Stokes-Einstein equation (Equation 2). The higher viscosity of artificial sebum with

Eudragit® RS nanoparticles reduced the dexamethasone diffusion coefficient, release and partitioning into the donor compartment.

$$D = \frac{k \times T}{6 \times \pi \times \eta \times r}$$ Equation 2

where D is the diffusion coefficient, k the Boltzmann´s constant, T the absolute temperature, η the viscosity of the media and r the radius of the dissolved molecule.

The dexamethasone release from ethyl cellulose nanoparticles was significantly faster with artificial sebum soaked membranes compared to paraffin and water soaked membranes, because ethyl cellulose nanoparticles dissolved in the artificial sebum and released the drug faster (Figure 29c and d). The higher viscosity of artificial sebum with ethyl cellulose nanoparticles (Figure 26) did not reduced the dexamethasone release of the ethyl cellulose nanoparticles in contrast to Eudragit® RS nanoparticles, because the fast dissolution of ethyl cellulose nanoparticles after the contact with sebum resulting in a fast drug release, overruled the effect of the increased viscosity. Interestingly the drug release decreased considerably with decreasing loading capacity, because a lower loading capacity was achieved by increasing the amount of the polymer in the disperse phase to keep the amount of suspension applied in the donor phase constant. Therefore the applied polymer amount increased resulting in a higher viscosity of the artificial sebum decreasing the dexamethasone release.

The dexamethasone release of ethyl cellulose nanoparticles with paraffin and water soaked membranes was slower compared to sebum soaked membrane because dexamethasone-loaded ethyl cellulose nanoparticles did not dissolve in water and paraffin. Therefore the dexamethasone is released in a diffusion controlled manner of the matrix structure of the ethyl cellulose nanoparticles. The drug release decreased with decreasing loading capacity, too because there is a high degree of drug encapsulation and probable formation of a high tortuous path (Figure 29c and d).

3.2.5. *Ex vivo* follicular penetration study

The *ex vivo* follicular penetration of the nanoparticles was performed in cooperation with the research group of Prof. Dr. Dr.-Ing. Jürgen Lademann using porcine ear skin,

because the hair follicle remains open after the surgical removal in contrast to human skin. In human skin, the skin contracts after surgical removal and as a result the hair follicles remain closed (Patzelt et al., 2008b). Furthermore, porcine tissue has a comparable tissue structure to human skin and is therefore a suitable *ex vivo* model to human skin (Jacobi et al., 2007).

The *ex vivo* follicular penetration of aqueous 5% (w/w) ethyl cellulose and 5% (w/w) Eudragit® RS nanosuspensions with 1.25% PVA (w/v) was investigated (Figure 30).

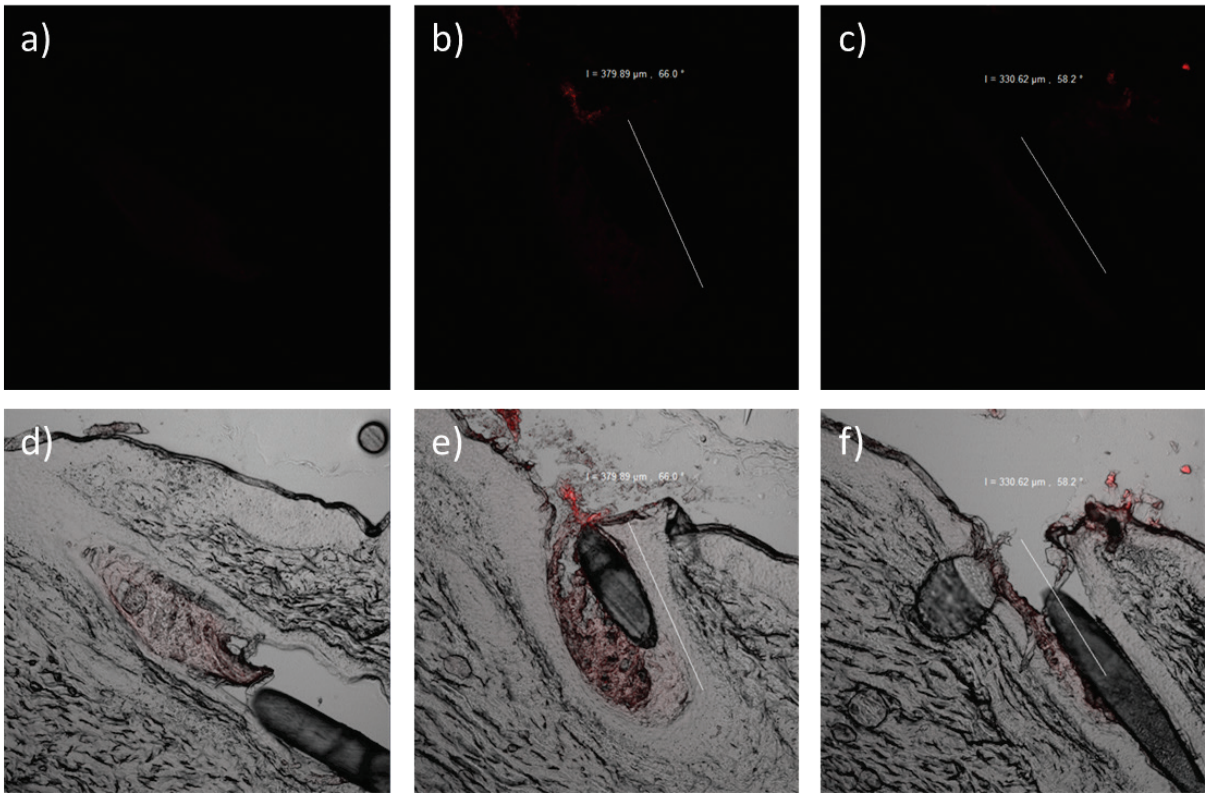

Figure 30: Typical CLSM images of a histological section of a porcine ear skin containing a hair follicle: red fluorescence emission image of a) untreated hair follicle, b) hair follicle treated with Nile red-loaded ethyl cellulose nanoparticles and c) Eudragit® RS nanoparticles and the superimposed image of the transmittance mode and the fluorescence emission image of d) untreated hair follicle, e) hair follicle treated with ethyl cellulose nanoparticles and f) Eudragit® RS nanoparticles.

Both nanoparticles were loaded with 0.004% (w/w) Nile red and the sizes of the ethyl cellulose and Eudragit® RS nanoparticles were 159 ± 1 nm and 90 ± 1 nm, respectively. The PDI values were 0.132 ± 0.009 and 0.211 ± 0.002, respectively. Furthermore, the ethyl cellulose nanoparticles were investigated with n-hexane washed and Sebutape® tapped skins, what reduce the sebum amount on skin and inside the hair follicles (Campbell et al., 2012; Pagnoni et al., 1994).

The hair follicular penetration depth of ethyl cellulose and Eudragit® RS nanoparticles was comparable (285 ± 75 µm and 306 ± 30 µm, respectively). This was expected as the nanoparticles had comparable particle sizes, the main factor that determines the hair follicular penetration depth of nanoparticles (Patzelt et al., 2011).

The fluorescence intensity of ethyl cellulose nanoparticles inside the hair follicles in untreated porcine ear skin was higher than in sebum reduced porcine ear skin (Figure 31).

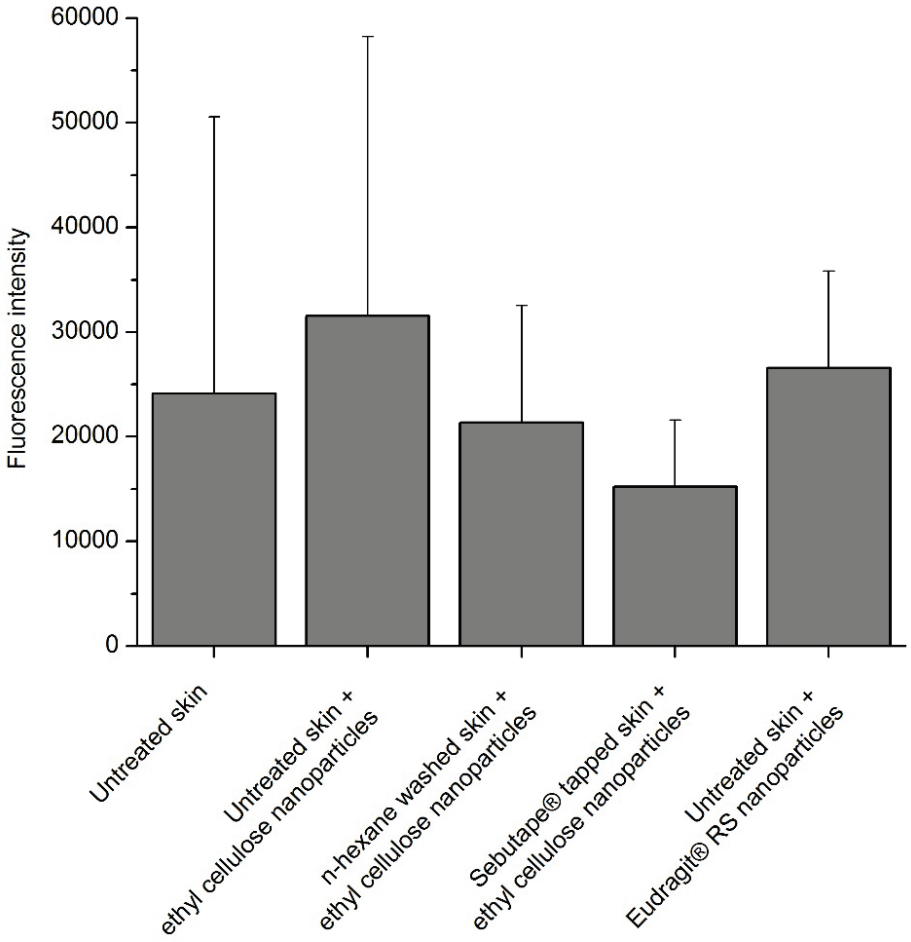

Figure 31: Fluorescence intensity inside porcine ear skin hair follicles of untreated skin, untreated skin with Nile red-loaded ethyl cellulose and Eudragit® RS nanoparticles, n-hexane washed skin with Nile red-loaded ethyl cellulose nanoparticles and Sebutape® tapped skin with Nile red-loaded ethyl cellulose nanoparticles.

This is in line with the *in vitro* results that the sebum dissolved ethyl cellulose nanoparticles inside the hair follicle and the fluorescent dye is released quickly. Without sebum, the ethyl cellulose nanoparticles remain intact and the dye is released slower (Figure 29). Additionally the fluorescence intensity of Eudragit® RS nanoparticles was

lower inside the hair follicles with untreated porcine ear skin in comparison to ethyl cellulose nanoparticles (Figure 31). Eudragit® RS nanoparticles were insoluble in sebum and sebum reduced the drug release of Eudragit® RS nanoparticles in contrast to ethyl cellulose nanoparticles (Figure 29), what is reflected by the *ex vivo* follicular penetration study. The difference in fluorescence intensity of the released dye and the dye inside the nanoparticles can be explained by the self-quenching between the unreleased fluorescence molecules inside the nanoparticles what reduces the fluorescence intensity (Imhof et al., 1999).

3.2.6. Conclusions

Promising sebum-responsive polymeric nanoparticles were prepared and characterized. Ethyl cellulose was the only sebum soluble polymer among the ten different polymers screened. Ethyl cellulose exhibited a sebum solubility of 20% (w/w) without changing the thermal behavior of the artificial sebum. Ethyl cellulose microparticle dissolved fast inside artificial sebum and the *in vitro* drug release of dexamethasone-loaded ethyl cellulose nanoparticles was increased in sebum. *Ex vivo* Nile red-loaded ethyl cellulose nanoparticles exhibited a higher fluorescence intensity in hair follicles of untreated porcine ear skin than in sebum reduced porcine ear skin. These results indicated that ethyl cellulose nanoparticles will dissolve inside hair follicles after coming in contact with sebum and release the loaded drug close to the target site.

Therefore, sebum-responsive ethyl cellulose nanoparticles could be established which could improve the treatment efficiency of drugs for hair follicle associated skin diseases. Ethyl cellulose nanoparticles will penetrate into the hair follicle and after contact with sebum release the loaded drug in close proximity to the target structure.

However, CLSM is a semi-quantitative method and it is difficult to exactly quantify the amount of dye that was released by the nanoparticles. Thus, this method should be complemented with other sensitive, precise and accurate analytical *ex* and *in vivo* methods to further investigate the clinical potential of ethyl cellulose nanoparticles.

Nevertheless, the viscosity of artificial sebum increased and the viscoelastic behavior changed after the addition of ethyl cellulose nanoparticles. Therefore, the irrational

potential to skin and hair follicle of ethyl cellulose nanoparticles should be investigated *in vivo*.

3.3. Part III: Comparison of *in vitro* drug release methods[4]

In vitro drug release is one of the most important methods used to assess the quality of and estimate the *in vivo* performance of a nanocarrier. To date, there is no compendial method available to evaluate drug release from various pharmaceutical nanocarriers. Consequently, various *in vitro* drug release techniques have been used. These methods can be broadly categorized in sample and separate, dialysis membrane, and *in situ* methods (D'Souza, 2014).

The different techniques may give different results as the methods are different in their working principles and even with the same method different results might be obtained when working under sink and non-sink conditions (Mishra et al., 2009; Murdande et al., 2015).

The choice of a drug release method for analysis of nanocarriers has in most cases been random without giving an account about their reproducibility and ability to discriminate release between different dosage forms. Therefore, the objective of this study was to assess and compare the reproducibility and discrimination potentials of three *in vitro* drug release methods, namely dialysis bags, Franz diffusion cells and the *in situ* drug release Sirius® inForm apparatus. The nanocarriers investigated include nanocrystals, polymeric nanoparticles and lipid nanoparticles under sink and non-sink conditions. Furthermore, the obtained *in vitro* results were correlated with *ex vivo* experiments with excised human skin to investigate the clinical relevance of the *in vitro* results.

3.3.1. Nanocarrier formulation and characterization

Different types of dexamethasone-loaded nanocarriers with different properties were prepared for the release experiments (Table 7).

As expected, the viscosity of the nanocrystals and ethyl cellulose nanosuspensions increased upon formulating them into HEC gels and their flow behavior changed from

[4] Parts of this chapter were taken from: B. Balzus, M. Colombo, F.F. Sahle, G. Zoubari, S. Staufenbiel, R. Bodmeier, Comparison of different in vitro release methods used to investigate nanocarriers intended for dermal application, Int. J. Pharm., 513 (2016) 247-254.

Newtonian to shear-thinning type (Figure 32). The increase in viscosity was proportional to the concentration of HEC used. Microscopic observations and dynamic light scattering results showed that the nanocarriers did not agglomerate upon addition of HEC.

Table 7: Composition, size, PDI and encapsulation efficiency of the investigated nanocarriers containing 0.05% (w/w) dexamethasone.

Nanocarrier	**Composition**	**Z-Average (nm)**	**PDI**	**Encapsulation efficiency (%)**
Nanocrystals	0.49% (w/v) poloxamer 407	268 ± 8	0.127 ± 0.041	-
Lipid nanoparticles	7.5% (w/w) Gelucire®, 2.5% (w/w) Witepsol®	112 ± 13	0.186 ± 0.133	93.6 ± 0.9
Eudragit® RS nanoparticles	5% (w/w) Eudragit® RS, 2.5% (w/v) PVA	70 ± 1	0.200 ± 0.008	66.8 ± 0.4
Ethyl cellulose nanoparticles	5% (w/w) ethyl cellulose, 2.5% (w/v) PVA	140 ± 1	0.119 ± 0.008	88.2 ± 0.1

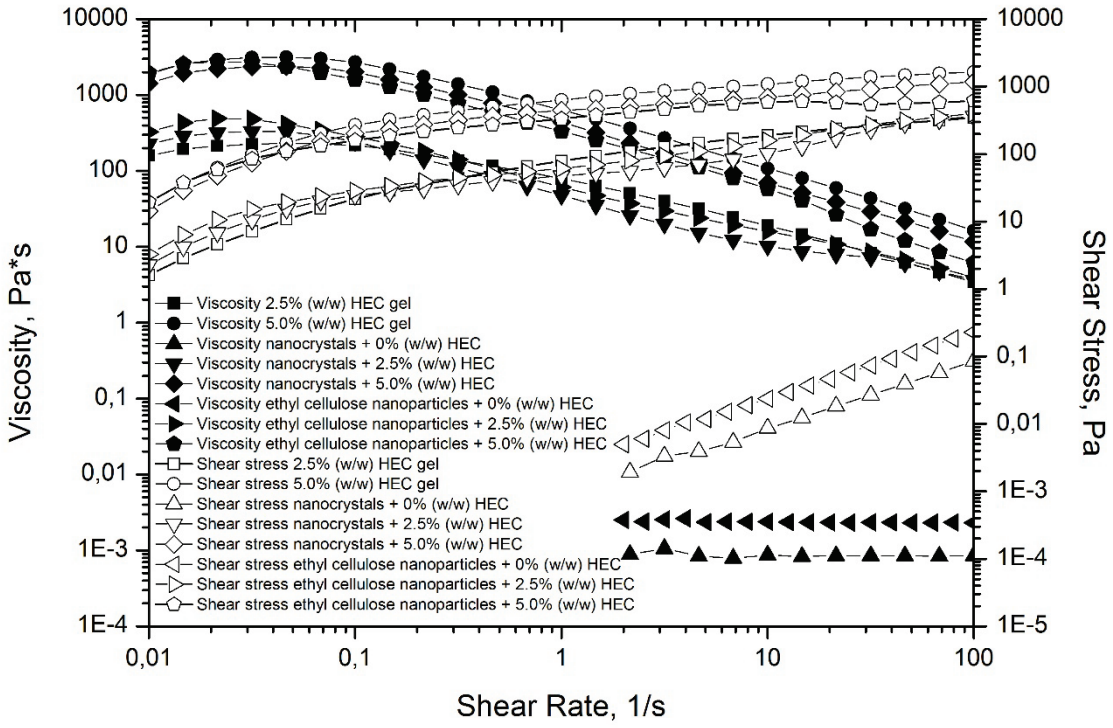

Figure 32: Rheological properties of nanocrystals and ethyl cellulose nanoparticles before and after incorporation of different amount of HEC.

However, the size of the ethyl cellulose nanoparticles decreased from 140 nm to 88 nm and 71 nm and the PDI values increased from 0.119 to 0.216 and 0.283, respectively, upon incorporation of 2.5% and 5.0% (w/w) HEC. This could be attributed to the addition of a relatively high amount of the polymer HEC, which affected the average particle size obtained with the dynamic light scattering. The dynamic light scattering data of the 2.5% and 5.0% HEC dispersion prepared by the same method but without the nanocarriers gave sizes of 40 ± 2 nm and 26 ± 2 nm, respectively. As a result, the average size of the peak decreased and the PDI increased.

3.3.2. Drug release investigations and method comparison

3.3.2.1. In situ drug release investigation using Sirius® inForm

Sirius® inForm is a relatively new instrument which is designed to carry out a number of formulation and preformulation investigations, including drug release studies, in a short period of time. Accordingly, its potential use in assessing dexamethasone release *in situ* from colloidal dispersions of nanocrystals, lipid nanoparticles and Eudragit® RS nanoparticles under sink and non-sink conditions was assessed (Figure 33).

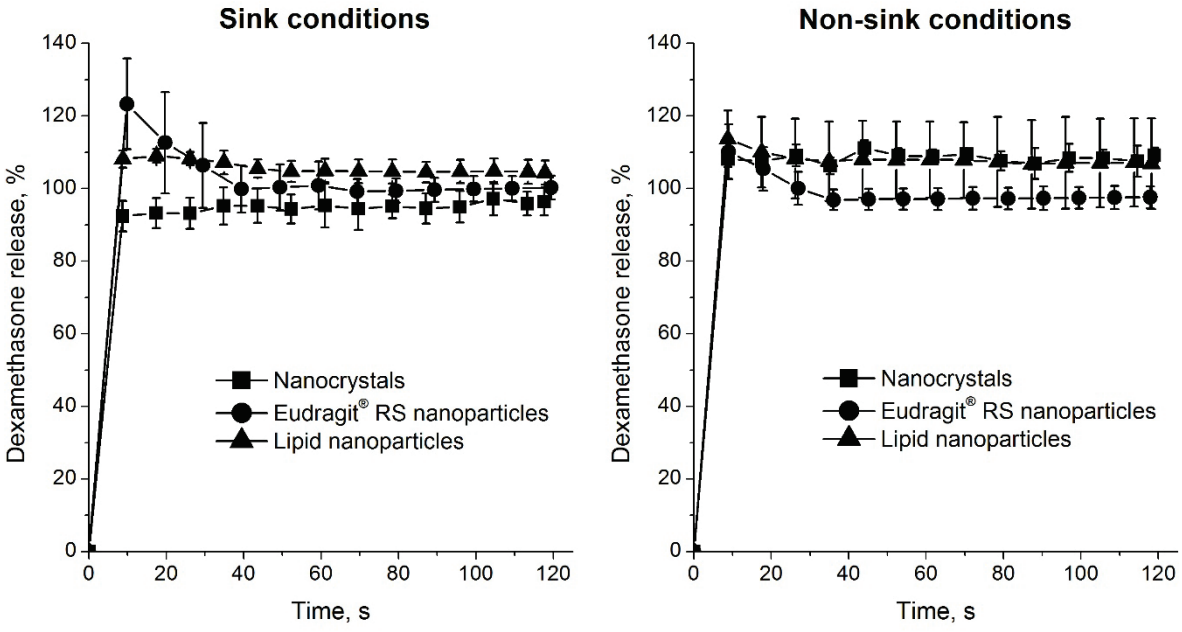

Figure 33: Dexamethasone release from different nanocarriers under sink and non-sink conditions as investigated *in situ* by using Sirius® inForm.

However, drug release was completed in few seconds and no significant difference in drug release between the nanocarriers was observed. Besides, drug release from ethyl

cellulose nanoparticles could not be investigated both under sink and non-sink conditions due to the high background scattering caused by the dispersed nanoparticles, which significantly interfered with the UV readings.

In situ drug release from lyophilized nanocrystals and Eudragit® RS nanoparticles was also investigated under sink condition (Figure 34).

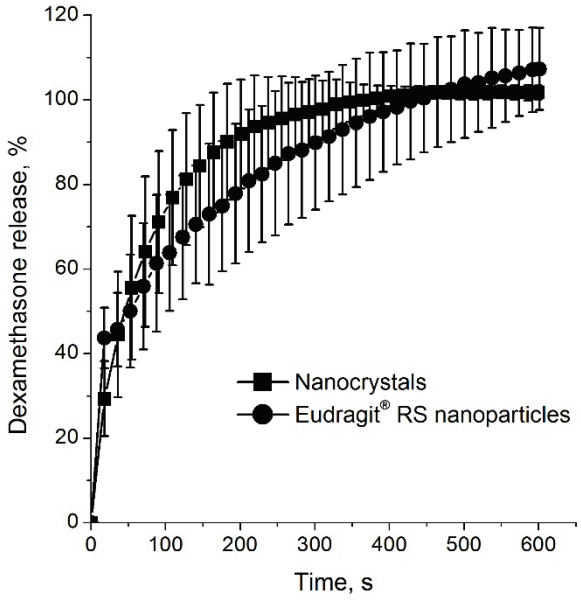

Figure 34: Dexamethasone release from freeze-dried nanocrystals and Eudragit® RS nanoparticles under sink conditions as investigated *in situ* by using Sirius® inform.

Like with the liquid nanocarrier dispersions, no significant difference in drug release between the nanocarriers was observed. However, the release/dissolution from/of the freeze-dried nanocarriers was slower because of the time need for nanocarrier wetting and drug dissolution. The nanocrystals and Eudragit® RS nanoparticles were redispersible without any significant change in particle size (289.7 nm; PDI 0.068 and 72.8 nm; PDI 0.209, respectively).

3.3.2.2. In vitro drug release investigation using Franz diffusion cells

The Franz diffusion cell is a commonly used apparatus to assess release of drugs from various dosage forms intended for application to the skin. The release from nanocrystals and Eudragit® RS nanoparticles was faster than from lipid nanoparticles and ethyl cellulose nanoparticles under both sink and non-sink conditions (Figure 35).

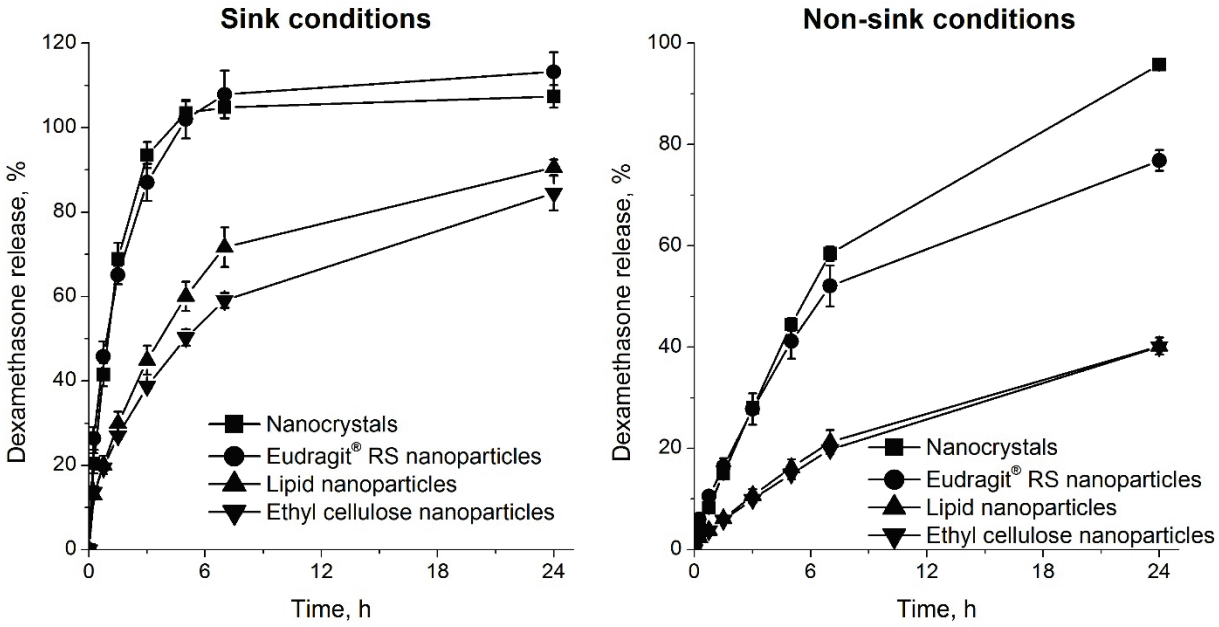

Figure 35: Dexamethasone release from different nanocarriers under sink and non-sink conditions investigated with Franz diffusion cells (n=4, mean ± SD).

With nanocrystals, the dispersion phase is saturated with the drug and a burst release as a result of dissolved drug is expected. Faster drug release is also expected with Eudragit® RS nanoparticles due to low drug encapsulation efficiency and their more hydrophilic character. The release profiles clearly reflect these phenomena showing that the method is discriminative. However, both under sink and non-sink conditions, there was no significant difference in drug release between nanocrystals and Eudragit® RS nanoparticles and between lipid nanoparticles and ethyl cellulose nanoparticles. This suggests that the nanocarriers exhibited similar drug release or the method is not adequate to show the differences in drug release.

3.3.2.3. In vitro drug release investigation using dialysis bags

Assessment of dexamethasone release from the different nanocarriers using dialysis bags indicated that, unlike Franz diffusion cell experiments, under both sink and non-sink conditions drug release from nanocrystals was faster than the drug release from Eudragit® RS nanoparticles (Figure 36).

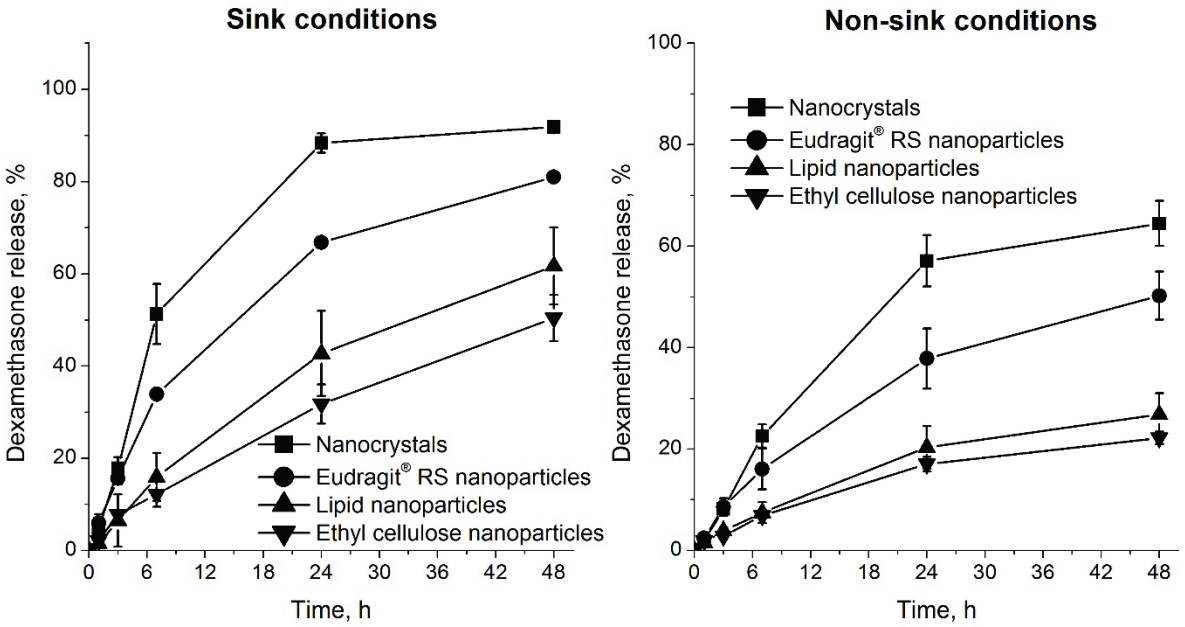

Figure 36: Dexamethasone release from different nanocarriers under sink and non-sink conditions investigated with dialysis bags.

In addition, like with Franz diffusion cell experiments, release from nanocrystals and Eudragit® RS nanoparticles was faster than from lipid nanoparticles and ethyl cellulose nanoparticles although there was no significant difference in drug release between the lipid nanoparticles and ethyl cellulose nanoparticles, especially under non-sink conditions.

Although the dialysis bag method is more discriminative it was also associated with some drawbacks. The method was less reproducible than the Franz diffusion cell experiments as shown by the larger error bars on the release profile curves (Figure 35 and Figure 36). This can be due to a lack of complete control over the area of the diffusion membrane unlike with the Franz diffusion cell, which is always given by the size of the diameter of the cell. In addition, during the release experiments the volume of the colloidal dispersion in the dialysis bags decreased significantly. The volume shrinkage was associated to water diffusion from the donor compartment into the acceptor compartment due to osmolality differences. Thus drug release using dialysis bags would also be significantly affected by the osmolality differences between the donor and acceptor media.

Another problem observed with both dialysis bags and Franz diffusion cells was that under non-sink conditions the nanocrystals agglomerated in the donor compartment during the release experiments (Figure 37a and Figure 37b).

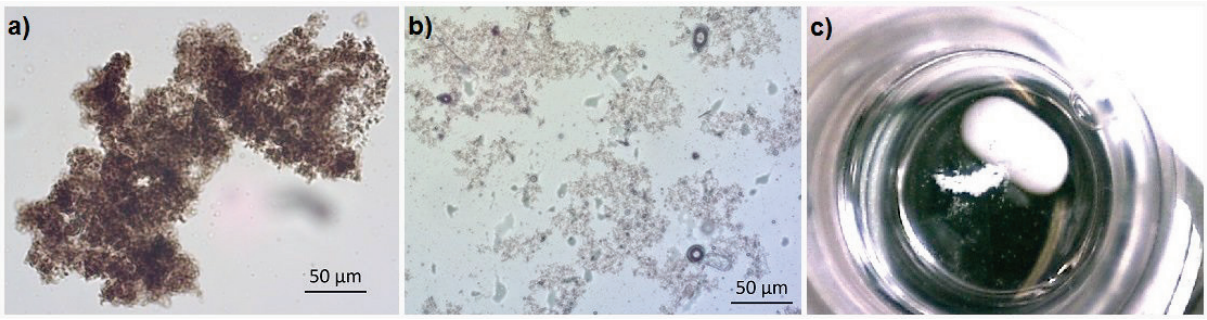

Figure 37: Agglomerates of nanocrystals detected after *in vitro* release experiments conducted under non-sink conditions: a) microscopic images in dialysis bags, b) microscopic images on the surface of Franz diffusion cell membrane, c) images on the surface of Franz diffusion cell membrane-experiment conducted after adjusting the osmolality of the donor compartment.

The instability could be associated to the differences in medium osmolality in the donor and acceptor compartments, which might cause diffusion of electrolytes from the acceptor compartment into the donor compartment, which could have a salting out effect on the dispersed nanocarriers, and/ or rapid diffusion of the stabilizer from the donor compartment into the acceptor compartment. To better understand this a set of experiments were conducted. Adjusting the osmolality of the donor compartment to that of the acceptor compartment with sodium chloride resulted in rapid particle agglomeration even before the start of the release experiment. A significant decrease of zeta potential from -12.7 ± 0.1 mV to -2.7 ± 0.3 mV (poor data quality due to particle agglomeration) was also observed. At the end of the release experiment, few large fluffy agglomerates formed (Figure 37c). The same agglomerates were also formed on the surface of the membrane, which could only be observed under the microscope, when water or a 0.49% (w/v) poloxamer solution was used in place of pH 7.4 phosphate buffer in the acceptor compartment. However, drug release was significantly faster when the 0.49% (w/v) poloxamer solution was used (Figure 38). This indicated that diffusion of the surfactant contributed to the nanocrystal agglomeration.

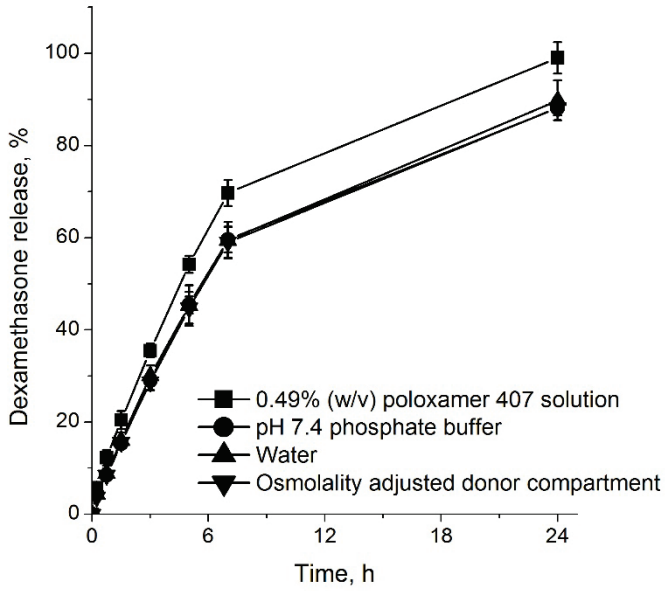

Figure 38: Effect of type of the release media in acceptor compartment and the osmolality of the release media in the donor compartment in Franz diffusion cells on dexamethasone release from nanocrystals under non-sink conditions.

3.3.2.4. Drug release from nanocarriers formulated into HEC gels

For easy application onto the skin it is advantageous to formulate nanocarriers into semisolid dosage forms like gels or creams. Thus, the drug release from HEC gels of nanocrystals and ethyl cellulose nanoparticles was investigated using Franz diffusion cells under non-sink condition (Figure 39). Interestingly, the method was adequate to discriminate dexamethasone release from the HEC gels and between nanocarriers. As expected, the release decreased with increasing HEC concentration and was more rapid with the nanocrystals.

The dexamethasone flux from nanocrystals and ethyl cellulose nanoparticles also decreased by ~2 and ~1.5 folds, respectively, when the aqueous suspensions were formulated into 2.5% (w/w) HEC gel (Figure 40). However, increasing the HEC concentration from 2.5% to 5.0% (w/w) did not affect drug flux significantly. The difference in drug release between nanocrystals and ethyl cellulose nanoparticles is significant at all HEC concentrations.

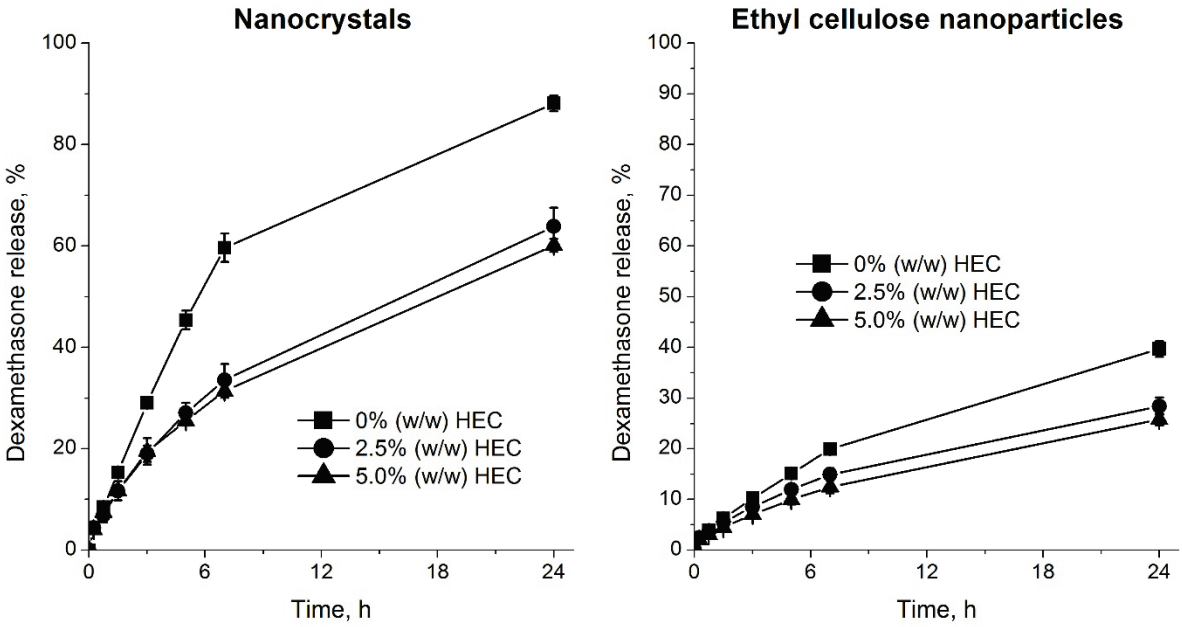

Figure 39: Dexamethasone release from HEC gels of nanocrystals and ethyl cellulose nanoparticles investigated with Franz diffusion cells under non-sink conditions.

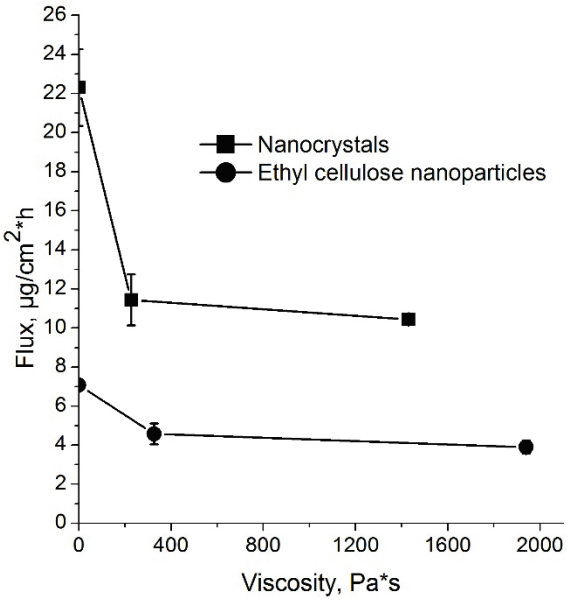

Figure 40: Effect of viscosity of the continuous phase on flux of dexamethasone from nanocrystals and ethyl cellulose nanoparticles through Franz diffusion cell membrane.

However, it was not easy to use dialysis bags for the investigation of drug release from the gels because of the difficulty to uniformly distribute the gels inside the dialysis bags. The Sirius® inForm was also not used for gels because of rapid dispersion of the gels in the dissolution vessel.

To summarize, each *in vitro* release method has its advantages and drawbacks and discriminates drug release to a different extent (Table 8).

Table 8: Summary of advantages/disadvantages of the different methods used to investigate drug release from different nanocarriers.

Attribute	**Release Method**		
	***In situ* drug release - Sirius® inForm**	**Franz diffusion cell**	**Dialysis bag**
Discriminative power	No (very rapid drug release)	Yes	Yes
Release duration	< 10 min	24 - 48 h	48 - 72 h
Simplicity	Sophisticated instrument, simple set up	Longer set-up time	Intermediate
Sample type	Difficult to work with highly scattering samples and semisolids	Easily used with both colloidal dispersions and semisolids	More tedious to use with semisolids
Membrane	No	Fixed surface area, release control by membrane?	Variable surface area, osmolality effects on bag volume?, release control by membrane?
Reproducibility	Good (sometimes too high background scattering)	Good (because of constant surface area)	More variability because of less controllable surface area

3.3.2.5. In vitro - ex vivo correlation of drug release/penetration experiments

The *in vitro* drug release experiments revealed a significant difference in dexamethasone dissolution/release profiles between nanocrystals and ethyl cellulose nanoparticles. To examine if this difference in drug dissolution/release from nanocrystals and ethyl cellulose nanoparticles is potentially consistent with their *in vivo* performance dexamethasone dissolution/release and penetration of both nanoparticles were investigated *ex vivo* with excised human skin in cooperation with the research groups of Prof. Dr. Sarah Hedtrich and of PD Dr. med. Annika Vogt. The

ex vivo experiments were performed with two different methods: Franz diffusion cell method and intradermal microdialysis (Figure 41).

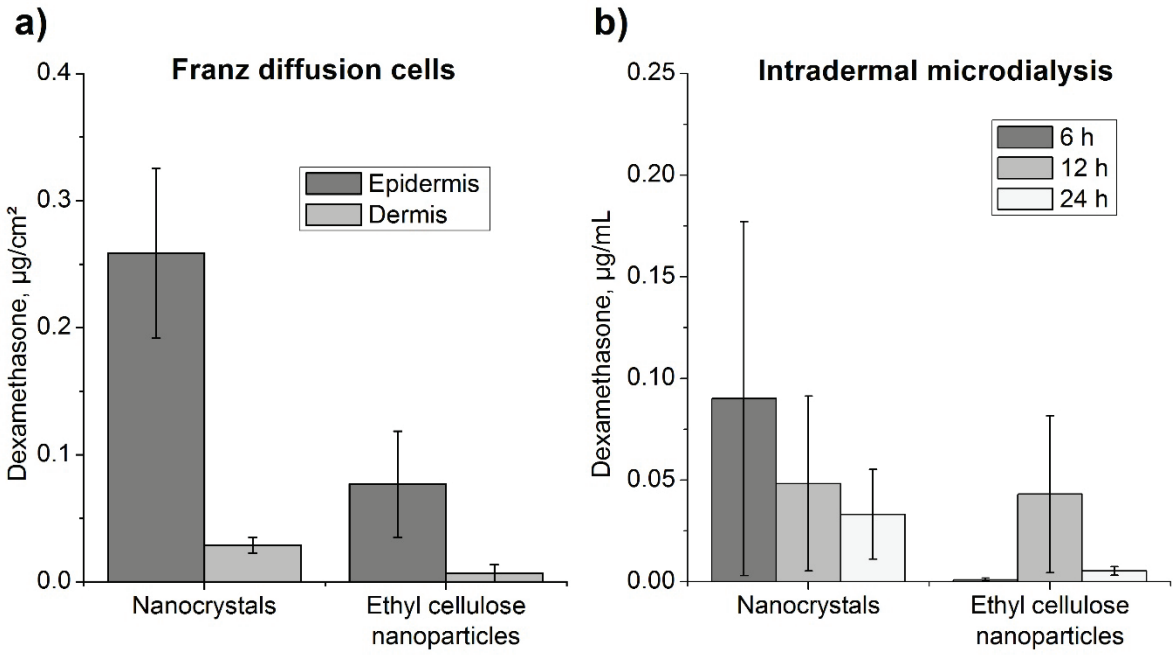

Figure 41: a) Franz diffusion cell experiment with excised human skin: Dexamethasone amount in epidermis and dermis extracts 6 h after topical application of ethyl cellulose nanocarriers and nanocrystals (5 µg/cm^2, n = 4). b) Intradermal microdialysis experiment with excised human skin: Dexamethasone concentration (µg/ml) in dermis eluates 6, 12 and 24 h after topical application of 5 µg/cm^2 dexamethasone (Döge et al., 2016)

Using Franz diffusion cell method with excised human skin, the amount of dexamethasone penetrated into the epidermis and dermis was determined. In contrast, intradermal microdialysis allowed the continuous monitoring of drug penetration and was used to examines the drug dissolution/release kinetic of nanocarriers into the dermis.

In the Franz diffusion cell experiments, with dexamethasone nanocrystals and ethyl cellulose nanoparticles, an insignificant amount of dexamethasone was recovered in the acceptor compartment. With nanocrystals more dexamethasone was recovered in epidermis and dermis in comparison to ethyl cellulose nanoparticles 6 h after topical application indicating a faster dexamethasone penetration of nanocrystals.

In the intradermal microdialysis experiments the dexamethasone release into the dermis was faster from nanocrystals in comparison to ethyl cellulose nanoparticles.

Already after 6 h high dexamethasone concentrations in the dermis were detected with nanocrystals which was in line with the *ex vivo* Franz diffusion cell results. In the case of ethyl cellulose nanoparticles dexamethasone release was slower and only after 12 h a higher dexamethasone concentration in the dermis was reached.

Results of both *ex vivo* experiments were consistent with the results of *in vitro* drug release experiments where the dexamethasone dissolution of nanocrystals was significantly faster in comparison to the dexamethasone release from ethyl cellulose nanoparticles.

3.3.3. Conclusions

Dialysis bag and Franz diffusion cell method discriminated drug release from different nanocarriers but not the *in situ* method using the Sirius® inForm. Drug release investigation using Franz diffusion cells had better repeatability/reproducibility than the release assessment performed using dialysis bags. The drug release profiles of the nanocarriers obtained with the different methods at both sink and non-sink conditions were not the same. However, the drug dissolution/release from nanocrystals and ethyl cellulose nanoparticles with all investigated methods was significantly different, except with the *in situ* method. *Ex vivo* experiments with human skin using Franz diffusion cells and intradermal microdialysis revealed that the difference between nanocrystals and ethyl cellulose nanoparticles was consistent with their *ex vivo* performance. In conclusion the investigated dialysis methods (Franz diffusion cell and dialysis bag methods) can be used to discriminate drug release profiles of nanocarriers that might differ in their *in vivo* performance.

4. Summary[5]

Controlled delivery of corticosteroids to the skin and hair follicle using nanoparticles may reduce their side effects and maximize treatment effectiveness. To assess the quality of nanoparticles and estimate their *in vivo* performance, *in vitro* drug release measurement is one of the most important methods.

Dexamethasone-loaded polymeric nanoparticles should be prepared, which adhere well to the skin and release the drug slowly, in a controlled manner. Additionally, sebum-responsive nanoparticles should be prepared, which are able to penetrate deep into the hair follicle and release the drug triggered by their dissolution in sebum.

The discriminative power and reproducibility of three *in vitro* drug release methods for nanoparticles, namely dialysis bags, Franz diffusion cells and an *in situ* drug release method using Sirius® inForm apparatus should be assessed. The investigated nanoparticles were nanocrystals, polymeric nanoparticles and lipid nanoparticles.

Dexamethasone-loaded ethyl cellulose, Eudragit® RS and ethyl cellulose/Eudragit® RS nanoparticles were prepared by the solvent evaporation method. Dexamethasone release from the polymeric nanoparticles was investigated *in vitro* using Franz diffusion cells. Drug penetration was assessed *ex vivo* using excised human skin. Follicular penetration of nanoparticles was investigated *ex vivo* using pig ear skin.

Eudragit® RS nanoparticles were smaller and positively charged but had a lower dexamethasone loading capacity (0.3–0.7%) than ethyl cellulose nanoparticles (1.4–2.2%). By blending the two polymers (1:1), small (105 nm), positively charged (+37 mV) nanoparticles with sufficient dexamethasone loading (1.3%) were obtained. Dexamethasone release and penetration significantly decreased with decreasing drug

[5] Parts of this were taken from:

1. B. Balzus, F.F. Sahle, S. Hönzke, C. Gerecke, F. Schumacher, S. Hedtrich, B. Kleuser, R. Bodmeier, Formulation and ex vivo evaluation of polymeric nanoparticles for controlled delivery of corticosteroids to the skin and the corneal epithelium, Eur. J. Pharm. Biopharm., 115 (2017) 122-130.
2. B. Balzus, M. Colombo, F.F. Sahle, G. Zoubari, S. Staufenbiel, R. Bodmeier, Comparison of different in vitro release methods used to investigate nanocarriers intended for dermal application, Int. J. Pharm., 513 (2016) 247-254.

to polymer ratio and increased when Eudragit® RS was blended with ethyl cellulose. *Ex vivo*, drug release and penetration from the nanoparticles was slower than a conventional cream.

Ethyl cellulose dissolved fast in artificial sebum, whereas Eudragit® RS was insoluble. Artificial sebum increased the drug release from ethyl cellulose nanoparticles, whereas it reduced the drug release from Eudragit® RS nanoparticles indicating a sebum-responsive drug release from ethyl cellulose nanoparticles. The hair follicle penetration depth of Eudragit® RS (330 µm) and ethyl cellulose nanoparticles (380 µm) was comparable, but the fluorescence intensity inside the hair follicle was higher from Nile red-loaded ethyl cellulose nanoparticles compared to Eudragit® RS nanoparticles.

In conclusion, the prepared nanoparticles showed great potential to control the release and penetration of corticosteroids on the skin and in the hair follicle to maximize treatment effectiveness.

The comparison of the different *in vitro* drug release methods indicated that the methods differ in their discriminative power and reproducibility. The *in situ* measurement was a simple and fast method, but not adequately discriminating because of a too rapid drug dissolution/release. Franz diffusion cells and dialysis bags were in most cases discriminative for the different nanoparticles with the drug dissolution/release being in the order of nanocrystals > Eudragit® RS nanoparticles > lipid nanoparticles ≥ ethyl cellulose nanoparticles. However, drug release experiments with Franz diffusion cells had the highest reproducibility.

5. Zusammenfassung[6]

Die kontrollierte Abgabe von Kortikosteroiden auf der Haut und im Haarfollikel unter Verwendung von Nanopartikeln könnte ihre Nebenwirkungen reduzieren und die Wirksamkeit der Behandlung maximieren. Zur Beurteilung der Qualität von Nanopartikeln und ihres *in vivo* Verhaltens, ist die Untersuchung der *in vitro* Freisetzung eine der wichtigsten Methoden.

Es sollten mit Dexamethason beladene Polymernanopartikel hergestellt werden, die gut auf der Haut haften und den Arzneistoff langsam und kontrolliert freisetzen. Zusätzlich sollten Talg sensitive Nanopartikel hergestellt werden, die in der Lage sind, tief in den Haarfollikel einzudringen und durch ihre Auflösung im Talg den Arzneistoff freizusetzen.

Die diskriminierenden Eigenschaften und die Reproduzierbarkeit der folgenden drei *in vitro* Freisetzungsmethoden für Nanopartikel sollten bewertet werden: Dialysebeutel, Franz-Diffusionszellen und eine *in situ* Freisetzungsmethode mit dem Sirius® inForm. Die untersuchten Nanopartikel waren Nanokristalle, Polymernanopartikel und Lipidnanopartikel.

Mit Dexamethason beladene Ethylcellulose, Eudragit® RS und Ethylcellulose / Eudragit® RS-Nanopartikel wurden durch das Lösungsmittelverdampfungsverfahren hergestellt. Die Dexamethason-Freisetzung aus den Polymernanopartikeln wurde *in vitro* mit Franz-Diffusionszellen untersucht. Die Arzneistoffpenetration wurde *ex vivo* unter Verwendung von exzidierter menschlicher Haut ermittelt. Die follikulare Penetration von Nanopartikeln wurde *ex vivo* unter Verwendung von Schweineohrhaut untersucht.

[6] Teile dieses Abschnittes wurden entnommen aus:

1. B. Balzus, F.F. Sahle, S. Hönzke, C. Gerecke, F. Schumacher, S. Hedtrich, B. Kleuser, R. Bodmeier, Formulation and ex vivo evaluation of polymeric nanoparticles for controlled delivery of corticosteroids to the skin and the corneal epithelium, Eur. J. Pharm. Biopharm., 115 (2017) 122-130.
2. B. Balzus, M. Colombo, F.F. Sahle, G. Zoubari, S. Staufenbiel, R. Bodmeier, Comparison of different in vitro release methods used to investigate nanocarriers intended for dermal application, Int. J. Pharm., 513 (2016) 247-254.

Eudragit® RS-Nanopartikel waren kleiner und positiv geladen, hatten jedoch eine geringere Dexamethason-Beladungskapazität (0,3-0,7%) als Ethylcellulose-Nanopartikel (1,4-2,2%). Durch Mischen der beiden Polymere (1:1) wurden kleine (105 nm), positiv geladene (+37 mV) Nanopartikel mit ausreichender Dexamethason-Beladung (1,3%) erhalten. Die Dexamethason-Freisetzung und Penetration nahm mit abnehmendem Verhältnis von Wirkstoff zu Polymer signifikant ab und stieg, wenn Eudragit® RS mit Ethylcellulose gemischt wurde. *Ex vivo*, war die Arzneistofffreisetzung und -penetration der Nanopartikel langsamer als bei einer herkömmlichen Creme.

Ethylcellulose löste sich schnell in künstlichem Talg auf, während Eudragit® RS unlöslich war. Künstlicher Talg erhöhte die Freisetzung von Ethylcellulose-Nanopartikeln, während er die Freisetzung von Eudragit® RS-Nanopartikeln reduzierte, was auf eine Talg-abhängige Freisetzung von Ethylcellulose-Nanopartikeln hindeutet. Die Penetration von Eudragit® RS- (330 µm) und Ethylcellulose-Nanopartikeln (380 µm) in die Haarfollikel war vergleichbar, aber die Fluoreszenzintensität im Haarfollikel von Nilrot-beladenen Ethylcellulose-Nanopartikeln war im Vergleich zu Eudragit® RS-Nanopartikeln höher.

Zusammenfassend zeigten die hergestellten Nanopartikel ein großes Potenzial, die Freisetzung und Penetration von Kortikosteroiden auf der Haut und im Haarfollikel zu kontrollieren und somit die Wirksamkeit der Behandlung zu maximieren.

Der Vergleich der verschiedenen *in vitro* Freisetzungsmethoden zeigte, dass sich die Methoden in ihren diskriminierenden Eigenschaften und der Reproduzierbarkeit unterscheiden. Die *in situ* Messung war eine einfache und schnelle Methode, die jedoch wegen einer zu schnellen Arzneistoffauflösung / -freisetzung nicht ausreichend diskriminierend war. Franz-Diffusionszellen und Dialysebeutel konnten die verschiedenen Nanopartikel in den meisten Fällen differenzieren, wobei die Auflösung- / Freisetzungs-geschwindigkeit des Wirkstoffs in folgender Reihenfolge abgenommen hat Nanokristalle > Eudragit® RS-Nanopartikel > Lipidnanopartikel ≥ Ethylcellulose-Nanopartikel. Freisetzungsexperimente mit Franz-Diffusionszellen wiesen die höchste Reproduzierbarkeit auf.

6. References

Abbas, S., Bashari, M., Akhtar, W., Li, W.W., Zhang, X., 2014. Process optimization of ultrasound-assisted curcumin nanoemulsions stabilized by OSA-modified starch. Ultrason. Sonochem. 21, 1265-1274.

Abdel-Mottaleb, M.M., Moulari, B., Beduneau, A., Pellequer, Y., Lamprecht, A., 2012. Nanoparticles enhance therapeutic outcome in inflamed skin therapy. Eur. J. Pharm. Biopharm. 82, 151-157.

Abdel-Mottaleb, M.M., Neumann, D., Lamprecht, A., 2011. Lipid nanocapsules for dermal application: a comparative study of lipid-based versus polymer-based nanocarriers. Eur. J. Pharm. Biopharm. 79, 36-42.

Albery, W.J., Hadgraft, J., 1979. Percutaneous absorption: theoretical description. J. Pharm. Pharmacol. 31, 129-139.

Ali, S.M., Yosipovitch, G., 2013. Skin pH: From basic science to basic skin care. Acta Derm. Venereol. 93, 261-269.

Almawi, W.Y., Lipman, M.L., Stevens, A.C., Zanker, B., Hadro, E.T., Strom, T.B., 1991. Abrogation of glucocorticoid-mediated inhibition of T cell proliferation by the synergistic action of IL-1, IL-6, and IFN-gamma. J. Immunol. 146, 3523-3527.

Ammoury, N., Fessi, H., Devissaguet, J.P., Puisieux, F., Benita, S., 1990. In vitro release kinetic pattern of indomethacin from poly(D, L-lactide) nanocapsules. J. Pharm. Sci. 79, 763-767.

Anderson, J.M., Shive, M.S., 2012. Biodegradation and biocompatibility of PLA and PLGA microspheres. Adv Drug Deliv Rev 64, 72-82.

Anhalt, K., Geissler, S., Harms, M., Weigandt, M., Fricker, G., 2012. Development of a new method to assess nanocrystal dissolution based on light scattering. Pharm. Res. 29, 2887-2901.

Azagury, A., Khoury, L., Enden, G., Kost, J., 2014. Ultrasound mediated transdermal drug delivery. Adv Drug Deliv Rev 72, 127-143.

Baroli, B., 2010. Penetration of nanoparticles and nanomaterials in the skin: fiction or reality? J. Pharm. Sci. 99, 21-50.

Benson, H.A.E., 2005. Transdermal drug delivery: Penetration enhancement techniques. Curr Drug Deliv 2, 23-33.

Blagus, T., Markelc, B., Cemazar, M., Kosjek, T., Preat, V., Miklavcic, D., Sersa, G., 2013. In vivo real-time monitoring system of electroporation mediated control of transdermal and topical drug delivery. J. Control. Release 172, 862-871.

Bodmeier, R., Chen, H., Tyle, P., Jarosz, P., 1991. Spontaneous formation of drug-containing acrylic nanoparticles. J. Microencapsul. 8, 161-170.

Boistelle, R., Astier, J.P., 1988. Crystallization mechanisms in solution. J Cryst Growth 90, 14-30.

Bolzinger, M.-A., Briançon, S., Pelletier, J., Chevalier, Y., 2012. Penetration of drugs through skin, a complex rate-controlling membrane. Curr Opin Colloid In 17, 156-165.

Bowman, D.M., van Calster, G., Friedrichs, S., 2010. Nanomaterials and regulation of cosmetics. Nat Nanotechnol 5, 92.

Brandner, J.M., Kief, S., Grund, C., Rendl, M., Houdek, P., Kuhn, C., Tschachler, E., Franke, W.W., Moll, I., 2002. Organization and formation of the tight junction system in human epidermis and cultured keratinocytes. Eur. J. Cell Biol. 81, 253-263.

Brandner, J.M., McIntyre, M., Kief, S., Wladykowski, E., Moll, I., 2003. Expression and localization of tight junction-associated proteins in human hair follicles. Arch. Dermatol. Res. 295, 211-221.

Brandner, J.M., Zorn-Kruppa, M., Yoshida, T., Moll, I., Beck, L.A., De Benedetto, A., 2015. Epidermal tight junctions in health and disease. Tissue Barriers 3, e974451.

Buckton, G., Beezer, A.E., 1992. The relationship between particle size and solubility. Int. J. Pharm. 82, R7-R10.

Burton, A.C., 1935. Human calorimetryii. The average temperature of the tissues of the body: Three figures. J. Nutr. 9, 261-280.

Callen, J., Chamlin, S., Eichenfield, L.F., Ellis, C., Girardi, M., Goldfarb, M., Hanifin, J., Lee, P., Margolis, D., Paller, A.S., Piacquadio, D., Peterson, W., Kaulback, K., Fennerty, M., Wintroub, B.U., 2007. A systematic review of the safety of topical therapies for atopic dermatitis. Br. J. Dermatol. 156, 203-221.

Campbell, C.S., Contreras-Rojas, L.R., Delgado-Charro, M.B., Guy, R.H., 2012. Objective assessment of nanoparticle disposition in mammalian skin after topical exposure. J. Control. Release 162, 201-207.

Cetin, M., Atila, A., Kadioglu, Y., 2010. Formulation and in vitro characterization of Eudragit(R) L100 and Eudragit(R) L100-PLGA nanoparticles containing diclofenac sodium. AAPS PharmSciTech 11, 1250-1256.

Cevc, G., Blume, G., 2001. New, highly efficient formulation of diclofenac for the topical, transdermal administration in ultradeformable drug carriers, Transfersomes. Biochim. Biophys. Acta 1514, 191-205.

Chattopadhyay, A., London, E., 1984. Fluorimetric determination of critical micelle concentration avoiding interference from detergent charge. Anal. Biochem. 139, 408-412.

Chidambaram, N., Burgess, D.J., 1999. A novel in vitro release method for submicron-sized dispersed systems. AAPS PharmSci 1, 32-40.

Christoffersen, J., Rostrup, E., Christoffersen, M.R., 1991. Relation between interfacial surface tension of electrolyte crystals in aqueous suspension and their solubility; a simple derivation based on surface nucleation. J Cryst Growth 113, 599-605.

Coldman, M.F., Poulsen, B.J., Higuchi, T., 1969. Enhancement of percutaneous absorption by the use of volatile: Nonvolatile systems as vehicles. J. Pharm. Sci. 58, 1098-1102.

Colombo, M., Staufenbiel, S., Ruhl, E., Bodmeier, R., 2017. In situ determination of the saturation solubility of nanocrystals of poorly soluble drugs for dermal application. Int. J. Pharm. 521, 156-166.

Contri, R.V., Fiel, L.A., Alnasif, N., Pohlmann, A.R., Guterres, S.S., Schafer-Korting, M., 2016. Skin penetration and dermal tolerability of acrylic nanocapsules: influence of the surface charge and a chitosan gel used as vehicle. Int. J. Pharm. 507, 12-20.

Contri, R.V., Katzer, T., Ourique, A.F., da Silva, A.L.M., Beck, R.C., Pohlmann, A.R., Guterres, S.S., 2014. Combined effect of polymeric nanocapsules and chitosan hydrogel on the increase of capsaicinoids adhesion to the skin surface. J. Biomed. Nanotechnol. 10, 820-830.

Corrias, F., Schlich, M., Sinico, C., Pireddu, R., Valenti, D., Fadda, A.M., Marceddu, S., Lai, F., 2017. Nile red nanosuspensions as investigative model to study the follicular targeting of drug nanocrystals. Int. J. Pharm. 524, 1-8.

Crisp, M.T., Tucker, C.J., Rogers, T.L., Williams, R.O., 3rd, Johnston, K.P., 2007. Turbidimetric measurement and prediction of dissolution rates of poorly soluble drug nanocrystals. J. Control. Release 117, 351-359.

D'Souza, S., 2014. A review of in vitro drug release test methods for nano-sized dosage forms. Adv. Pharm. 2014, 12.

Davidovich-Pinhas, M., Barbut, S., Marangoni, A.G., 2015. The gelation of oil using ethyl cellulose. Carbohydr Polym 117, 869-878.

Dingler, A., Blum, R.P., Niehus, H., Muller, R.H., Gohla, S., 1999. Solid lipid nanoparticles (SLN/Lipopearls)--a pharmaceutical and cosmetic carrier for the application of vitamin E in dermal products. J. Microencapsul. 16, 751-767.

Döge, N., Hönzke, S., Schumacher, F., Balzus, B., Colombo, M., Hadam, S., Rancan, F., Blume-Peytavi, U., Schafer-Korting, M., Schindler, A., Ruhl, E., Skov, P.S., Church, M.K., Hedtrich, S., Kleuser, B., Bodmeier, R., Vogt, A., 2016. Ethyl cellulose nanocarriers and nanocrystals differentially deliver dexamethasone into intact, tape-stripped or sodium lauryl sulfate-exposed ex vivo human skin - assessment by intradermal microdialysis and extraction from the different skin layers. J. Control. Release 242, 25-34.

Elias, P.M., 2005. Stratum corneum defensive functions: An integrated view. J. Gen. Intern. Med. 20, 183-200.

Elias, P.M., Friend, D.S., 1975. The permeability barrier in mammalian epidermis. J. Cell Biol. 65, 180-191.

Eloy, J.O., Claro de Souza, M., Petrilli, R., Barcellos, J.P., Lee, R.J., Marchetti, J.M., 2014. Liposomes as carriers of hydrophilic small molecule drugs: strategies to enhance encapsulation and delivery. Colloids Surf B Biointerfaces 123, 345-363.

Elsayed, M.M., Abdallah, O.Y., Naggar, V.F., Khalafallah, N.M., 2007. Lipid vesicles for skin delivery of drugs: reviewing three decades of research. Int. J. Pharm. 332, 1-16.

Erbetta, C.D.A.C., Alves, R.J., Resende, J.M., de Souza Freitas, R.F., de Sousa, R.G., 2012. Synthesis and characterization of poly (D, L-lactide-co-glycolide) copolymer. J Biomater Nanobiotechnol 3, 208.

Finnin, B.C., Morgan, T.M., 1999. Transdermal penetration enhancers: Applications, limitations, and potential. J. Pharm. Sci. 88, 955-958.

Furue, M., Terao, H., Rikihisa, W., Urabe, K., Kinukawa, N., Nose, Y., Koga, T., 2003. Clinical dose and adverse effects of topical steroids in daily management of atopic dermatitis. Br. J. Dermatol. 148, 128-133.

Garcia Ortiz, P., Hansen, S.H., Shah, V.P., Menne, T., Benfeldt, E., 2009. Impact of adult atopic dermatitis on topical drug penetration: assessment by cutaneous microdialysis and tape stripping. Acta Derm. Venereol. 89, 33-38.

Garti, N., Zour, H., 1997. The effect of surfactants on the crystallization and polymorphic transformation of glutamic acid. J Cryst Growth 172, 486-498.

Gattu, S., Maibach, H.I., 2011. Modest but increased penetration through damaged skin: an overview of the in vivo human model. Skin Pharmacol. Physiol. 24, 2-9.

Grijpma, D.W., Pennings, A.J., 1994. (Co)polymers of L-lactide, 1. Synthesis, thermal properties and hydrolytic degradation. Macromol. Chem. Phys. 195, 1633-1647.

Guttman-Yassky, E., Nograles, K.E., Krueger, J.G., 2011. Contrasting pathogenesis of atopic dermatitis and psoriasis--part I: clinical and pathologic concepts. J. Allergy Clin. Immunol. 127, 1110-1118.

Guzmán, H.R., Tawa, M., Zhang, Z., Ratanabanangkoon, P., Shaw, P., Gardner, C.R., Chen, H., Moreau, J.P., Almarsson, Ö., Remenar, J.F., 2007. Combined use of crystalline salt forms and precipitation inhibitors to improve oral absorption of celecoxib from solid oral formulations. J. Pharm. Sci. 96, 2686-2702.

Gysler, A., Lange, K., Korting, H.C., Schäfer-Korting, M., 1997. Prednicarbate biotransformation in human foreskin keratinocytes and fibroblasts. Pharm. Res. 14, 793-797.

Haag, R., Vogtle, F., 2004. Highly branched macromolecules at the interface of chemistry, biology, physics, and medicine. Angew. Chem. Int. Ed. Engl. 43, 272-273.

Haj-Ahmad, R., Khan, H., Arshad, M.S., Rasekh, M., Hussain, A., Walsh, S., Li, X., Chang, M.W., Ahmad, Z., 2015. Microneedle coating techniques for transdermal drug delivery. Pharmaceutics 7, 486-502.

Hamid, Q., Boguniewicz, M., Leung, D.Y., 1994. Differential in situ cytokine gene expression in acute versus chronic atopic dermatitis. J. Clin. Invest. 94, 870-876.

Haque, M.E., Das, A.R., Moulik, S.P., 1999. Mixed Micelles of Sodium Deoxycholate and Polyoxyethylene Sorbitan Monooleate (Tween 80). J. Colloid Interface Sci. 217, 1-7.

Heine, D.R., Petersen, M.K., Grest, G.S., 2010. Effect of particle shape and charge on bulk rheology of nanoparticle suspensions. J. Chem. Phys. 132.

Heng, D., Cutler, D.J., Chan, H.K., Yun, J., Raper, J.A., 2008. What is a suitable dissolution method for drug nanoparticles? Pharm. Res. 25, 1696-1701.

Honari, G., Maibach, H., 2014. Skin structure and function, Applied Dermatotoxicology, pp. 1-10.

Hughes, J., Rustin, M., 1997. Corticosteroids. Clin. Dermatol. 15, 715-721.

Imhof, A., Megens, M., Engelberts, J.J., de Lang, D.T.N., Sprik, R., Vos, W.L., 1999. Spectroscopy of fluorescein (FITC) dyed colloidal silica spheres. J. Phys. Chem. B 103, 1408-1415.

Ishida-Yamamoto, A., Igawa, S., 2014. Genetic skin diseases related to desmosomes and corneodesmosomes. J. Dermatol. Sci. 74, 99-105.

Ita, K.B., 2015. Chemical penetration enhancers for transdermal drug delivery - Success and challenges. Curr Drug Deliv 12, 645-651.

Jacobi, U., Kaiser, M., Toll, R., Mangelsdorf, S., Audring, H., Otberg, N., Sterry, W., Lademann, J., 2007. Porcine ear skin: an in vitro model for human skin. Skin Res. Technol. 13, 19-24.

Jaeger, A., Weiss, D.G., Jonas, L., Kriehuber, R., 2012. Oxidative stress-induced cytotoxic and genotoxic effects of nano-sized titanium dioxide particles in human HaCaT keratinocytes. Toxicology 296, 27-36.

Jain, S., Jain, P., Umamaheshwari, R.B., Jain, N.K., 2003. Transfersomes--a novel vesicular carrier for enhanced transdermal delivery: development, characterization, and performance evaluation. Drug Dev. Ind. Pharm. 29, 1013-1026.

Jain, S., Tiwary, A.K., Sapra, B., Jain, N.K., 2007. Formulation and evaluation of ethosomes for transdermal delivery of lamivudine. AAPS PharmSciTech 8, 249.

Jansen, J.F.G.A., de Brabander-van den Berg, E.M.M., Meijer, E.W., 1994. Encapsulation of guest molecules into a dendritic box. Science 266, 1226-1229.

Jenning, V., Gohla, S.H., 2001. Encapsulation of retinoids in solid lipid nanoparticles (SLN). J. Microencapsul. 18, 149-158.

Jin, H., Zhou, W., Cao, J., Stoyanov, S.D., Blijdenstein, T.B.J., de Groot, P.W.N., Arnaudov, L.N., Pelan, E.G., 2012. Super stable foams stabilized by colloidal ethyl cellulose particles. Soft Matter 8, 2194-2205.

Jose Morilla, M., Lilia Romero, E., 2016. Carrier deformability in drug delivery. Curr. Pharm. Des. 22, 1118-1134.

Katakam, M., Bell, L.N., Banga, A.K., 1995. Effect of surfactants on the physical stability of recombinant human growth hormone. J. Pharm. Sci. 84, 713-716.

Kayaert, P., Li, B., Jimidar, I., Rombaut, P., Ahssini, F., Van den Mooter, G., 2010. Solution calorimetry as an alternative approach for dissolution testing of nanosuspensions. Eur. J. Pharm. Biopharm. 76, 507-513.

Kesisoglou, F., Panmai, S., Wu, Y., 2007. Nanosizing--oral formulation development and biopharmaceutical evaluation. Adv Drug Deliv Rev 59, 631-644.

Kim, Y.I., Fluckiger, L., Hoffman, M., Lartaud-Idjouadiene, I., Atkinson, J., Maincent, T., 1997. The antihypertensive effect of orally administered nifedipine-loaded nanoparticles in spontaneously hypertensive rats. Br. J. Pharmacol. 120, 399-404.

Kimura, E., Kawano, Y., Todo, H., Ikarashi, Y., Sugibayashi, K., 2012. Measurement of skin permeation/penetration of nanoparticles for their safety evaluation. Biol. Pharm. Bull. 35, 1476-1486.

Kirschner, N., Poetzl, C., von den Driesch, P., Wladykowski, E., Moll, I., Behne, M.J., Brandner, J.M., 2009. Alteration of tight junction proteins is an early event in psoriasis: putative involvement of proinflammatory cytokines. Am. J. Pathol. 175, 1095-1106.

Kroll, A., Pillukat, M.H., Hahn, D., Schnekenburger, J., 2009. Current in vitro methods in nanoparticle risk assessment: limitations and challenges. Eur. J. Pharm. Biopharm. 72, 370-377.

Küchler, S., Abdel-Mottaleb, M., Lamprecht, A., Radowski, M.R., Haag, R., Schafer-Korting, M., 2009a. Influence of nanocarrier type and size on skin delivery of hydrophilic agents. Int. J. Pharm. 377, 169-172.

Küchler, S., Herrmann, W., Panek-Minkin, G., Blaschke, T., Zoschke, C., Kramer, K.D., Bittl, R., Schafer-Korting, M., 2010. SLN for topical application in skin diseases--characterization of drug-carrier and carrier-target interactions. Int. J. Pharm. 390, 225-233.

Küchler, S., Radowski, M.R., Blaschke, T., Dathe, M., Plendl, J., Haag, R., Schafer-Korting, M., Kramer, K.D., 2009b. Nanoparticles for skin penetration enhancement--a comparison of a dendritic core-multishell-nanotransporter and solid lipid nanoparticles. Eur. J. Pharm. Biopharm. 71, 243-250.

Kumar, S., Alnasif, N., Fleige, E., Kurniasih, I., Kral, V., Haase, A., Luch, A., Weindl, G., Haag, R., Schafer-Korting, M., Hedtrich, S., 2014. Impact of structural differences in hyperbranched polyglycerol-polyethylene glycol nanoparticles on dermal drug delivery and biocompatibility. Eur. J. Pharm. Biopharm. 88, 625-634.

Kurihara-Bergstrom, T., Knutson, K., DeNoble, L.J., Goates, C.Y., 1990. Percutaneous absorption enhancement of an ionic molecule by ethanol–water systems in human skin. Pharm. Res. 7, 762-766.

Lademann, J., Knorr, F., Richter, H., Jung, S., Meinke, M.C., Rühl, E., Alexiev, U., Calderon, M., Patzelt, A., 2015. Hair follicles as a target structure for nanoparticles. J Innov Opt Health Sci 08, 1530004.

Lademann, J., Meinke, M.C., Schanzer, S., Richter, H., Darvin, M.E., Haag, S.F., Fluhr, J.W., Weigmann, H.J., Sterry, W., Patzelt, A., 2012. In vivo methods for the analysis of the penetration of topically applied substances in and through the skin barrier. Int. J. Cosmet. Sci. 34, 551-559.

Lademann, J., Otberg, N., Jacobi, U., Hoffman, R.M., Blume-Peytavi, U., 2005. Follicular penetration and targeting. J. Investig. Dermatol. Symp. Proc. 10, 301-303.

Lademann, J., Otberg, N., Richter, H., Weigmann, H.J., Lindemann, U., Schaefer, H., Sterry, W., 2001. Investigation of follicular penetration of topically applied substances. Skin Pharmacol. Physiol. 14(suppl 1), 17-22.

Lademann, J., Patzelt, A., Richter, H., Antoniou, C., Sterry, W., Knorr, F., 2009. Determination of the cuticula thickness of human and porcine hairs and their potential influence on the penetration of nanoparticles into the hair follicles. Journal of biomedical optics 14, 021014.

Lademann, J., Richter, H., Knorr, F., Patzelt, A., Darvin, M.E., Ruhl, E., Cheung, K.Y., Lai, K.K., Renneberg, R., Mak, W.C., 2016. Triggered release of model drug from AuNP-doped BSA nanocarriers in hair follicles using IRA radiation. Acta Biomater 30, 388-396.

Lademann, J., Richter, H., Schaefer, U.F., Blume-Peytavi, U., Teichmann, A., Otberg, N., Sterry, W., 2006. Hair follicles - a long-term reservoir for drug delivery. Skin Pharmacol. Physiol. 19, 232-236.

Lademann, J., Richter, H., Teichmann, A., Otberg, N., Blume-Peytavi, U., Luengo, J., Weiss, B., Schaefer, U.F., Lehr, C.M., Wepf, R., Sterry, W., 2007. Nanoparticles--an efficient carrier for drug delivery into the hair follicles. Eur. J. Pharm. Biopharm. 66, 159-164.

Langbein, L., Grund, C., Kuhn, C., Praetzel, S., Kartenbeck, J., Brandner, J.M., Moll, I., Franke, W.W., 2002. Tight junctions and compositionally related junctional structures in mammalian stratified epithelia and cell cultures derived therefrom. Eur. J. Cell Biol. 81, 419-435.

Lange, K., Kleuser, B., Gysler, A., Bader, M., Maia, C., Scheidereit, C., Korting, H.C., Schäfer-Korting, M., 2000. Cutaneous inflammation and proliferation in vitro: Differential effects and mode of action of topical glucocorticoids. Skin Pharmacol Appl Skin Physio 13, 93-103.

Lauterbach, A., Müller-Goymann, C.C., 2014. Comparison of rheological properties, follicular penetration, drug release, and permeation behavior of a novel topical drug delivery system and a conventional cream. Eur. J. Pharm. Biopharm. 88, 614-624.

Li, Y., Zheng, J., Xiao, H., McClements, D.J., 2012. Nanoemulsion-based delivery systems for poorly water-soluble bioactive compounds: Influence of formulation parameters on Polymethoxyflavone crystallization. Food Hydrocoll 27, 517-528.

Liang, X.W., Xu, Z.P., Grice, J., Zvyagin, A.V., Roberts, M.S., Liu, X., 2013. Penetration of nanoparticles into human skin. Curr. Pharm. Des. 19, 6353-6366.

Lin, Y.K., Yang, S.H., Chen, C.C., Kao, H.C., Fang, J.Y., 2015. Using Imiquimod-induced psoriasis-like skin as a model to measure the skin penetration of anti-psoriatic drugs. PLoS One 10, e0137890.

Liu, H., Slamovich, E.B., Webster, T.J., 2006. Less harmful acidic degradation of poly(lactic-co-glycolic acid) bone tissue engineering scaffolds through titania nanoparticle addition. Int J Nanomedicine 1, 541-545.

Liu, P., De Wulf, O., Laru, J., Heikkila, T., van Veen, B., Kiesvaara, J., Hirvonen, J., Peltonen, L., Laaksonen, T., 2013. Dissolution studies of poorly soluble drug nanosuspensions in non-sink conditions. AAPS PharmSciTech 14, 748-756.

Lohan, S.B., Icken, N., Teutloff, C., Saeidpour, S., Bittl, R., Lademann, J., Fleige, E., Haag, R., Haag, S.F., Meinke, M.C., 2016. Investigation of cutaneous penetration properties of stearic acid loaded to dendritic core-multi-shell (CMS) nanocarriers. Int. J. Pharm. 501, 271-277.

Loira-Pastoriza, C., Sapin-Minet, A., Diab, R., Grossiord, J.L., Maincent, P., 2012. Low molecular weight heparin gels, based on nanoparticles, for topical delivery. Int. J. Pharm. 426, 256-262.

Lu, G.W., Valiveti, S., Spence, J., Zhuang, C., Robosky, L., Wade, K., Love, A., Hu, L.Y., Pole, D., Mollan, M., 2009. Comparison of artificial sebum with human and hamster sebum samples. Int. J. Pharm. 367, 37-43.

Lu, G.W., Warner, K.S., Wang, F., 2014. Development of pilosebaceous unit-targeted drug products, Topical Drug Bioavailability, Bioequivalence, and Penetration. Springer, pp. 181-215.

Lu, X., Weiss, R., 1992. Relationship between the glass transition temperature and the interaction parameter of miscible binary polymer blends. Macromolecules 25, 3242-3246.

Luengo, J., Weiss, B., Schneider, M., Ehlers, A., Stracke, F., Konig, K., Kostka, K.H., Lehr, C.M., Schaefer, U.F., 2006. Influence of nanoencapsulation on human skin transport of flufenamic acid. Skin Pharmacol. Physiol. 19, 190-197.

Margulis-Goshen, K., Weitman, M., Major, D.T., Magdassi, S., 2011. Inhibition of crystallization and growth of celecoxib nanoparticles formed from volatile microemulsions. J. Pharm. Sci. 100, 4390-4400.

Marks, R., Barlow, J.W., Funder, J.W., 1982. Steroid-induced vasoconstriction: Glucocorticoid antagonist studies. J. Clin. Endocrinol. Metab. 54, 1075-1077.

Marro, D., Guy, R.H., Begoña Delgado-Charro, M., 2001. Characterization of the iontophoretic permselectivity properties of human and pig skin. J. Control. Release 70, 213-217.

Mathes, S.H., Ruffner, H., Graf-Hausner, U., 2014. The use of skin models in drug development. Adv Drug Deliv Rev 69-70, 81-102.

Mehnert, W., Mäder, K., 2001. Solid lipid nanoparticles: Production, characterization and applications. Advanced Drug Delivery Reviews 47, 165-196.

Merisko-Liversidge, E., Liversidge, G.G., Cooper, E.R., 2003. Nanosizing: a formulation approach for poorly-water-soluble compounds. Eur. J. Pharm. Sci. 18, 113-120.

Mishra, P.R., Al Shaal, L., Muller, R.H., Keck, C.M., 2009. Production and characterization of Hesperetin nanosuspensions for dermal delivery. Int. J. Pharm. 371, 182-189.

Mojumdar, E.H., Gooris, G.S., Groen, D., Barlow, D.J., Lawrence, M.J., Deme, B., Bouwstra, J.A., 2016. Stratum corneum lipid matrix: Location of acyl ceramide and cholesterol in the unit cell of the long periodicity phase. Biochim. Biophys. Acta 1858, 1926-1934.

Montenegro, L., Trapani, A., Fini, P., Mandracchia, D., Latrofa, A., Cioffi, N., Chiarantini, L., Giusi, G.P., Brundu, S., Puglisi, G., 2014. Chitosan nanoparticles for topical co-administration of the antioxidants glutathione and idebenone: characterization and in vitro release. Br. J. Pharm. Res. 4, 2387-2406.

Moreno-Bautista, G., Tam, K.C., 2011. Evaluation of dialysis membrane process for quantifying the in vitro drug-release from colloidal drug carriers. Colloid Surface A 389, 299-303.

Moss, G.P., Dearden, J.C., Patel, H., Cronin, M.T.D., 2002. Quantitative structure–permeability relationships (QSPRs) for percutaneous absorption. Toxicol. In Vitro 16, 299-317.

Müller, R.H., Gohla, S., Keck, C.M., 2011. State of the art of nanocrystals--special features, production, nanotoxicology aspects and intracellular delivery. Eur. J. Pharm. Biopharm. 78, 1-9.

Müller, R.H., Radtke, M., Wissing, S.A., 2002. Solid lipid nanoparticles (SLN) and nanostructured lipid carriers (NLC) in cosmetic and dermatological preparations. Adv Drug Deliv Rev 54, Supplement, S131-S155.

Murdande, S.B., Shah, D.A., Dave, R.H., 2015. Impact of nanosizing on solubility and dissolution rate of poorly soluble pharmaceuticals. J. Pharm. Sci. 104, 2094-2102.

Murota, H., Matsui, S., Ono, E., Kijima, A., Kikuta, J., Ishii, M., Katayama, I., 2015. Sweat, the driving force behind normal skin: an emerging perspective on functional biology and regulatory mechanisms. J. Dermatol. Sci. 77, 3-10.

Nakatsuji, T., Kao, M.C., Zhang, L., Zouboulis, C.C., Gallo, R.L., Huang, C.M., 2010. Sebum free fatty acids enhance the innate immune defense of human sebocytes by upregulating beta-defensin-2 expression. J. Invest. Dermatol. 130, 985-994.

Nel, A., Xia, T., Mädler, L., Li, N., 2006. Toxic potential of materials at the nanolevel. Science 311, 622-627.

Nohynek, G.J., Lademann, J., Ribaud, C., Roberts, M.S., 2007. Grey goo on the skin? Nanotechnology, cosmetic and sunscreen safety. Crit. Rev. Toxicol. 37, 251-277.

Otberg, N., Richter, H., Schaefer, H., Blume-Peytavi, U., Sterry, W., Lademann, J., 2004. Variations of hair follicle size and distribution in different body sites. J. Invest. Dermatol. 122, 14-19.

Otberg, N., Teichmann, A., Rasuljev, U., Sinkgraven, R., Sterry, W., Lademann, J., 2007. Follicular Penetration of Topically Applied Caffeine via a Shampoo Formulation. Skin Pharmacol. Physiol. 20, 195-198.

Pagnoni, A., Kligman, A.M., Gammal, S.E., Stoudemayer, T., 1994. Determination of density of follicles on various regions of the face by cyanoacrylate biopsy: correlation with sebum output. Br. J. Dermatol. 131, 862-865.

Pal, A., Srivastava, A., Bhattacharya, S., 2009. Role of capping ligands on the nanoparticles in the modulation of properties of a hybrid matrix of nanoparticles in a 2D film and in a supramolecular organogel. Chem. Eur. J. 15, 9169-9182.

Patzelt, A., Knorr, F., Blume-Peytavi, U., Sterry, W., Lademann, J., 2008a. Hair follicles, their disorders and their opportunities. Drug Discov. Today Dis. Mech. 5, e173-e181.

Patzelt, A., Mak, W.C., Jung, S., Knorr, F., Meinke, M.C., Richter, H., Ruhl, E., Cheung, K.Y., Tran, N., Lademann, J., 2017. Do nanoparticles have a future in dermal drug delivery? J. Control. Release 246, 174-182.

Patzelt, A., Richter, H., Buettemeyer, R., Huber, H.J., Blume-Peytavi, U., Sterry, W., Lademann, J., 2008b. Differential stripping demonstrates a significant reduction of the hair follicle reservoir in vitro compared to in vivo. Eur. J. Pharm. Biopharm. 70, 234-238.

Patzelt, A., Richter, H., Knorr, F., Schafer, U., Lehr, C.M., Dahne, L., Sterry, W., Lademann, J., 2011. Selective follicular targeting by modification of the particle sizes. J. Control. Release 150, 45-48.

Pireddu, R., Caddeo, C., Valenti, D., Marongiu, F., Scano, A., Ennas, G., Lai, F., Fadda, A.M., Sinico, C., 2016. Diclofenac acid nanocrystals as an effective strategy to reduce in vivo skin inflammation by improving dermal drug bioavailability. Colloids Surf B Biointerfaces 143, 64-70.

Poblet, E., Ortega, F., Jiménez, F., 2002. The arrector pili muscle and the follicular unit of the scalp: A microscopic anatomy study. Dermatol. Surg. 28, 800-803.

Ponec, M., Kempenaar, J.A., 1983. Biphasic entry of glucocorticoids into cultured human skin keratinocytes and fibroblasts. Arch. Dermatol. Res. 275, 334-344.

Ponec, M., Kempenaar, J.A., De Kloet, E.R., 1981. Corticoids and cultured human epidermal keratinocytes: Specific intracellular binding and clinical efficacy. J. Invest. Dermatol. 76, 211-214.

Potts, R.O., Guy, R.H., 1995. A predictive algorithm for skin permeability: The effects of molecular size and hydrogen bond activity. Pharm. Res. 12, 1628-1633.

Prow, T.W., Grice, J.E., Lin, L.L., Faye, R., Butler, M., Becker, W., Wurm, E.M., Yoong, C., Robertson, T.A., Soyer, H.P., Roberts, M.S., 2011. Nanoparticles and microparticles for skin drug delivery. Adv Drug Deliv Rev 63, 470-491.

Puglia, C., Offerta, A., Rizza, L., Zingale, G., Bonina, F., Ronsisvalle, S., 2013. Optimization of curcumin loaded lipid nanoparticles formulated using high shear homogenization (HSH) and ultrasonication (US) methods. J Nanosci Nanotechno 13, 6888-6893.

Rabinow, B.E., 2004. Nanosuspensions in drug delivery. Nat Rev Drug Discov 3, 785-796.

Radtke, M., Patzelt, A., Knorr, F., Lademann, J., Netz, R.R., 2017. Ratchet effect for nanoparticle transport in hair follicles. Eur. J. Pharm. Biopharm. 116, 12-16.

Raghavan, S.L., Trividic, A., Davis, A.F., Hadgraft, J., 2001. Crystallization of hydrocortisone acetate: influence of polymers. Int. J. Pharm. 212, 213-221.

Rancan, F., Papakostas, D., Hadam, S., Hackbarth, S., Delair, T., Primard, C., Verrier, B., Sterry, W., Blume-Peytavi, U., Vogt, A., 2009. Investigation of polylactic acid (PLA) nanoparticles as drug delivery systems for local dermatotherapy. Pharm. Res. 26, 2027-2036.

Rancan, F., Todorova, A., Hadam, S., Papakostas, D., Luciani, E., Graf, C., Gernert, U., Ruhl, E., Verrier, B., Sterry, W., Blume-Peytavi, U., Vogt, A., 2012. Stability of polylactic acid particles and release of fluorochromes upon topical application on human skin explants. Eur. J. Pharm. Biopharm. 80, 76-84.

Rao, G.S., 1981. Mode of entry of steroid and thyroid hormones into cells. Mol. Cell. Endocrinol. 21, 97-108.

Rao, J.P., Geckeler, K.E., 2011. Polymer nanoparticles: preparation techniques and size-control parameters. Prog. Polym. Sci. 36, 887-913.

Reddy, M.B., Guy, R.H., Bunge, A.L., 2000. Does epidermal turnover reduce percutaneous penetration? Pharm. Res. 17, 1414-1419.

Rekhi, G.S., Jambhekar, S.S., 1995. Ethylcellulose-A polymer review. Drug Dev. Ind. Pharm. 21, 61-77.

Roberts, D., Marks, R., 1980. The determination of regional and age variations in the rate of desquamation: A comparison of four techniques. J. Invest. Dermatol. 74, 13-16.

Rodriguez-Hornedo, N., Murphy, D., 2004. Surfactant-facilitated crystallization of dihydrate carbamazepine during dissolution of anhydrous polymorph. J. Pharm. Sci. 93, 449-460.

Rojanasakul, Y., Robinson, J.R., 1989. Transport mechanisms of the cornea: characterization of barrier permselectivity. Int. J. Pharm. 55, 237-246.

Roll, A., Cozzio, A., Fischer, B., Schmid-Grendelmeier, P., 2004. Microbial colonization and atopic dermatitis. Curr. Opin. Allergy Clin. Immunol. 4, 373-378.

Rosenblatt, K.M., Douroumis, D., Bunjes, H., 2007. Drug release from differently structured monoolein/poloxamer nanodispersions studied with differential pulse polarography and ultrafiltration at low pressure. J. Pharm. Sci. 96, 1564-1575.

Ryman-Rasmussen, J.P., Riviere, J.E., Monteiro-Riviere, N.A., 2006. Penetration of intact skin by quantum dots with diverse physicochemical properties. Toxicol. Sci. 91, 159-165.

Sahle, F.F., Balzus, B., Gerecke, C., Kleuser, B., Bodmeier, R., 2016. Formulation and in vitro evaluation of polymeric enteric nanoparticles as dermal carriers with pH-dependent targeting potential. Eur. J. Pharm. Sci. 92, 98-109.

Sahle, F.F., Giulbudagian, M., Bergueiro, J., Lademann, J., Calderon, M., 2017. Dendritic polyglycerol and N-isopropylacrylamide based thermoresponsive nanogels as smart carriers for controlled delivery of drugs through the hair follicle. Nanoscale 9, 172-182.

Sahu, S., Saraf, S., Kaur, C.D., Saraf, S., 2013. Biocompatible nanoparticles for sustained topical delivery of anticancer phytoconstituent quercetin. Pak. J. Biol. Sci. 16, 601.

Saint-Leger, D., Cohen, E., 1985. Practical study of qualitative and quantitative sebum excretion on the human forehead. Br. J. Dermatol. 113, 551-557.

Sanna, V., Roggio, A.M., Siliani, S., Piccinini, M., Marceddu, S., Mariani, A., Sechi, M., 2012. Development of novel cationic chitosan-and anionic alginate-coated poly(D,L-lactide-co-glycolide) nanoparticles for controlled release and light protection of resveratrol. Int J Nanomedicine 7, 5501-5516.

Saski, W., Shah, S.G., 1965. Availability of drugs in the presence of surface-active agents I critical micelle concentrations of some oxyethylene oxypropylene polymers. J. Pharm. Sci. 54, 71-74.

Schafer-Korting, M., Mehnert, W., Korting, H.C., 2007. Lipid nanoparticles for improved topical application of drugs for skin diseases. Adv Drug Deliv Rev 59, 427-443.

Schaller, M., Korting, H.C., 1996. Interaction of liposomes with human skin: the role of the stratum corneum. Adv Drug Deliv Rev 18, 303-309.

Scheinman, R.I., Cogswell, P.C., Lofquist, A.K., Baldwin, A.S., 1995. Role of transcriptional activation of iκbα in mediation of immunosuppression by glucocorticoids. Science 270, 283-286.

Scheuplein, R.J., 1967. Mechanism of Percutaneous Absorption. J. Invest. Dermatol. 48, 79-88.

Schirren, C.G., 1955. Does the glass electrode determine the same pH-values on the skin surface as the quinhydrone electrode? J. Invest. Dermatol. 24, 485-488.

Schmid-Wendtner, M.H., Korting, H.C., 2006. The pH of the skin surface and its impact on the barrier function. Skin Pharmacol. Physiol. 19, 296-302.

Schmidt, C., Bodmeier, R., 1999. Incorporation of polymeric nanoparticles into solid dosage forms. J. Control. Release 57, 115-125.

Schmuth, M., Blunder, S., Dubrac, S., Gruber, R., Moosbrugger-Martinz, V., 2015. Epidermal barrier in hereditary ichthyoses, atopic dermatitis, and psoriasis. J Dtsch Dermatol Ges 13, 1119-1123.

Schoepe, S., Schäcke, H., May, E., Asadullah, K., 2006. Glucocorticoid therapy-induced skin atrophy. Exp. Dermatol. 15, 406-420.

Shim, J., Seok Kang, H., Park, W.S., Han, S.H., Kim, J., Chang, I.S., 2004. Transdermal delivery of mixnoxidil with block copolymer nanoparticles. J. Control. Release 97, 477-484.

Sklar, L.R., Burnett, C.T., Waibel, J.S., Moy, R.L., Ozog, D.M., 2014. Laser assisted drug delivery: a review of an evolving technology. Lasers Surg. Med. 46, 249-262.

Souto, E.B., Wissing, S.A., Barbosa, C.M., Muller, R.H., 2004. Development of a controlled release formulation based on SLN and NLC for topical clotrimazole delivery. Int. J. Pharm. 278, 71-77.

Sparavigna, A., Setaro, M., Gualandri, V., 1999. Cutaneous pH in children affected by atopic dermatitis and in healthy children: a multicenter study. Skin Res. Technol. 5, 221-227.

Stegemann, S., Leveiller, F., Franchi, D., de Jong, H., Linden, H., 2007. When poor solubility becomes an issue: from early stage to proof of concept. Eur. J. Pharm. Sci. 31, 249-261.

Subongkot, T., Wonglertnirant, N., Songprakhon, P., Rojanarata, T., Opanasopit, P., Ngawhirunpat, T., 2013. Visualization of ultradeformable liposomes penetration pathways and their skin interaction by confocal laser scanning microscopy. Int. J. Pharm. 441, 151-161.

Sullivan, S.P., Koutsonanos, D.G., Del Pilar Martin, M., Lee, J.W., Zarnitsyn, V., Choi, S.O., Murthy, N., Compans, R.W., Skountzou, I., Prausnitz, M.R., 2010. Dissolving polymer microneedle patches for influenza vaccination. Nat. Med. 16, 915-920.

Swed, A., Cordonnier, T., Fleury, F., Boury, F., 2014. Protein encapsulation into PLGA nanoparticles by a novel phase separation method using non-toxic solvents. J Nanomed Nanotechnol 2014.

Tan, J.P., Goh, C.H., Tam, K.C., 2007. Comparative drug release studies of two cationic drugs from pH-responsive nanogels. Eur. J. Pharm. Sci. 32, 340-348.

Tantra, R., Schulze, P., Quincey, P., 2010. Effect of nanoparticle concentration on zeta-potential measurement results and reproducibility. Particuology 8, 279-285.

Taylor, K.M.G., Taylor, G., Kellaway, I.W., Stevens, J., 1990. Drug entrapment and release from multilamellar and reverse-phase evaporation liposomes. Int. J. Pharm. 58, 49-55.

Teichmann, A., Jacobi, U., Ossadnik, M., Richter, H., Koch, S., Sterry, W., Lademann, J., 2005. Differential stripping: Determination of the amount of topically applied substances penetrated into the hair follicles. J. Invest. Dermatol. 20, 264-269.

Teichmann, A., Ossadnik, M., Richter, H., Sterry, W., Lademann, J., 2006. Semiquantitative determination of the penetration of a fluorescent hydrogel formulation into the hair follicle with and without follicular closure by microparticles by means of differential stripping. Skin Pharmacol. Physiol. 19, 101-105.

Teskac, K., Kristl, J., 2010. The evidence for solid lipid nanoparticles mediated cell uptake of resveratrol. Int. J. Pharm. 390, 61-69.

Thakral, S., Thakral, N.K., Majumdar, D.K., 2013. Eudragit: a technology evaluation. Expert Opin Drug Deliv 10, 131-149.

Touitou, E., Dayan, N., Bergelson, L., Godin, B., Eliaz, M., 2000. Ethosomes — novel vesicular carriers for enhanced delivery: characterization and skin penetration properties. J. Control. Release 65, 403-418.

Triplett, M.D., Rathman, J.F., 2008. Optimization of β-carotene loaded solid lipid nanoparticles preparation using a high shear homogenization technique. J Nanopart Res 11, 601-614.

Uram, L., Szuster, M., Gargasz, K., Filipowicz, A., Walajtys-Rode, E., Wolowiec, S., 2013. In vitro cytotoxicity of the ternary PAMAM G3-pyridoxal-biotin bioconjugate. Int J Nanomedicine 8, 4707-4720.

Valiveti, S., Wesley, J., Lu, G.W., 2008. Investigation of drug partition property in artificial sebum. Int. J. Pharm. 346, 10-16.

van der Maaden, K., Trietsch, S.J., Kraan, H., Varypataki, E.M., Romeijn, S., Zwier, R., van der Linden, H.J., Kersten, G., Hankemeier, T., Jiskoot, W., Bouwstra, J., 2014. Novel hollow microneedle technology for depth-controlled microinjection-mediated dermal vaccination: a study with polio vaccine in rats. Pharm. Res. 31, 1846-1854.

Van Eerdenbrugh, B., Alonzo, D.E., Taylor, L.S., 2011. Influence of particle size on the ultraviolet spectrum of particulate-containing solutions: implications for in-situ concentration monitoring using UV/Vis fiber-optic probes. Pharm. Res. 28, 1643-1652.

van Smeden, J., Bouwstra, J.A., 2016. Stratum corneum lipids: Their role for the skin barrier function in healthy subjects and atopic dermatitis patients. Curr. Probl. Dermatol. 49, 8-26.

Vauthier, C., Bouchemal, K., 2009. Methods for the preparation and manufacture of polymeric nanoparticles. Pharm. Res. 26, 1025-1058.

Venkateswarlu, V., Manjunath, K., 2004. Preparation, characterization and in vitro release kinetics of clozapine solid lipid nanoparticles. J. Control. Release 95, 627-638.

Venuganti, V.V., Perumal, O.P., 2009. Poly(amidoamine) dendrimers as skin penetration enhancers: Influence of charge, generation, and concentration. J. Pharm. Sci. 98, 2345-2356.

Venuganti, V.V., Sahdev, P., Hildreth, M., Guan, X., Perumal, O., 2011. Structure-skin permeability relationship of dendrimers. Pharm. Res. 28, 2246-2260.

Vert, M., Mauduit, J., Li, S., 1994. Biodegradation of PLA/GA polymers: increasing complexity. Biomaterials 15, 1209-1213.

Visscher, G.E., Robison, R.L., Maulding, H.V., Fong, J.W., Pearson, J.E., Argentieri, G.J., 1985. Biodegradation of and tissue reaction to 50:50 poly(DL-lactide-co-glycolide) microcapsules. J. Biomed. Mater. Res. 19, 349-365.

Visscher, G.E., Robison, R.L., Maulding, H.V., Fong, J.W., Pearson, J.E., Argentieri, G.J., 1986. Biodegradation of and tissue reaction to poly(DL-lactide) microcapsules. J. Biomed. Mater. Res. 20, 667-676.

Vogt, A., Hadam, S., Heiderhoff, M., Audring, H., Lademann, J., Sterry, W., Blume-Peytavi, U., 2007. Morphometry of human terminal and vellus hair follicles. Exp. Dermatol. 16, 946-950.

Vogt, A., Mandt, N., Lademann, J., Schaefer, H., Blume-Peytavi, U., 2005. Follicular targeting--a promising tool in selective dermatotherapy. J. Investig. Dermatol. Symp. Proc. 10, 252-255.

Wallace, S.J., Li, J., Nation, R.L., Boyd, B.J., 2012. Drug release from nanomedicines: Selection of appropriate encapsulation and release methodology. Drug Deliv Transl Res 2, 284-292.

Washington, C., 1989. Evaluation of non-sink dialysis methods for the measurement of drug release from colloids: effects of drug partition. Int. J. Pharm. 56, 71-74.

Weigmann, H.J., Lademann, J., Meffert, H., Schaefer, H., Sterry, W., 1999. Determination of the horny layer profile by tape stripping in combination with optical spectroscopy in the visible range as a prerequisite to quantify percutaneous absorption. Skin Pharmacol. Physiol. 12, 34-45.

Wenkers, B.P., Lippold, B.C., 1999. Skin penetration of nonsteroidal antiinflammatory drugs out of a lipophilic vehicle: Influence of the viable epidermis. J. Pharm. Sci. 88, 1326-1331.

Westesen, K., Bunjes, H., Koch, M.H.J., 1997. Physicochemical characterization of lipid nanoparticles and evaluation of their drug loading capacity and sustained release potential. J. Control. Release 48, 223-236.

Witting, M., Molina, M., Obst, K., Plank, R., Eckl, K.M., Hennies, H.C., Calderon, M., Friess, W., Hedtrich, S., 2015. Thermosensitive dendritic polyglycerol-based nanogels for cutaneous delivery of biomacromolecules. Nanomedicine 11, 1179-1187.

Woodley, D., Sauder, D., Talley, M.J., Silver, M., Grotendorst, G., Qwarnstrom, E., 1983. Localization of basement membrane components after dermal-epidermal junction separation. J. Invest. Dermatol. 81, 149-153.

Wu, X., Landfester, K., Musyanovych, A., Guy, R.H., 2010. Disposition of charged nanoparticles after their topical application to the skin. Skin Pharmacol. Physiol. 23, 117-123.

Xu, X., Khan, M.A., Burgess, D.J., 2012. A two-stage reverse dialysis in vitro dissolution testing method for passive targeted liposomes. Int. J. Pharm. 426, 211-218.

Yoo, J.W., Giri, N., Lee, C.H., 2011. pH-sensitive Eudragit nanoparticles for mucosal drug delivery. Int. J. Pharm. 403, 262-267.

Yoshiike, T., Aikawa, Y., Sindhvananda, J., Suto, H., Nishimura, K., Kawamoto, T., Ogawa, H., 1993. Skin barrier defect in atopic dermatitis: increased permeability of the stratum corneum using dimethyl sulfoxide and theophylline. J. Dermatol. Sci. 5, 92-96.

Youn, S.W., 2010. The role of facial sebum secretion in acne pathogenesis: facts and controversies. Clin. Dermatol. 28, 8-11.

Zambito, Y., Pedreschi, E., Di Colo, G., 2012. Is dialysis a reliable method for studying drug release from nanoparticulate systems?-A case study. Int. J. Pharm. 434, 28-34.

Zhai, H., Maibach, H.I., 2001. Effects of skin occlusion on percutaneous absorption: An overview. Skin Pharmacol. Physiol. 14, 1-10.

Zhang, L.W., Monteiro-Riviere, N.A., 2008. Assessment of quantum dot penetration into intact, tape-stripped, abraded and flexed rat skin. Skin Pharmacol. Physiol. 21, 166-180.

Zhang, L.W., Monteiro-Riviere, N.A., 2009. Mechanisms of quantum dot nanoparticle cellular uptake. Toxicol. Sci. 110, 138-155.

Zhang, Y., Wang, H., Li, C., Sun, B., Wang, Y., Wang, S., Gao, C., 2014. A novel three-dimensional large-pore mesoporous carbon matrix as a potential nanovehicle for the fast release of the poorly water-soluble drug, celecoxib. Pharm. Res. 31, 1059-1070.

Zoubari, G., Staufenbiel, S., Volz, P., Alexiev, U., Bodmeier, R., 2017. Effect of drug solubility and lipid carrier on drug release from lipid nanoparticles for dermal delivery. Eur. J. Pharm. Biopharm. 110, 39-46.

7. Publications resulting from this work

7.1. Research publications

B. Balzus, M. Colombo, F.F. Sahle, G. Zoubari, S. Staufenbiel, R. Bodmeier, Comparison of different in vitro release methods used to investigate nanocarriers intended for dermal application, Int. J. Pharm., 513 (2016) 247-254. https://doi.org/10.1016/j.ijpharm.2016.09.033

B. Balzus, F.F. Sahle, S. Hönzke, C. Gerecke, F. Schumacher, S. Hedtrich, B. Kleuser, R. Bodmeier, Formulation and ex vivo evaluation of polymeric nanoparticles for controlled delivery of corticosteroids to the skin and the corneal epithelium, Eur. J. Pharm. Biopharm., 115 (2017) 122-130. https://doi.org/10.1016/j.ejpb.2017.02.001

F.F. Sahle, **B. Balzus**, C. Gerecke, B. Kleuser, R. Bodmeier, Formulation and in vitro evaluation of polymeric enteric nanoparticles as dermal carriers with pH-dependent targeting potential, Eur. J. Pharm. Sci., 92 (2016) 98-109. https://doi.org/10.1016/j.ejps.2016.07.004

N. Döge, S. Hönzke, F. Schumacher, **B. Balzus**, M. Colombo, S. Hadam, F. Rancan, U. Blume-Peytavi, M. Schafer-Korting, A. Schindler, E. Rühl, P.S. Skov, M.K. Church, S. Hedtrich, B. Kleuser, R. Bodmeier, A. Vogt, Ethyl cellulose nanocarriers and nanocrystals differentially deliver dexamethasone into intact, tape-stripped or sodium lauryl sulfate-exposed ex vivo human skin - assessment by intradermal microdialysis and extraction from the different skin layers, J. Control. Release, 242 (2016) 25-34 https://doi.org/10.1016/j.jconrel.2016.07.009

K. Obst, G. Yealland, **B. Balzus**, E. Miceli, M. Dimde, C. Weise, M. Eravci, R. Bodmeier, R. Haag, M. Calderon, N. Charbaji, S. Hedtrich, Protein corona formation on colloidal polymeric nanoparticles and polymeric nanogels: Impact on cellular uptake, toxicity, immunogenicity, and drug release properties, Biomacromolecules, 18 (2017) 1762-1771 https://doi.org/10.1021/acs.biomac.7b00158

7.2. Poster presentations

Balzus B., Bodmeier, R. *In situ* drug dissolution tests for nanocrystals based on light scattering or UV spectroscopy. Galenus Workshop 2015, Saarbrücken, Germany

Balzus B., Bodmeier, R. Polymeric nanoparticles with controlled drug release for topical skin therapy. Poster #T2283. AAPS Annual Meeting and Exposition 2015; Orlando, Florida, USA

Balzus B., Bodmeier, R. Incorporation of plasticizers into dexamethasone loaded polymeric nanoparticles for dermal application – Influence on particle size, drug loading and drug release. International Conference on Dermal Drug Delivery by Nanocarriers 2016; Berlin, Germany

Balzus B., Bodmeier, R. Investigation of different in vitro methods to discriminate drug release from various nanocarriers intended for dermal application. Galenus Workshop 2016, Berlin, Germany

8. Curriculum vitae

For reasons of data protection, the Curriculum vitae is not published in the online version

Der Lebenslauf ist in der Online-Version aus Gründen des Datenschutzes nicht enthalten